

Fig. 1

2H7scFv-Ig cDNA and predicted amino acid sequence:

```
HindIII      NcoI      2H7 VL Leader Peptide→
~~~~~      ~~~~~
      M D F Q V Q I F S F L L I S A S
1  AAGCTTGCCG CCATGGATTT TCAAGTGCAG ATTTTCAGCT TCCTGCTAAT CAGTGCTTCA

      2H7 VL→
      V I I A R G Q I V L S Q S P A I L S A S
61  GTCATAATTG CCAGAGGACA AATTGTTCTC TCCAGTCTC CAGCAATCCT GTCTGCATCT

      P G E K V T M T C R A S S S V S Y M H W
121  CCAGGGGAGA AGGTCACAAT GACTTGCAGG GCCAGCTCAA GTGTAAGTTA CATGCACTGG

      BamHI
      ~~~~~
      Y Q Q K P G S S P K P W I Y A P S N L A
181  TACCAGCAGA AGCCAGGATC CTCCCCAAA CCCTGGATTT ATGCCCCATC CAACCTGGCT

      S G V P A R F S G S G S G T S Y S L T I
241  TCTGGAGTCC CTGCTCGCTT CAGTGGCAGT GGGTCTGGGA CCTCTTACTC TCTACAATC

      S R V E A E D A A T Y Y C Q Q W S F N P
301  AGCAGAGTGG AGGCTGAAGA TGCTGCCACT TATTACTGCC AGCAGTGGAG TTTTAACCCA

      (Gly4Ser)3 Linker
      P T F G A G T K L E L K G G G G S G G G
361  CCCACGTTCTG GTGCTGGGAC CAAGCTGGAG CTGAAAGGTG GCGGTGGCTC GGGCGGTGGT

      2H7 VH→
      G S G G G G S S Q A Y L Q Q S G A E L V
421  GGATCTGGAG GAGGTGGGAG CTCTCAGGCT TATCTACAGC AGTCTGGGGC TGAGCTGGTG

      R P G A S V K M S C K A S G Y T F T S Y
481  AGGCCTGGGG CCTCAGTGAA GATGCCTG C AAGGCTTCTG GCTACACATT TACCAGTTAC

      N M H W V K Q T P R Q G L E W I G A I Y
541  AATATGCACT GGGTAAAGCA GACACCTAGA CAGGGCCTGG AATGGATTGG AGCTATTTAT

      P G N G D T S Y N Q K F K G K A T L T V
601  CCAGGAAATG GTGATACTTC CTACAATCAG AAGTTCAAGG GCAAGGCCAC ACTGACTGTA

      D K S S S T A Y M Q L S S L T S E D S A
661  GACAAATCCT CCAGCACAGC CTACATGCAG CTCAGCAGCC TGACATCTGA AGACTCTGCG

      V Y F C A R V V Y Y S N S Y W Y F D V W
721  GTCTATTTCT GTGCAAGAGT GGTGTACTAT AGTAACTCTT ACTGGTACTT CGATGTCTGG
```

Fig. 1 (continued)

BclI  
-----human IgG1 Fc domain →

781     G T G T T V T V S D Q E P K S C D K T H  
GGCACAGGGA CCACGGTCAC CGTCTCT**GAT** CAGGAGCCCA AATCTTGTGA CAAAACTCAC

841     T C P P C P A P E L L G G P S V F L F P  
ACATGCCCAC CGTGCCCAGC ACCTGAACTC CTGGGGGGAC CGTCAGTCTT CCTCTTCCCC

901     P K P K D T L M I S R T P E V T C V V V  
CCAAAACCCA AGGACACCCT CATGATCTCC CGGACCCCTG AGGTCACATG CGTGGTGGTG

961     D V S H E D P E V K F N W Y V D G V E V  
GACGTGAGCC ACGAAGACCC TGAGGTCAAG TTCAACTGGT ACGTGACGG CGTGGAGGTG

1021    H N A K T K P R E E Q Y N S T Y R V V S  
CATAATGCCA AGACAAAGCC GCGGGAGGAG CAGTACAACA GCACGTACCG TGTGGTCAGC

1081    V L T V L H Q D W L N G K E Y K C K V S  
GTCCTACCG TCCTGCACCA GGACTGGCTG AATGGCAAGG AGTACAAGTG CAAGGTCTCC

1141    N K A L P A P I E K T I S K A K G Q P R  
AACAAAGCCC TCCCAGCCCC CATCGAGAAA ACAATCTCCA AAGCCAAAGG GCAGCCCCGA

1201    E P Q V Y T L P P S R D E L T K N Q V S  
GAACCACAGG TGTACACCCT GCCCCATCC CGGGATGAGC TGACCAAGAA CCAGGTCAGC

1261    L T C L V K G F Y P S D I A V E W E S N  
CTGACCTGCC TGGTCAAAGG CTTCTATCCC AGCGACATCG CCGTGGAGTG GGAGAGCAAT

1321    G Q P E N N Y K T T P P V L D S D G S F  
GGGCAGCCGG AGAACAATA CAAGACCAG CCTCCCGTGC TGGACTCCGA CGGCTCCTTC

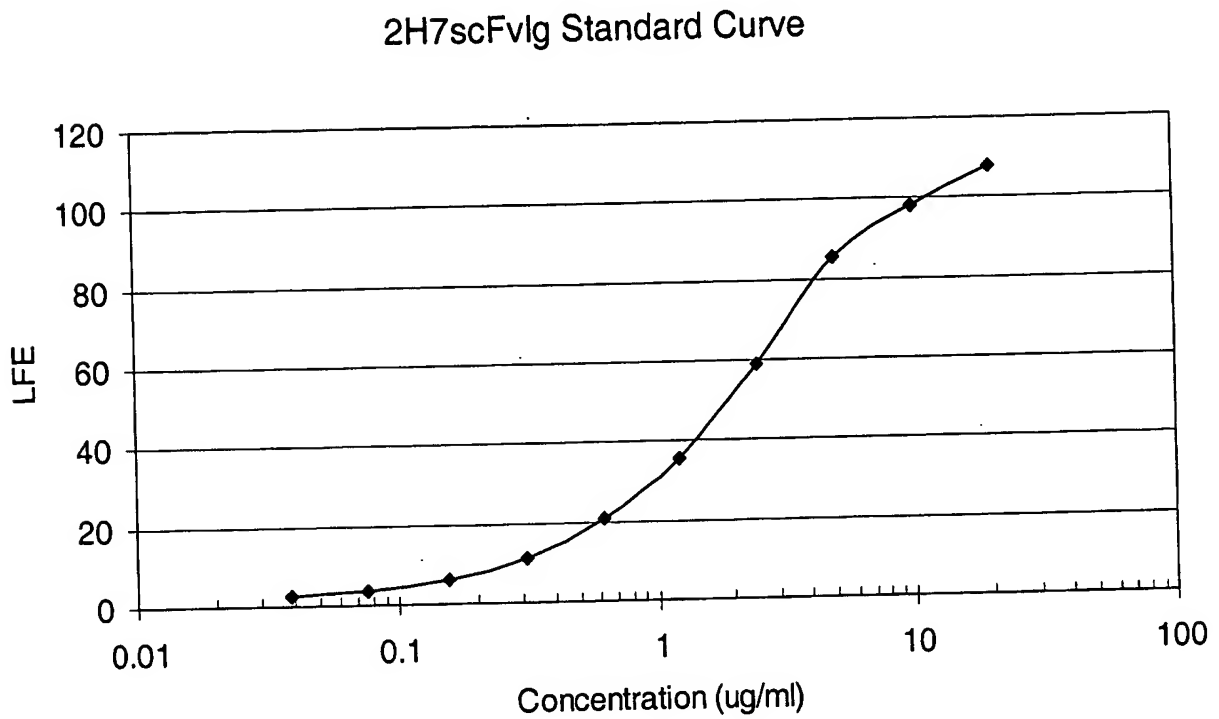
1381    F L Y S K L T V D K S R W Q Q G N V F S  
TTCCTCTACA GCAAGCTCAC CGTGGACAAG AGCAGGTGGC AGCAGGGGAA CGTCTTCTCA

1441    C S V M H E A L H N H Y T Q K S L S L S  
TGCTCCGTGA TGCATGAGGC TCTGCACAAC CACTACACGC AGAAGAGCCT CTCCCTGTCT

XbaI  
-----

1501    P G K \* S R  
CCGGGTAAAT GATCTAGA

Fig. 2  
Production Levels of 2H7 scFvIgG1 (SSS-S)H WCH2 WCH3  
by Stable CHO Lines



Clone	LFE @ 1:50 Estimated Concentration ( $\mu$ g/ml)
D2	26.156
IIIC6	25.755
IVA3	28.661
Spent bulk	29.664

Fig. 3  
SDS-PAGE Analysis of  
2H7 scFvIgG1 (SSS-S)H WCH2 WCH3 Protein.

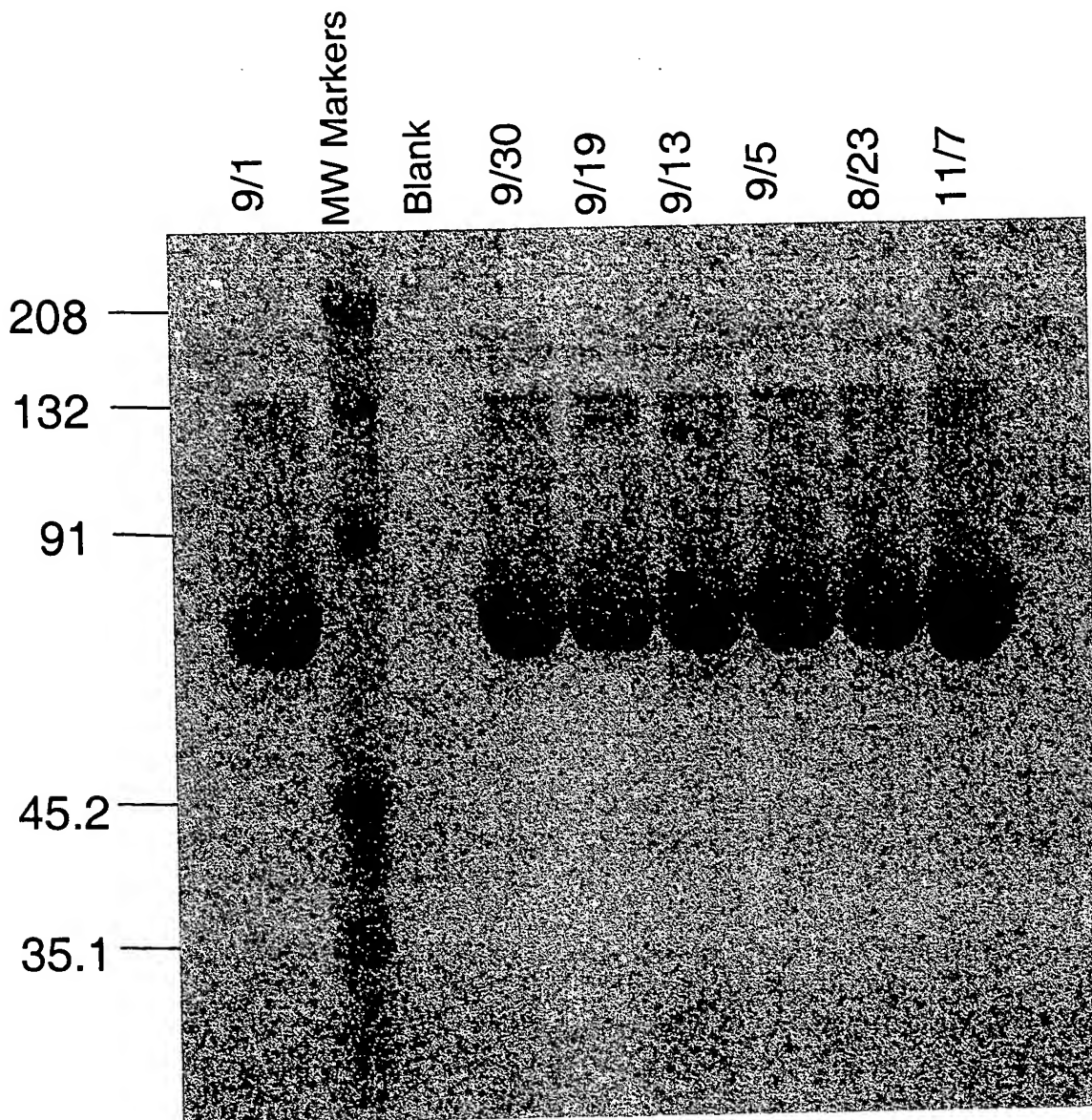


Fig. 4A

Complement Mediated B Cell Killing After Binding of  
CD20-targeted 2H7 scFvIgG1 (SSS-S)H WCH2 WCH3:

2H7scFv-Ig Concentration	RAMOS # live cells/total cells	BJAB # live cells/total cells
20 µg/ml + complement	- 0.16	- 0.07
5 µg/ml + complement	- 0.2	- N.D.
1.25 µg/ml + complement	- 0.32	- 0.1
Complement alone	- 0.98	- 0.94

\*Viability was determined by trypan blue exclusion and is tabulated as the fraction of viable cells out of the total number of cells counted.

\*\*N.D. (not determined).

Fig. 4B

Antibody-dependent cellular cytotoxicity (ADCC) mediated by 2H7scFv-IgG1  
(SSS-S)H WCH2 WCH3:

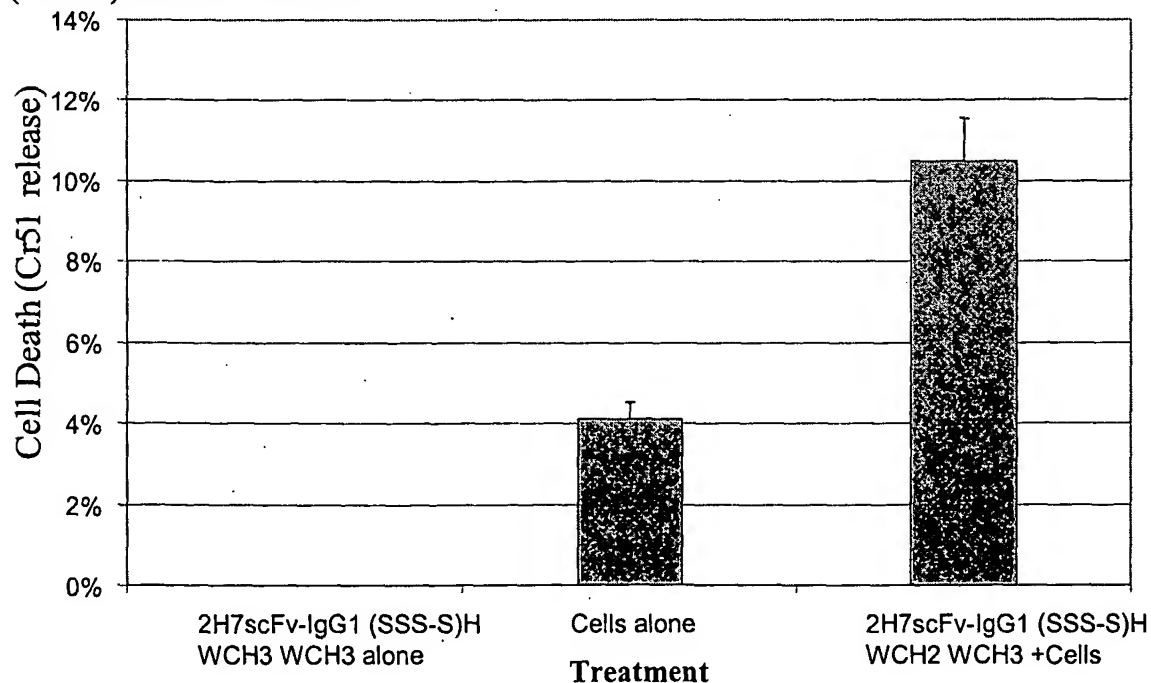


Fig. 5

Effects of Crosslinking of CD20 and CD40 Cell Surface Receptors  
on B Cell Proliferation:

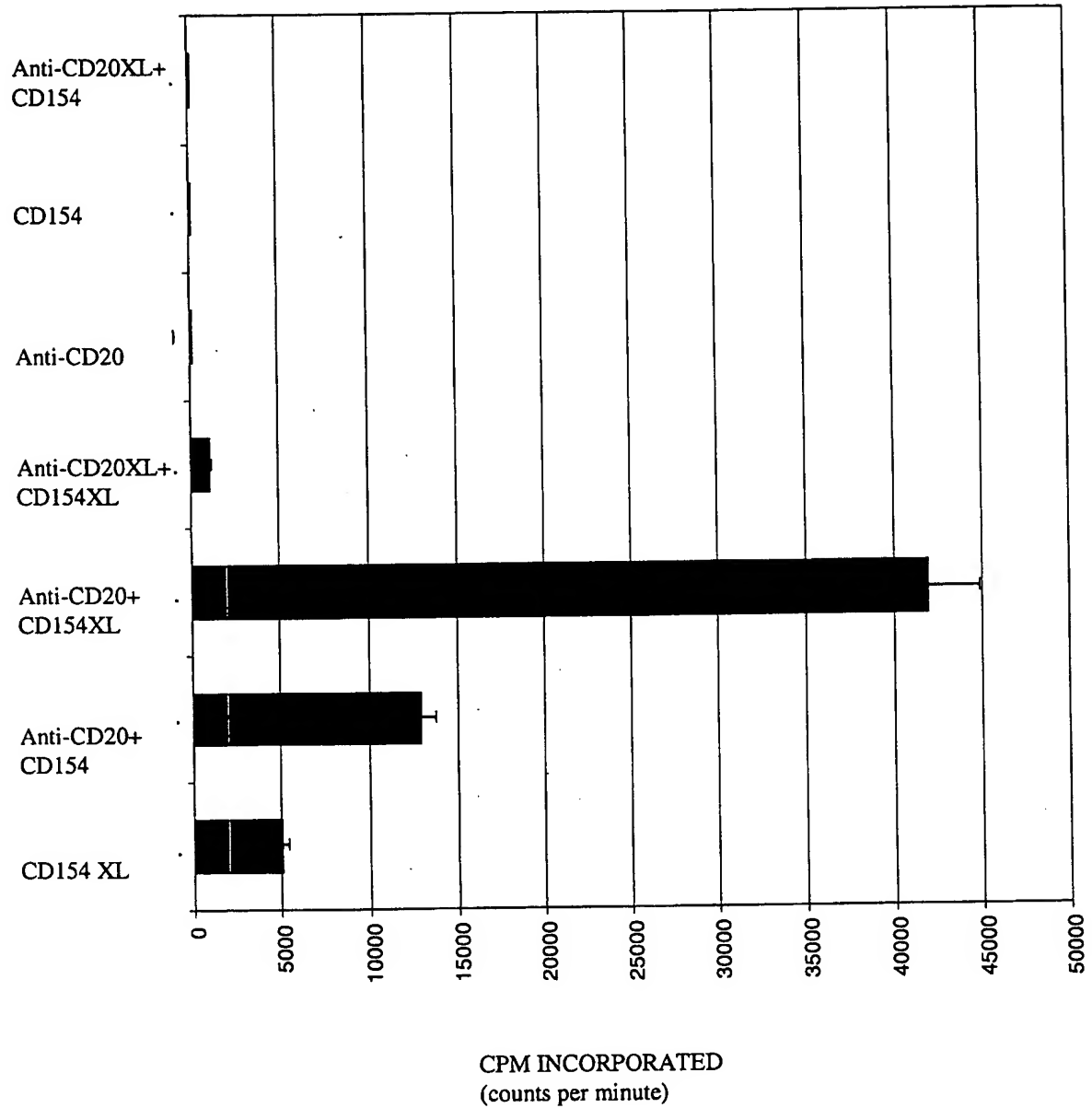


Fig. 6

Effect of Simultaneous ligation of CD20 and CD40  
on CD95 and apoptosis.

Fig. 6A.

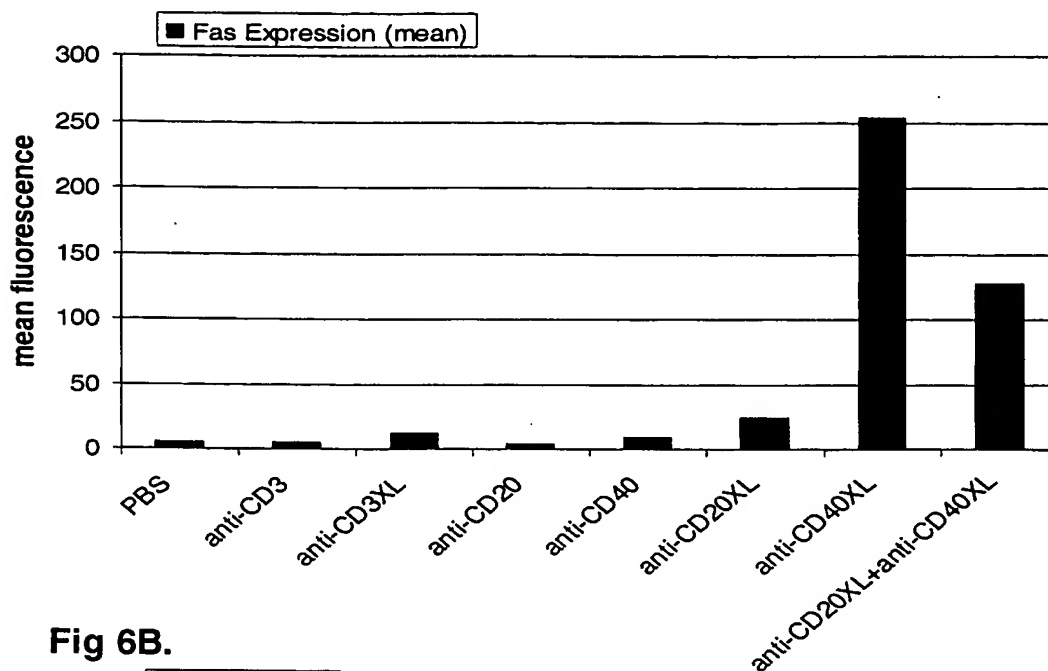
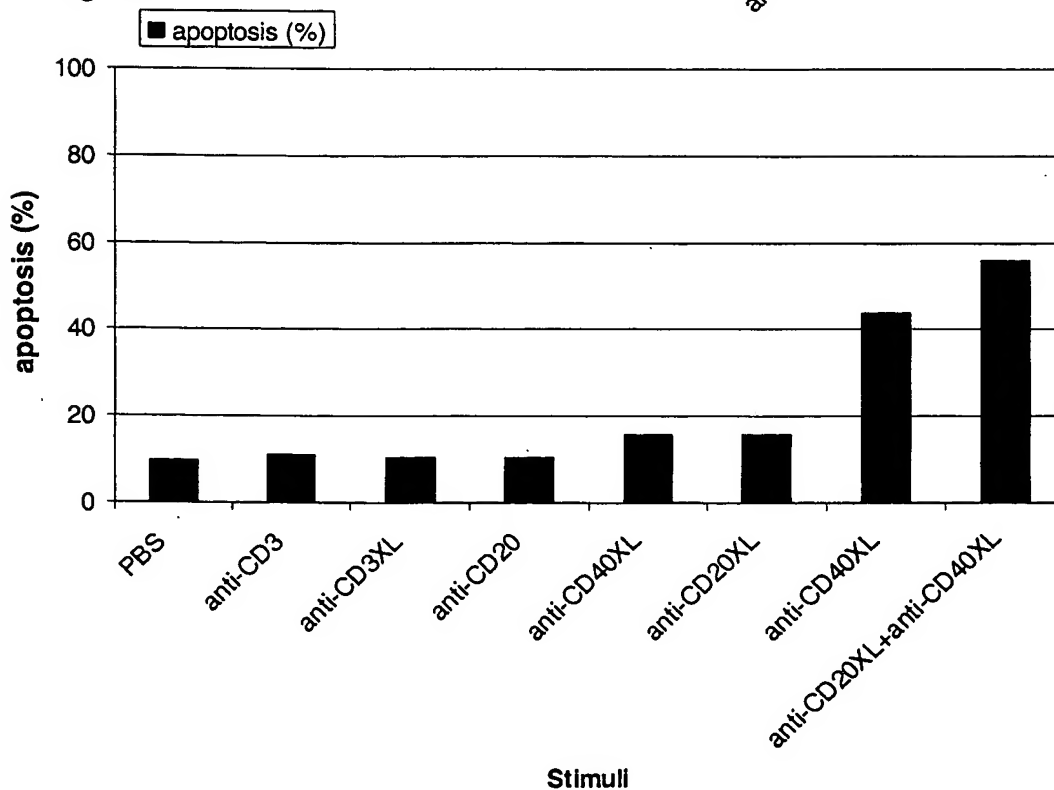


Fig 6B.



**BINDING CONSTRUCTS &  
METHODS OF USE THEREOF**  
Ledbetter, Jeffrey A.  
Docket: 49076.000004.CIP2

Fig. 7A

**2H7-CD154 L2 cDNA and predicted amino acid sequence:**

HindIII                  NcoI      2H7 V<sub>L</sub> Leader Peptide →  
~~~~~                  ~~~~~

1 AAGCTTGCCG CC ATGGATTT TCAAGTGCAG ATTTTCAGCT TCCTGCTAAT CAGTGCTTCA  
  
M D F Q V Q I F S F L L I S A S  
  
2H7 V<sub>L</sub> →  
61 GTCATAATTG CCAGAGGACA AATTGTTC TCACAGTCTC CAGCAATCCT GTCTGCATCT  
  
P G E K V T M T C R A S S S V S Y M H W  
121 CCAGGGGAGA AGGTCACAAT GACTTGCAGG GCCAGCTCAA GTGTAAGTTA CATGCACTGG  
  
BamHI  
~~~~~  
181 TACCAGCAGA AGCCAGGATC CTCCCCAAA CCCTGGATTT ATGCCCATC CAACCTGGCT  
  
S G V P A R F S G S G S G T S Y S L T I  
241 TCTGGAGTCC CTGCTCGCTT CAGTGGCAGT GGTCTGGGA CCTCTTACTC TCTCACAACT  
  
S R V E A E D A A T Y Y C Q Q W S F N P  
301 AGCAGAGTGG AGGCTGAAGA TGCTGCCACT TATTACTGCC AGCAGTGGAG TTTTAACCCA  
  
(Gly<sub>4</sub>Ser)<sub>3</sub> Linker →  
361 CCCACGTT CG GTGCTGGGAC CAAGCTGGAG CTGAAAGGTG GCGGTGGCTC GGGCGGTGGT  
  
2H7 V<sub>H</sub> →  
421 GGATCTGGAG GAGGTGGGAG CTCTCAGGCT TATCTACAGC AGTCTGGGGC TGAGCTGGTG  
  
R P G A S V K M S C K A S G Y T F T S Y  
481 AGGCCTGGGG CCTCAGTGAA GATGTCCTGC AAGGCTTCTG GCTACACATT TACCAGTTAC  
  
N M H W V K Q T P R Q G L E W I G A I Y  
541 AATATGCACT GGGTAAAGCA GACACCTAGA CAGGCGCTGG AATGGATTGG AGCTATTATT  
  
P G N G D T S Y N Q K F K G K A T L T V  
601 CCAGGAAATG GTGATACTTC CTACAATCAG AAGTTCAAGG GCAAGGCCAC ACTGACTGTA  
  
D K S S S T A Y M Q L S S L T S E D S A  
661 GACAAATCCT CCAGCACAGC CTACATGCAG CTCAGCAGCC TGACATCTGA AGACTCTGCG  
  
V Y F C A R V V Y Y S N S Y W Y F D V W  
721 GTCTATTTCT GTGCAAGAGT GGTGTAATAT AGTAATCTT ACTGGTACTT CGATGTCTGG

# Fig. 7A (continued)

human CD154/amino acid 48→

Bcl/Bam hybrid site

781 G T G T T V T V S D P R R L D K I E D E  
GGCACAGGGA CCACGGTCAC CGTCTC**tgat** CCAAGAAGGT TGGACAAGAT AGAAGATGAA

841 R N L H E D F V F M K T I Q R C N T G E  
AGGAATCTTC ATGAAGATTT TGTATTCATG AAAACGATAC AGAGATGCAA CACAGGAGAA

901 R S L S L L N C E E I K S Q F E G F V K  
AGATCCTTAT CCTTACTGAA CTGTGAGGAG ATTAAAAGCC AGTTTGAAGG CTTTGTGAAG

BclI

961 D I M L N K E E T K K E N S F E M Q K G  
GATATAATGT TAAACAAAGA GGAGACGAAG AAAGAAAACA GCTTTGAAAT GCAAAAAGGT

BclI  
~~~~~

1021 D Q N P Q I A A H V I S E A S S K T T S  
GATCAGAATC CTCAAATTGC GGCACATGTC ATAAGTGAGG CCAGCAGTAA AACAAATCAT

1081 V L Q W A E K G Y Y T M S N N L V T L E  
GTGTTACAGT GGGCTGAAAA AGGATACTAC ACCATGAGCA ACAACTTGGT AACCTTGGA

1141 N G K Q L T V K R Q G L Y Y I Y A Q V T  
AATGGGAAAC AGCTGACCGT TAAAAGACAA GGACTCTATT ATATCTATGC CCAAGTCACC

HindIII  
~~~~~

1201 F C S N R E A S S Q A P F I A S L C L K  
TTCTGTTCOA ATCGGGAAGC TTCGAGTCAA GCTCCATTTA TAGCCAGCCT CTGCCTAAAG

1261 S P G R F E R I L L R A A N T H S S A K  
TCCCCGGTA GATTCGAGAG AATCTTACTC AGAGCTGCAA ATACCCACAG TTCCGCCAAA

1321 P C G Q Q S I H L G G V F E L Q P G A S  
CCTTGCGGGC AACAATCCAT TCACTTGGGA GGAGTATTG AATTGCAACC AGGTGCTTCG

NcoI  
~~~~~

1381 V F V N V T D P S Q V S H G T G F T S F  
GTGTTTGTCA ATGTGACTGA TCCAAGCCAA GTGAGCCATG GCACTGGCTT CACGTCCTTT

XhoI XbaI  
~~~~~

1441 G L L K L E \* \* S R  
GGCTTACTCA AACTCGAGTG ATAATCTAGA

Fig. 7B.

2H7scFv-CD154 S4 cDNA and predicted amino acid sequence:

```

HindIII      NcoI
~~~~~      ~~~~~2H7 VL Leader Peptide→
                M D F Q V Q I F S F L L I S A S
1  AAGCTTGCCG CC  ATGGATTT TCAAGTGCAG ATTTTCAGCT TCCTGCTAAT CAGTGCTTCA

                2H7 VL →
        V I I A R G Q I V L S Q S P A I L S A S
61  GTCATAATTG CCAGAGGACA AATTGTTCTC TCCAGTCTC CAGCAATCCT GTCTGCATCT

        P G E K V T M T C R A S S S V S Y M H W
121 CCAGGGGAGA AGGTCACAAT GACTTGCAGG GCCAGCTCAA GTGTAAGTTA CATGCACTGG

                BamHI
                ~~~~~
        Y Q Q K P G S S P K P W I Y A P S N L A
181 TACCAGCAGA AGCCAGGATC CTCCCCCAAA CCCTGGATTT ATGCCCCATC CAACCTGGCT

        S G V P A R F S G S G S G T S Y S L T I
241 TCTGGAGTCC CTGCTCGCTT CAGTGGCAGT GGGTCTGGGA CCTCTTACTC TCTCACAATC

        S R V E A E D A A T Y Y C Q Q W S F N P
301 AGCAGAGTGG AGGCTGAAGA TGCTGCCACT TATTACTGCC AGCAGTGGAG TTTTAACCCA

(Gly4Ser)3 Linker →
        P T F G A G T K L E L K G G G G S G G G
361 CCCACGTTCTG GTGCTGGGAC CAAGCTGGAG CTGAAAGGTG GCGGTGGCTC GGGCGGTGGT

                2H7 VH →
        G S G G G G S S Q A Y L Q Q S G A E L V
421 GGATCTGGAG GAGGTGGGAG CTCTCAGGCT TATCTACAGC AGTCTGGGGC TGAGCTGGTG

        R P G A S V K M S C K A S G Y T F T S Y
481 AGGCCTGGGG CCTCAGTGAA GATGTCCTGC AAGGCTTCTG GCTACACATT TACCAGTTAC

        N M H W V K Q T P R Q G L E W I G A I Y
541 AATATGCACT GGGTAAAGCA GACACCTAGA CAGGGCCTGG AATGGATTGG AGCTATTTAT

        P G N G D T S Y N Q K F K G K A T L T V
601 CCAGGAAATG GTGATACTTC CTACAATCAG AAGTTCAAGG GCAAGGCCAC ACTGACTGTA

        D K S S S T A Y M Q L S S L T S E D S A
661 GACAAATCCT CCAGCACAGC CTACATGCAG CTCAGCAGCC TGACATCTGA AGACTCTGCG

        V Y F C A R V V Y Y S N S Y W Y F D V W
721 GTCTATTTCT GTGCAAGAGT GGTGTACTAT AGTAACTCTT ACTGGTACTT CGATGTCTGG

```

Fig. 7B

human CD154/amino acid 108 →

Bcl/Bam hybrid site

BclI

781 G T G T T V T V S D P E N S F E M Q K G  
GGCACAGGGA CCACGGTCAC CGTCTCTGAT CCAGAAAACA GCTTTGAAAT GCAAAAAGGT

BclI

841 D Q N P Q I A A H V I S E A S S K T T S  
GATCAGAATC CTCAAATTGC GGCACATGTC ATAAGTGAGG CCAGCAGTAA AACAAACATCT  
901 V L Q W A E K G Y Y T M S N N L V T L E  
GTGTTACAGT GGGCTGAAAA AGGATACTAC ACCATGAGCA ACAACTTGGT AACCCCTGGAA  
961 N G K Q L T V K R Q G L Y Y I Y A Q V T  
AATGGGAAAC AGCTGACCGT TAAAAGACAA GGACTCTATT ATATCTATGC CCAAGTCACC

HindIII

1021 F C S N R E A S S Q A P F I A S L C L K  
TTCTGTCCA ATCGGGAAGC TTCGAGTCAA GCTCCATTTA TAGCCAGCCT CTGCCTAAAG  
1081 S P G R F E R I L L R A A N T H S S A K  
TCCCCGGTA GATTCGAGAG AATCTTACTC AGAGCTGCAA ATACCCACAG TTCCGCCAAA  
1141 P C G Q Q S I H L G G V F E L Q P G A S  
CCTTGCGGGC AACAATCCAT TCACTTGGGA GGAGTATTTG AATTGCAACC AGGTGCTTCG

NcoI

1201 V F V N V T D P S Q V S H G T G F T S F  
GTGTTTGTCA ATGTGACTGA TCCAAGCCAA GTGAGCCATG GCACTGGCTT CACGTCCTTT

XhoI

XbaI

1261 G L L K L E \* \* S R  
GGCTTACTCA AACTCGAGTG ATAATCTAGA

Fig. 8

Simultaneous Binding of 2H7scFv-CD154  
Fusion Proteins to CD20 and CD40

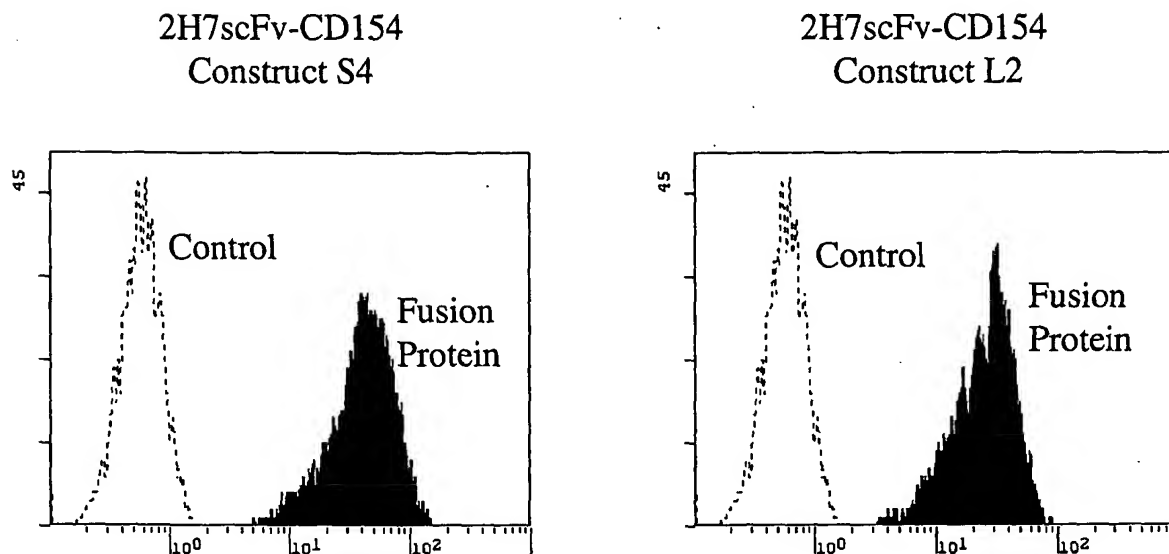
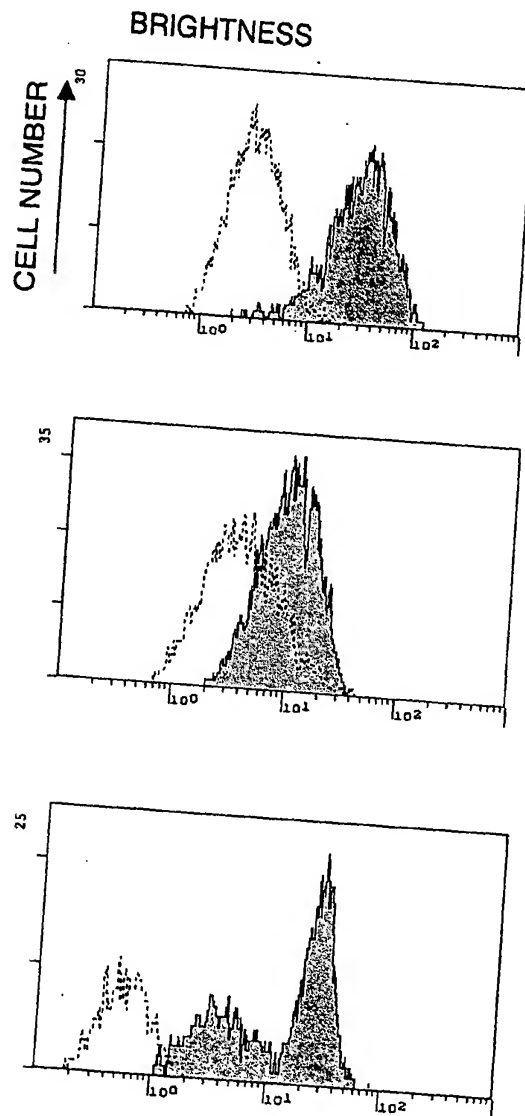


Fig. 9

Induction of Apoptosis Measured by Binding of Annexin V after  
incubation with 2H7scFv-CD154



.....control supernatant    — 2H7scFv-CD154 supernatant

Fig. 10

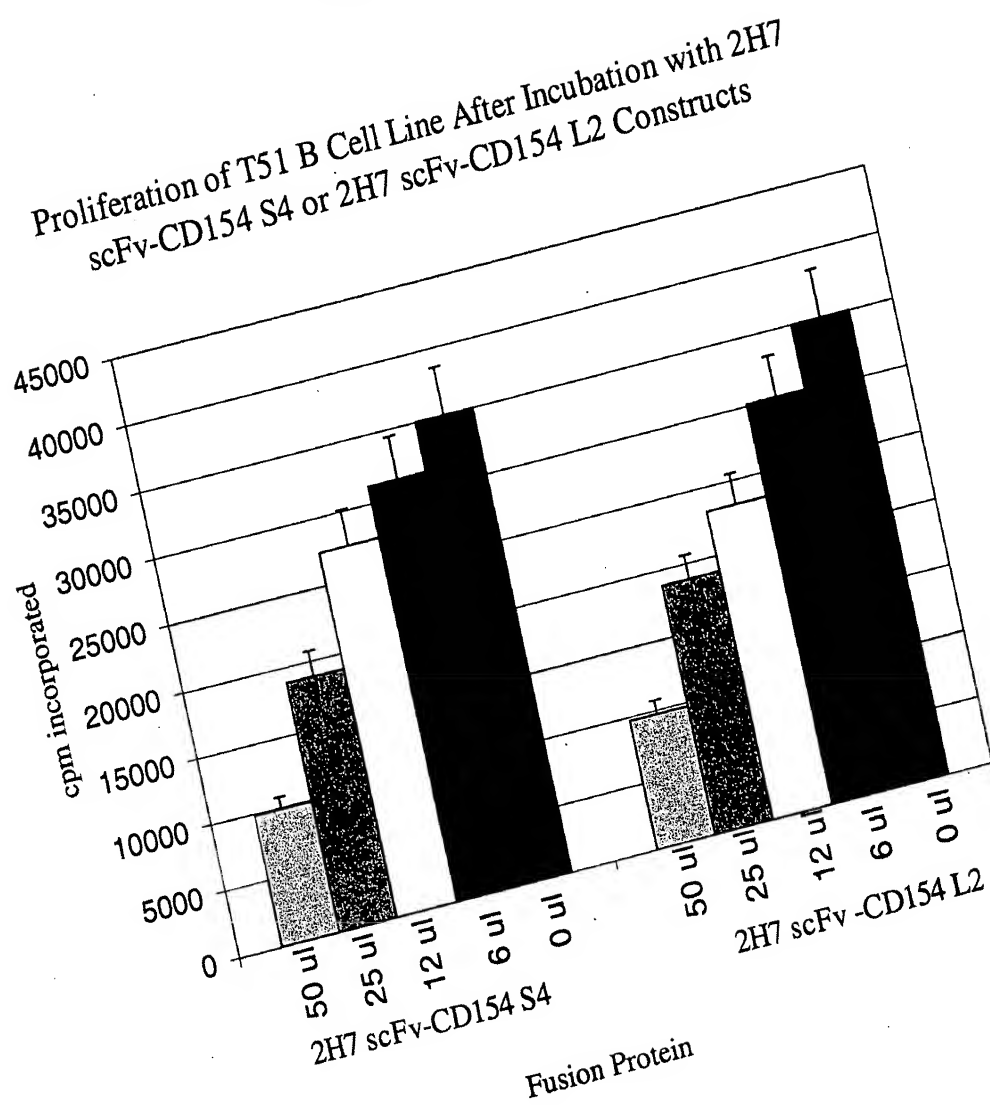




Fig. 12

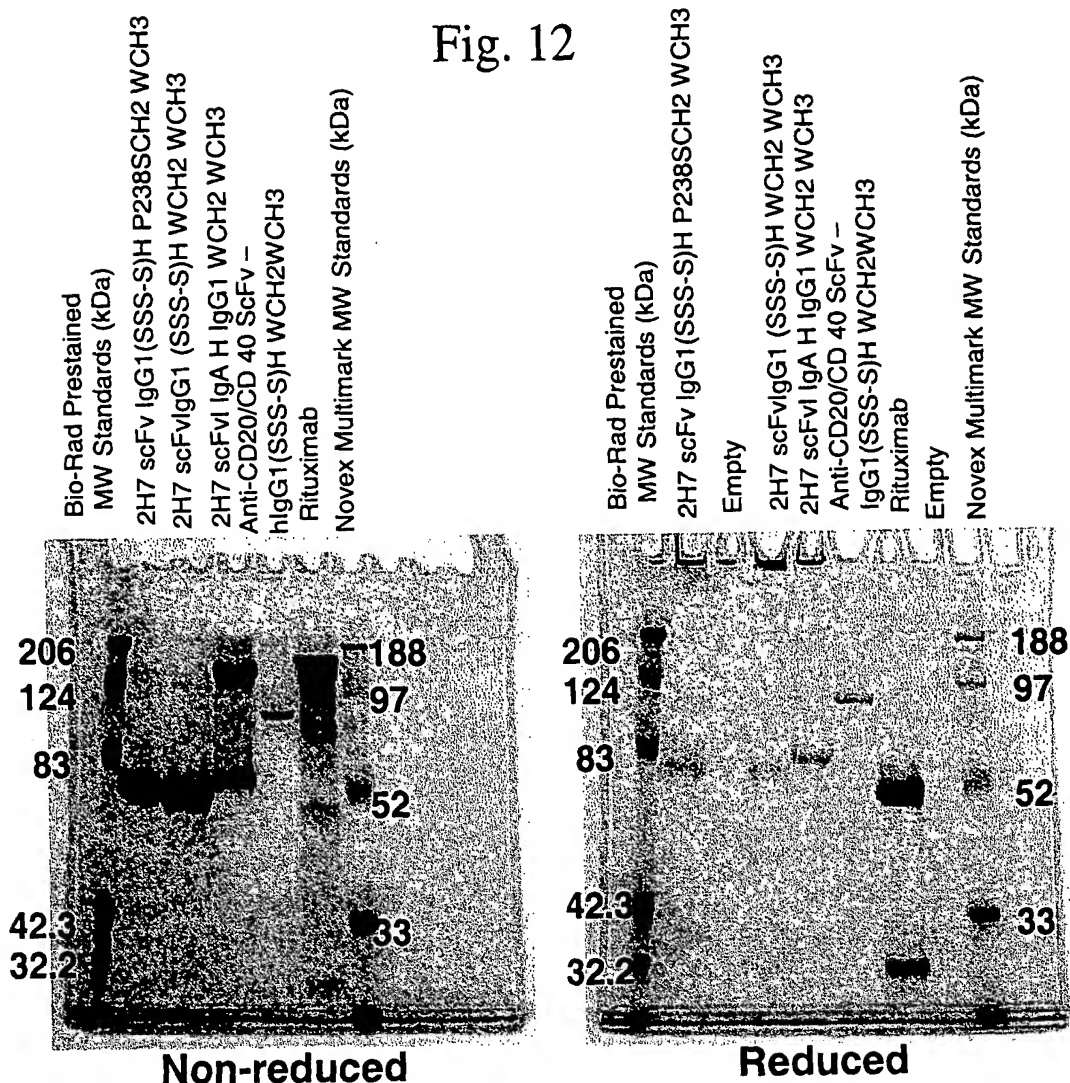


Figure 12: SDS-PAGE Analysis of CytoxB Derivatives. Purified fusion protein derivatives of CytoxB-scFvIg molecules and Rituximab were resuspended in SDS sample buffer, boiled, loaded onto 10% Novex Tris-Bis gels (Invitrogen, San Diego, CA) and subjected to nonreducing (left panel) or reducing (right panel) SDS-PAGE electrophoresis at 175 volts. Two different molecular weight markers, BioRad prestained markers, and Novex Multimark molecular weight markers were also loaded onto each gel and the approximate size in kDa of each marker band is indicated along each side of the photographed gels. Gels were stained in Coomassie Blue stain and photographed with a SONY Mavica Digital camera. The mutant hinge forms of 2H7 scFvIgG1 migrate at approximately 70 kDa under both nonreducing and reducing conditions, indicating that these molecules are monomeric rather than dimeric in structure. The IgA hinge form of 2H7scFvIg migrates at approximately 75 kDa under reducing conditions, but migrates predominately as a dimer of 140 kDa with a fraction of the protein migrating at 75 kDa under nonreducing conditions. Under nonreducing conditions, rituximab migrates as a diffuse band of between 150 and 200 kDa. The heavy and light chains resolve into separate bands of approximately 32 and 50 kDa when rituximab is reduced and subjected to SDS-PAGE.

Fig. 13  
ADCC Activity of Cytox B (2H7 scFvIg) Constructs.

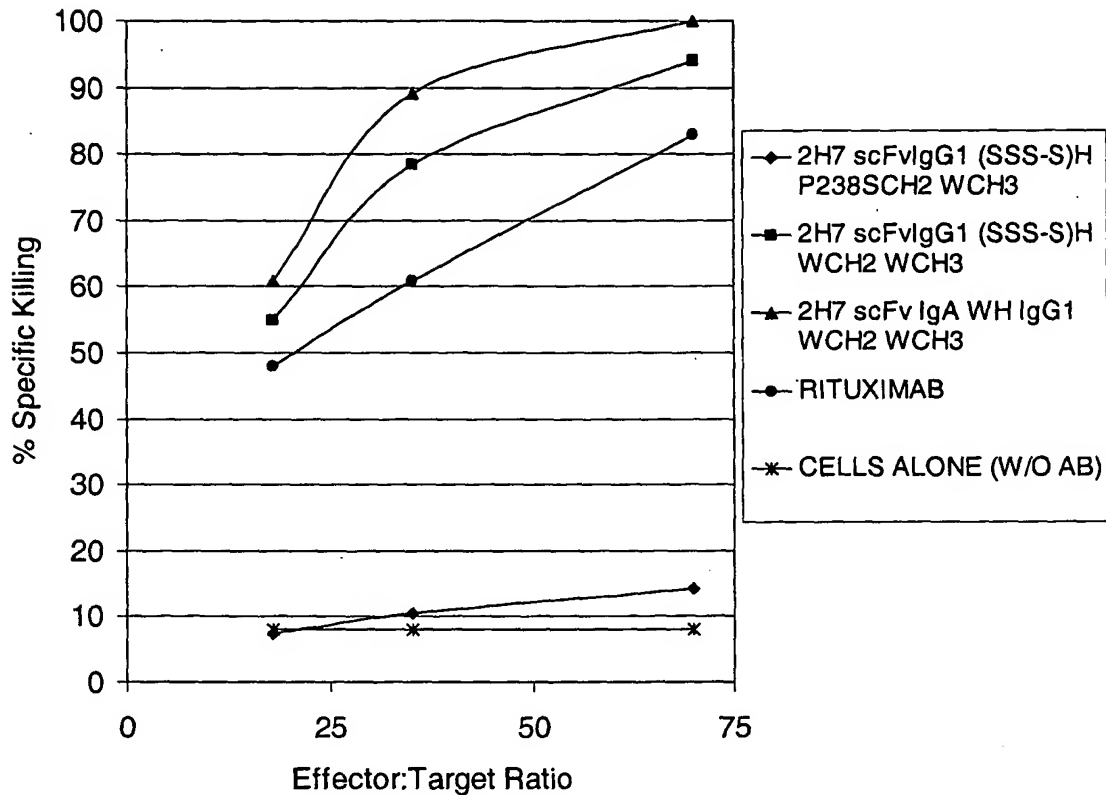


Figure 13: ADCC Activity of Cytox B Derivatives Compared to Rituximab. ADCC activity of Cytox B Derivatives or Rituximab was measured *in vitro* against BJAB B lymphoma cell line as target and using fresh human PBMC as effector cells. Effector to target ratios were varied as follows: 70:1, 35:1, and 18:1, with the number of BJAB cells per well remaining constant but varying the number of PBMC. Bjab cells were labeled for 2 hours with  $^{51}\text{Cr}$  and aliquoted at a cell density of  $5 \times 10^4$  cells/well to each well of flat-bottom 96 well plates. Purified fusion proteins or rituximab were added at a concentration of 10 mg/ml, and PBMC were added at  $9 \times 10^5$  cells/well (18:1),  $1.8 \times 10^6$  cells/well (35:1), or  $3.6 \times 10^6$  cells/well (70:1), in a final volume of 200  $\mu\text{l}$ . Spontaneous release was measured without addition of PBMC or fusion protein, and maximal release was measured by the addition of detergent (1% NP-40) to the appropriate wells. Reactions were incubated for 4 hours, and 100  $\mu\text{l}$  culture supernatant harvested to a Lumaplate (Packard Instruments) and allowed to dry overnight prior to counting cpm released on a Packard Top Count NXT Microplate Scintillation Counter.

Fig. 14  
CDC of Cytos B (2H7 scFvIg) Constructs

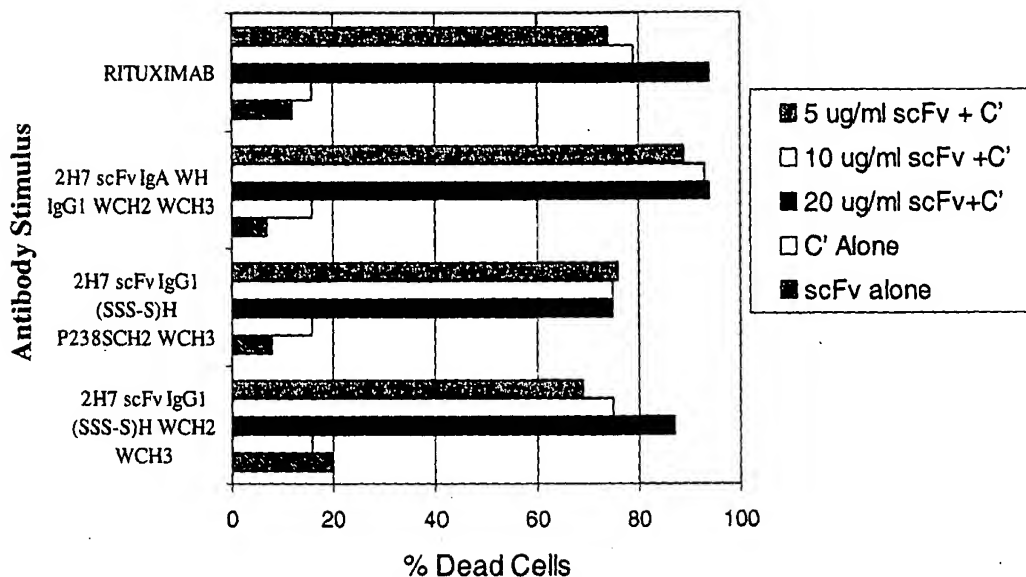
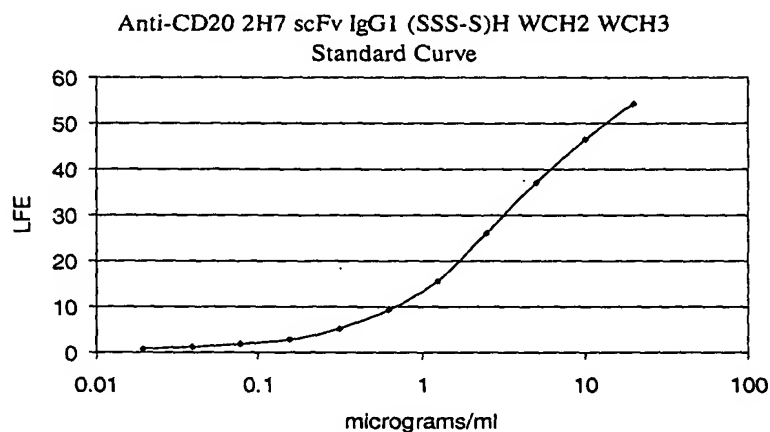


Figure 14: Complement Dependent Cytotoxicity (CDC) Activity of CytosB Derivatives Compared to Rituximab. 2H7 scFvIgG1 (SSS-S)H WCH2 WCH3, 2H7 scFvIgG1 (SSS-S)H WCH2 WCH3, and 2H7scFv.IgA WH IgG1 WCH2 WCH3 derivatives and Rituximab were compared for their ability to mediate complement dependent cytotoxicity. Rabbit complement (Pel-Freez) was diluted 1:10 and added to BJAB cells along with dilutions of each antibody derivative (20  $\mu$ g/ml, 10  $\mu$ g/ml, and 5  $\mu$ g/ml). Controls were also included without addition of complement (C') or scFv derivative. Reactions were allowed to continue for 1 hour, and cells from each well were then stained with trypan blue and the cell viability counted using a hemacytometer. Data is graphed as % of dead cells/total cells counted for each condition assayed.

Fig. 15  
2H7 (anti-CD20) scFv IgG1 (SSS-S)H WCH2 WCH3  
In Vivo Half Life



Macaque A99314

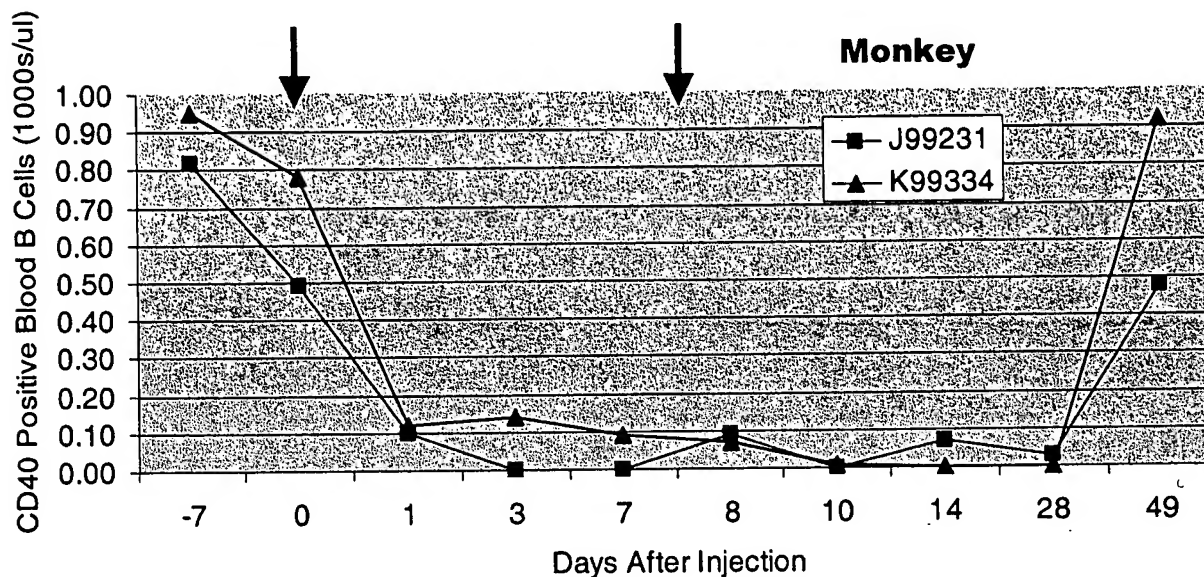
	Day	Binding intensity (LFE) @ 1:50 dilution of serum	estimated concentration (µg/ml)
Injection #1	-7	0.213	<0.1
	0	0.227	<0.1
	1	7.79	25.1
Injection #2	3	5.51	15.6
	7	3.37	9.4
	8	11.33	41.7
	10	5.45	15.4
	14	0.27	<0.1

Macaque F98081

	Day	Binding intensity (LFE) @ 1:50 dilution of serum	estimated concentration (µg/ml)
Injection #1	-7	0.208	<0.1
	0	0.219	<0.1
	1	6.73	21.9
Injection #2	3	6.14	19.3
	7	3.04	8.7
	8	9.83	33.8
	10	4.77	14.4
	14	0.231	<0.1

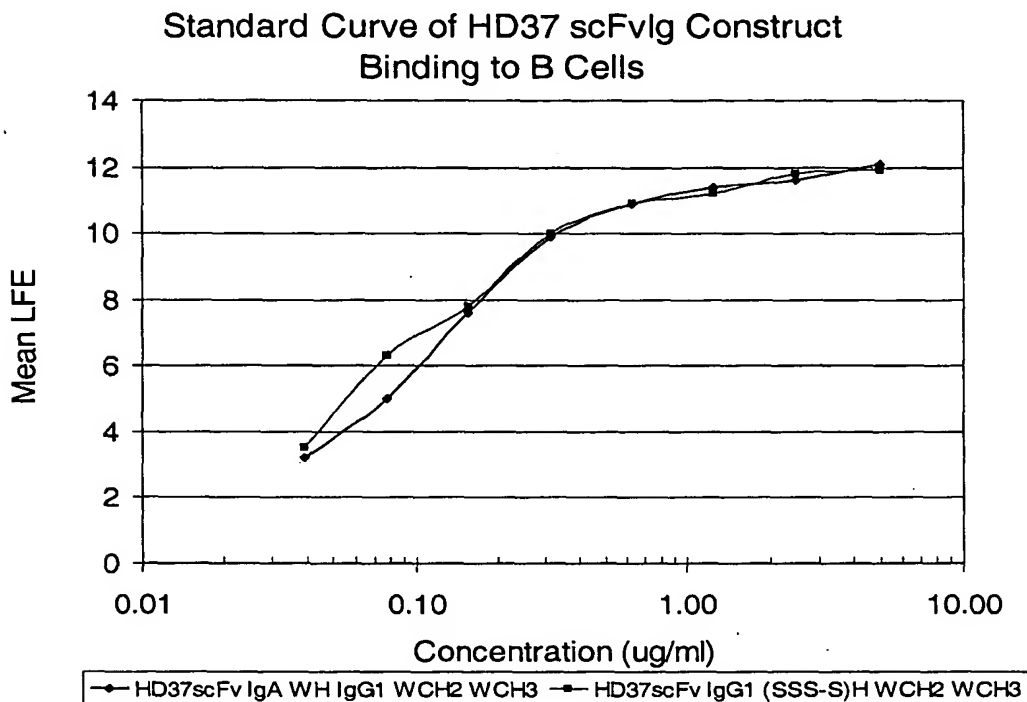
Fig. 16

B Cell Depletion in macaques mediated by Cytos B20  
(2H7 scFv IgG1 (SSS-S)H WCH2 WCH3) Construct



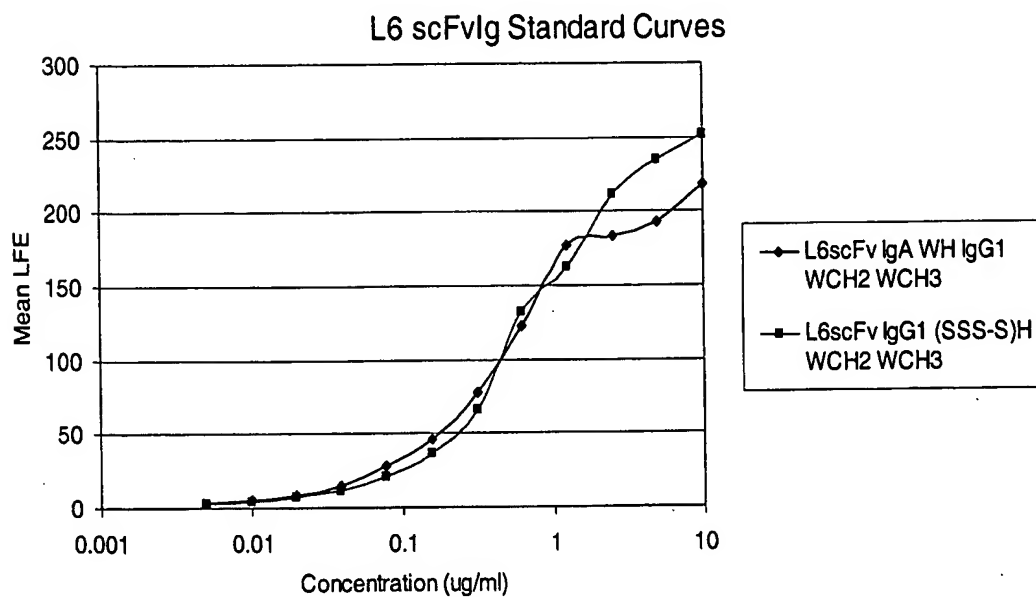
- CytosB20 injections of 6mg/kg yields 3 week B-cell depletion
- 3-4 day half-life *in vivo*
- CD20 saturation in lymph node B-cells at d14
- No first dose effects
- No anti-chimeric antibody development

Fig. 17  
Production Levels of HD37 scFvIg Constructs  
by CHO Cell Lines



Clone/Isolate	Mean LFE at 1:100	Estimated Concentration
Bulk HD37 scFv		
IgA WH IgG1 WCH2 WCH3	11.2	> 60 ug/ml
1B2	10.4	>50 ug/ml
6C5	10.5	>50 ug/ml
4B1	8.6	>40 ug/ml
Bulk HD37 scFv		
IgG1 (SSS-S)H WCH2 WCH3	10.9	> 50 ug/ml
2G8	10.6	> 50 ug/ml
3F3	8.3	>40 ug/ml
3D9	11.1	> 60 ug/ml

Fig. 18  
Production of L6 scFvIg constructs by CHO Cells



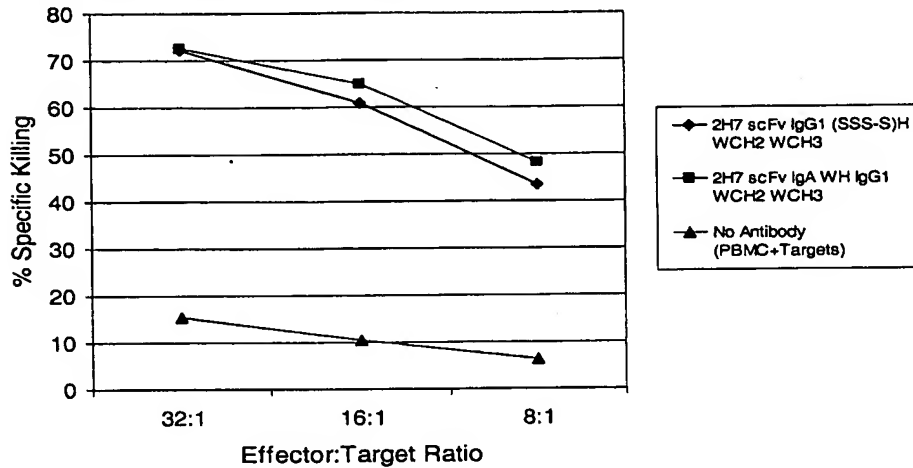
Construct	Mean LFE 1:20	Estimated Concentration
L6scFv IgA WH IgG1 WCH2 WCH3 unamplified CHO sup	51.1	6.25 ug/ml
L6scFv IgG1(SSS-S)H WCH2 WCH3 unamplified CHO sup	23.0	3.2 ug/ml

# Fig. 19

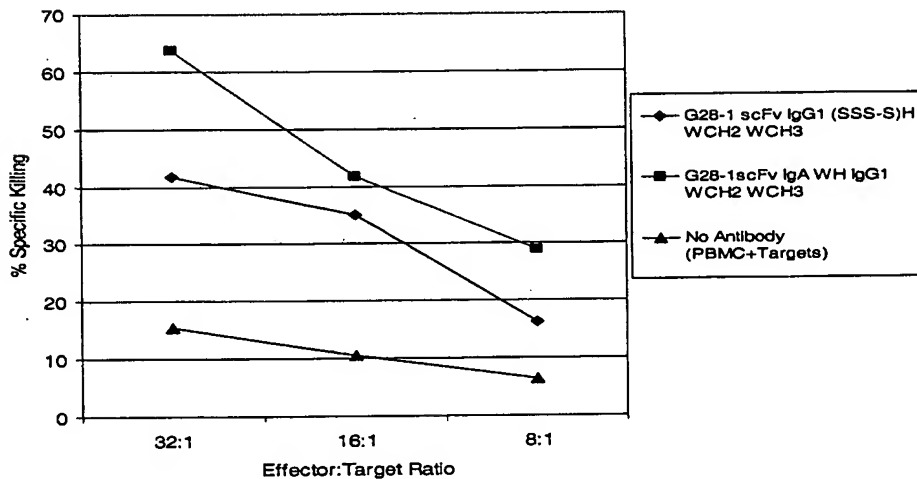
## ADCC Activity of 2H7 scFvIg, G28-1 scFvIg, and HD37 scFvIg Constructs

### ADCC Activity of scFvs Targeted to B Cell Antigens

A. 2H7 (anti-CD20) scFv constructs



B. G28-1 (anti-CD37) scFv constructs



C. HD37 (anti-CD19) scFv constructs

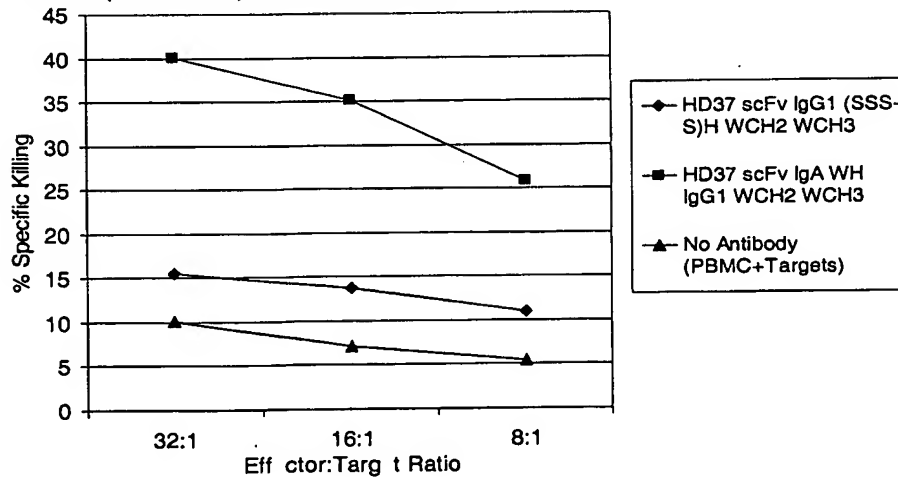


Fig. 20  
ADCC Activity of L6 scFvIg Constructs

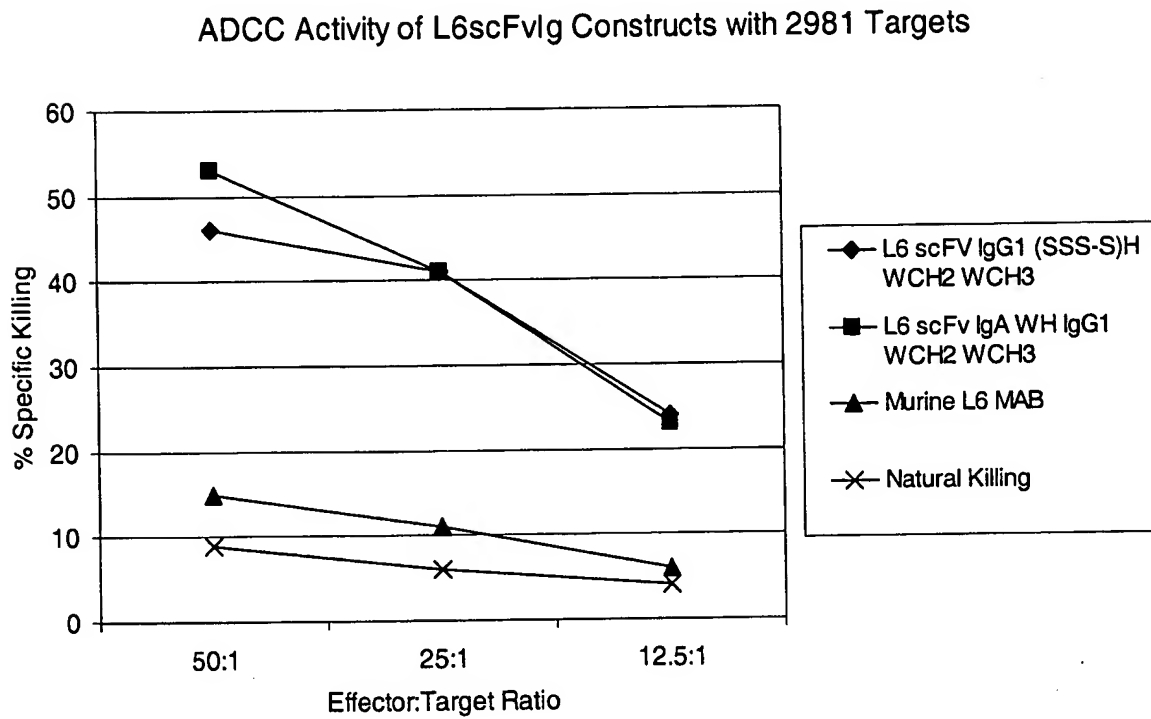


Fig. 21  
SDS-PAGE Analysis of L6 and 2H7  
scFvIg Fusion Proteins.

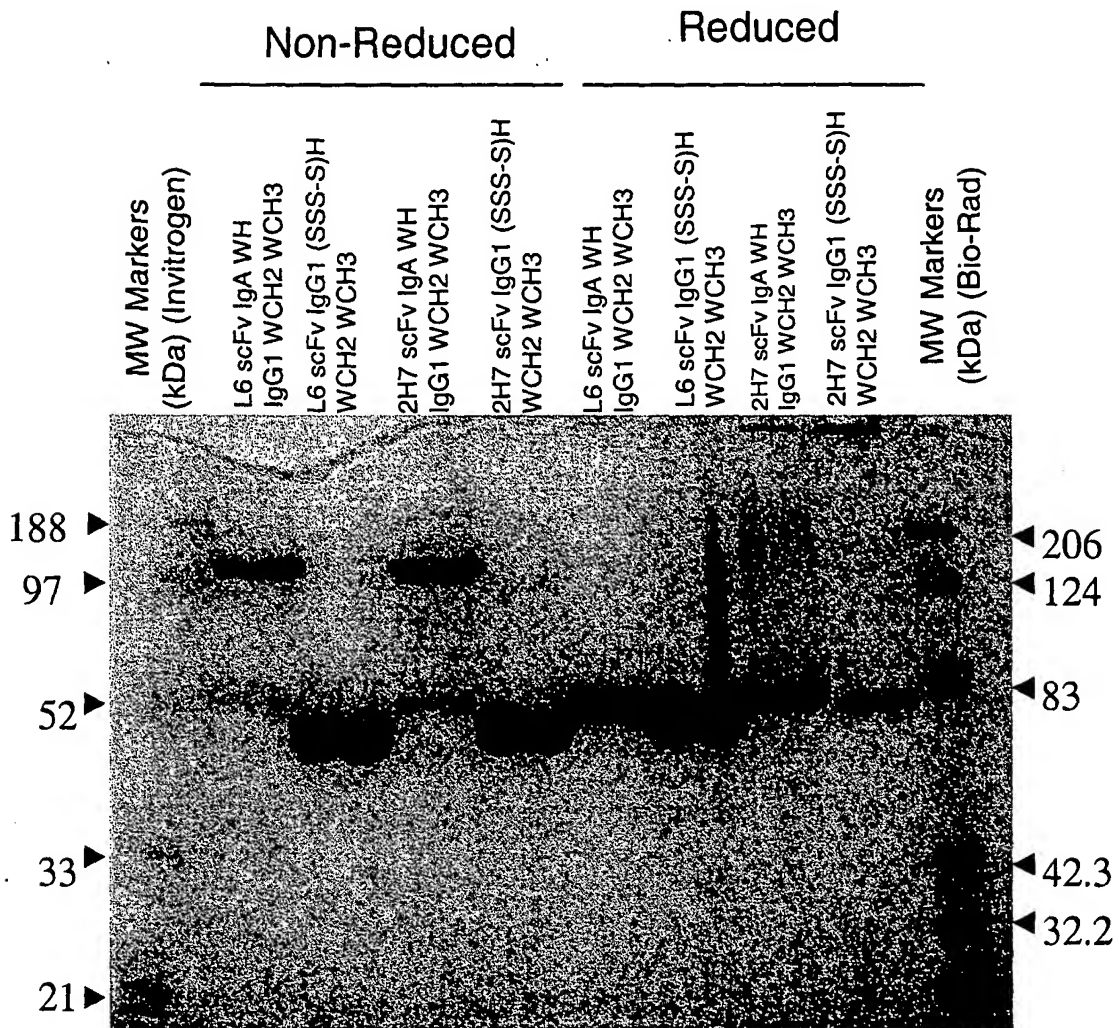


Fig. 22  
SDS-PAGE Analysis of G28-1 and HD37  
scFvlg Constructs.

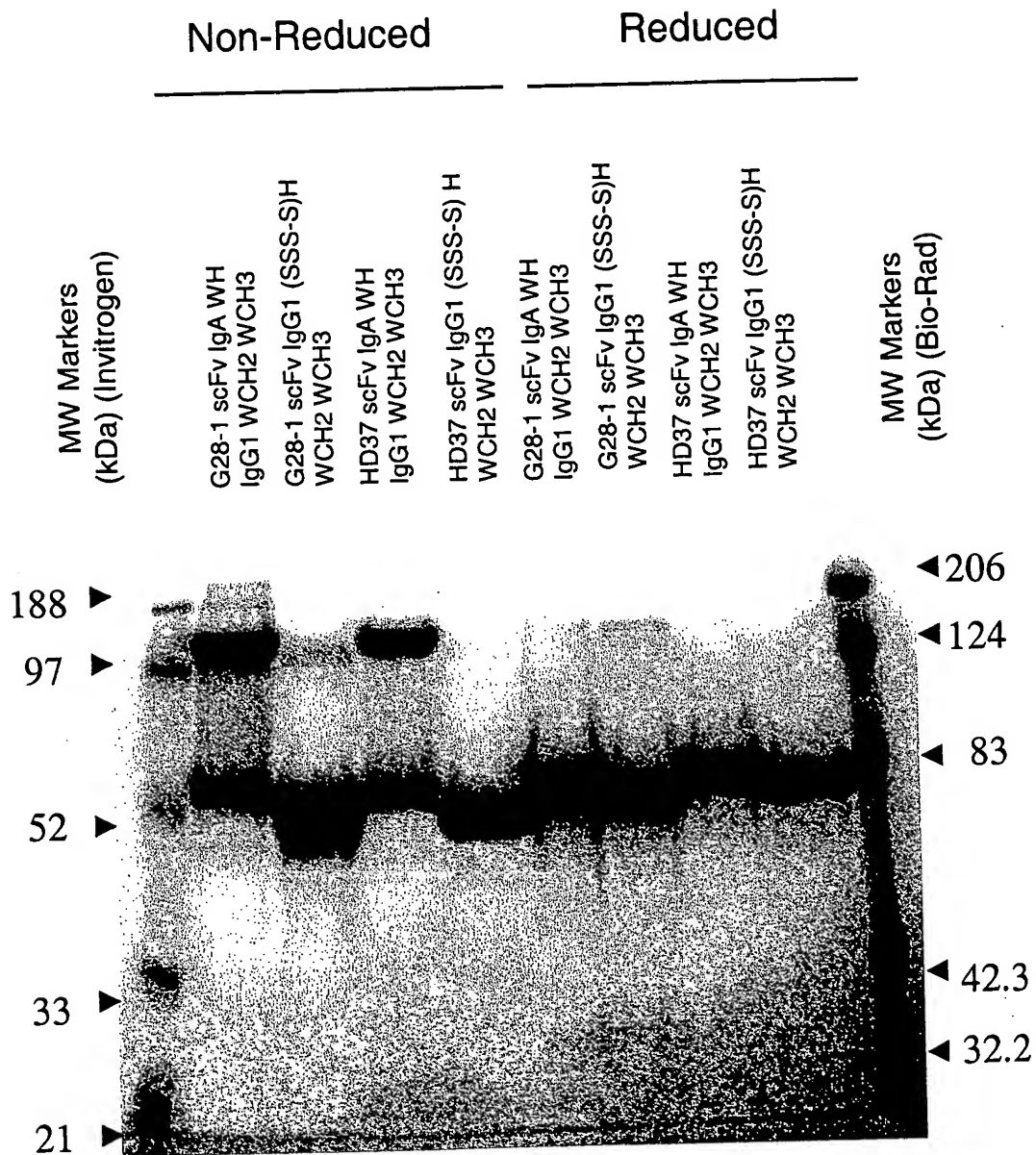


Fig. 23  
Sequence alignment of human and llama Fc regions.

	HINGE	CH2→
Human IgG1:	DQEPKSCDKT-----HTCPPC	PAPELLGGPSVFLFPPKPKDTLMISRTPEVTCVVVDVSHEDPEVKFNWYVDG
Llama IgG2:	DQEPKTPKPPQPPQPNPTTESKCPKC	PAPELLGGPSVFIFFPKPKDVLSISGRPEVTCVVVDVGQEDPEVSFNWYIDG
Llama IgG1:	--EPHGG-----CTCPQC	PAPELPGGPSVFVFPPKPKDVLSISGRPEVTCVVVDVGKEDPEVNFNWYIDG
Llama IgG3:	--AHSEDPT-----SKCPKC	PGPELLGGPTVFIFPPKAKDVLSITRKPEVTCVWWTWVKTLRSSSSWSVDD

VEVHNAKTKPREEQYNSTYRVVSVLTVLHQDWLNGKEYKCKVSNKALPAPIEKTISKAKGQPREPQVYTLPPSRDELTKNQVSLT  
TAEVRANTRPKEEQFNSTYRVVSVLPIQHQQDWLTGKEFKCKVNNKALPAPIEKTISKAKGQTPREPQVYTLAPHREELAKDTVSVT  
VEVRTANTKPKKEEQFNSTYRVVSVLPIQHQQDWLTGKEFKCKVNNKALPAPIERTISKAKGQTPREPQVYTLAPHREELAKDTVSVT  
TEVHTAETKPKKEEQFNSTYRVVSVLPIQHQQDWLTGKEFKCKVNNKALPAPIERTISKAKGQTPREPQVYTLAPHREELAKDTVSVT

CLVKGFYPSDIAVEWESNGQPEN--NYKTPPVLDSDGSFFLYSKLTVDKSRWQQGNVFSQSVMHEALHNHYTQKSLSLSPGK  
CLVKGFYPPDINVEWQRNGQPESXGTYATPPQLDNDGTYFLXSKXSVGKNTWQQGETFTCVVMHEALHNHYTQKSITQSSGK  
CLVKGFYPADINVEWQRNGQPESEGTANTPPQLDNDGTYFLYSRLSVGKNTWQRGETLTGVVMHEALHNHYTQKSITQSSGK  
CLVKGFFPADINVEWQRNGQPESEGTANTPPQLDNDGTYFLYSKLSVGKNTWQQGEVFTCVVMHEALHNHSTQKSITQSSGK

Fig. 24

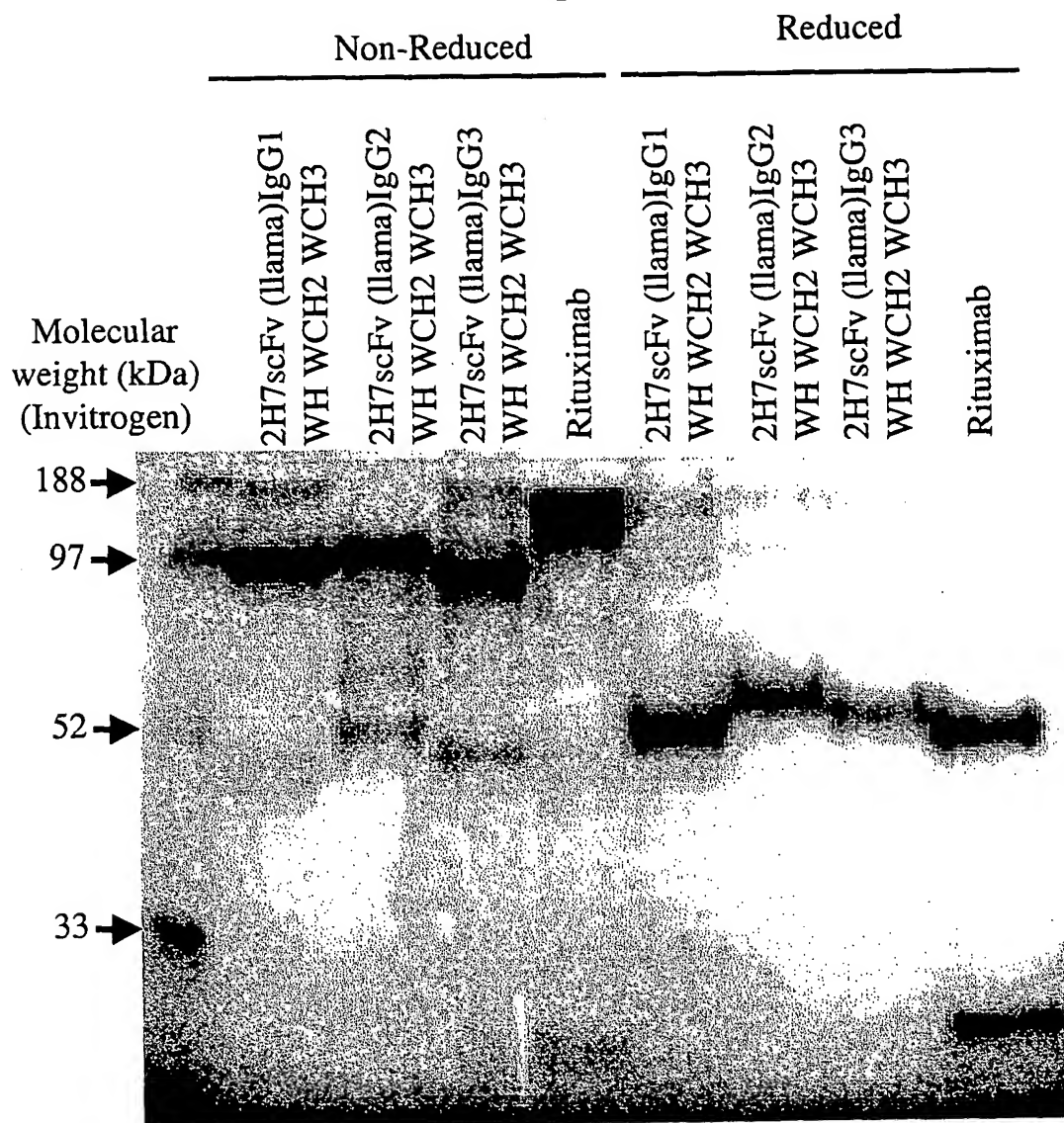


Fig. 25

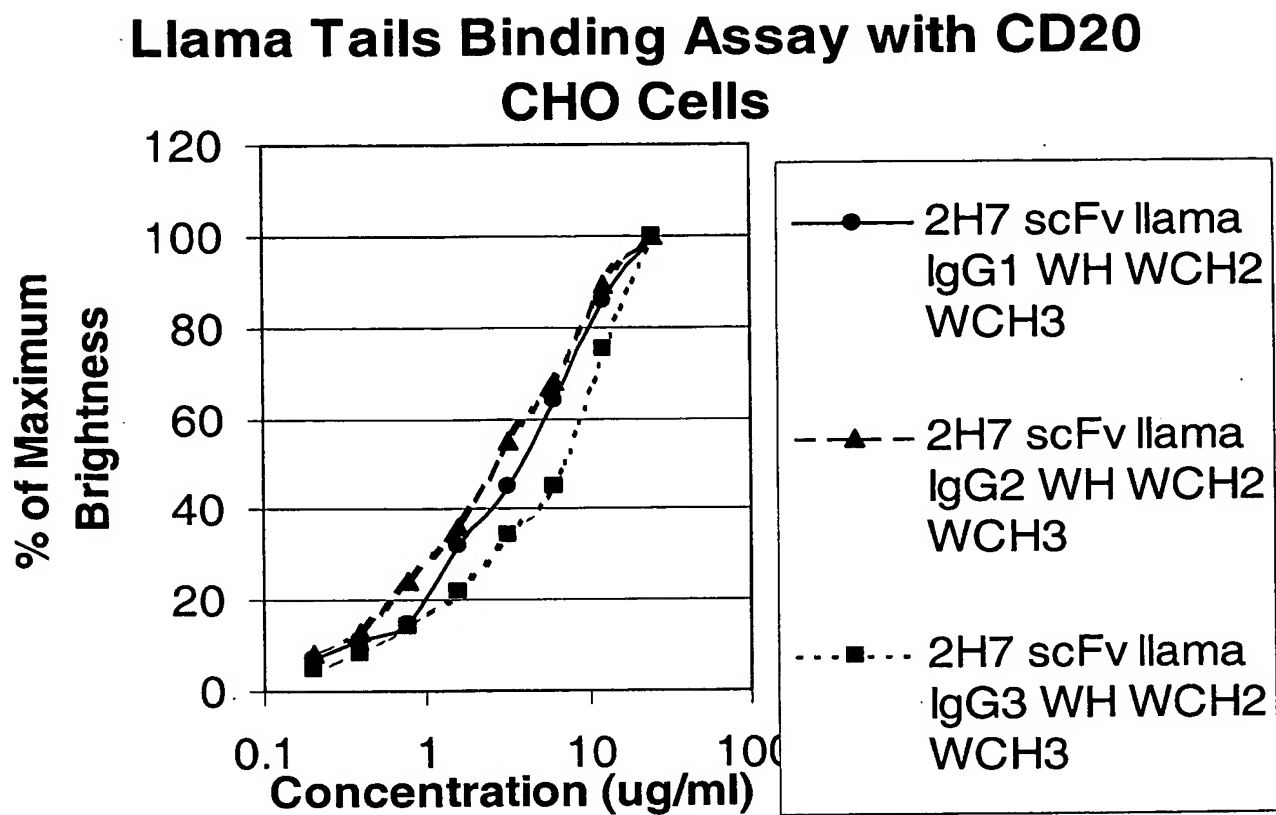
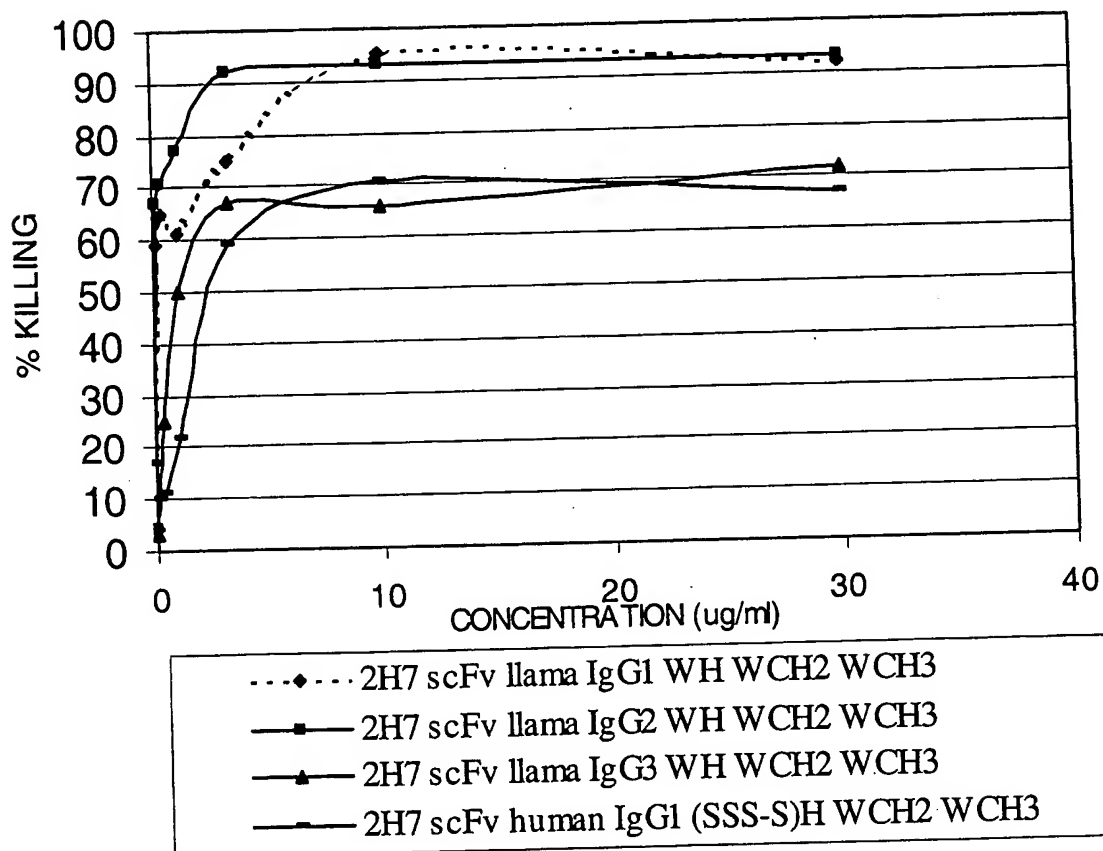


Fig. 26

2H7 scFvIg Llama Tails binding Assay with CD20 CHO Cells



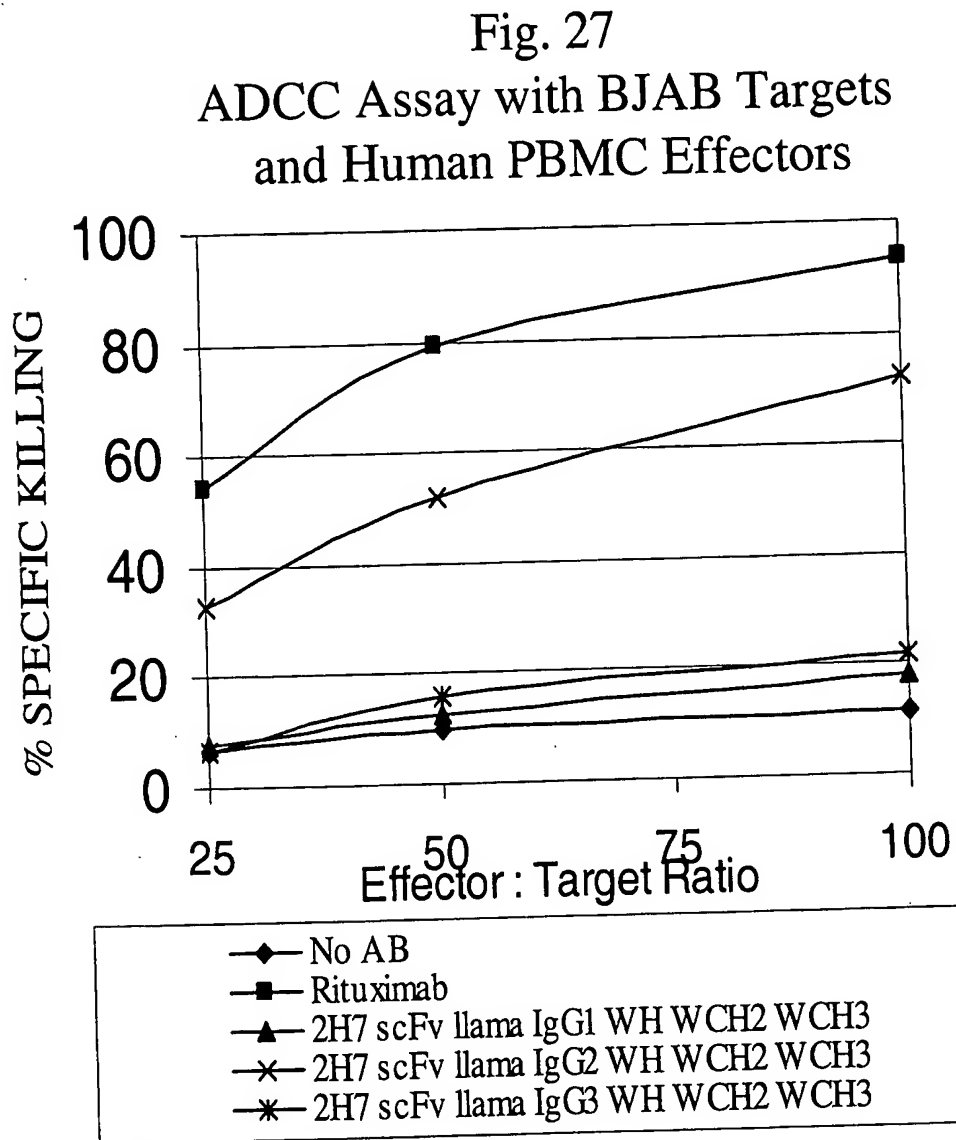


Fig. 28

ADCC Assay with BJAB Cells  
And Llama PBMC Effectors

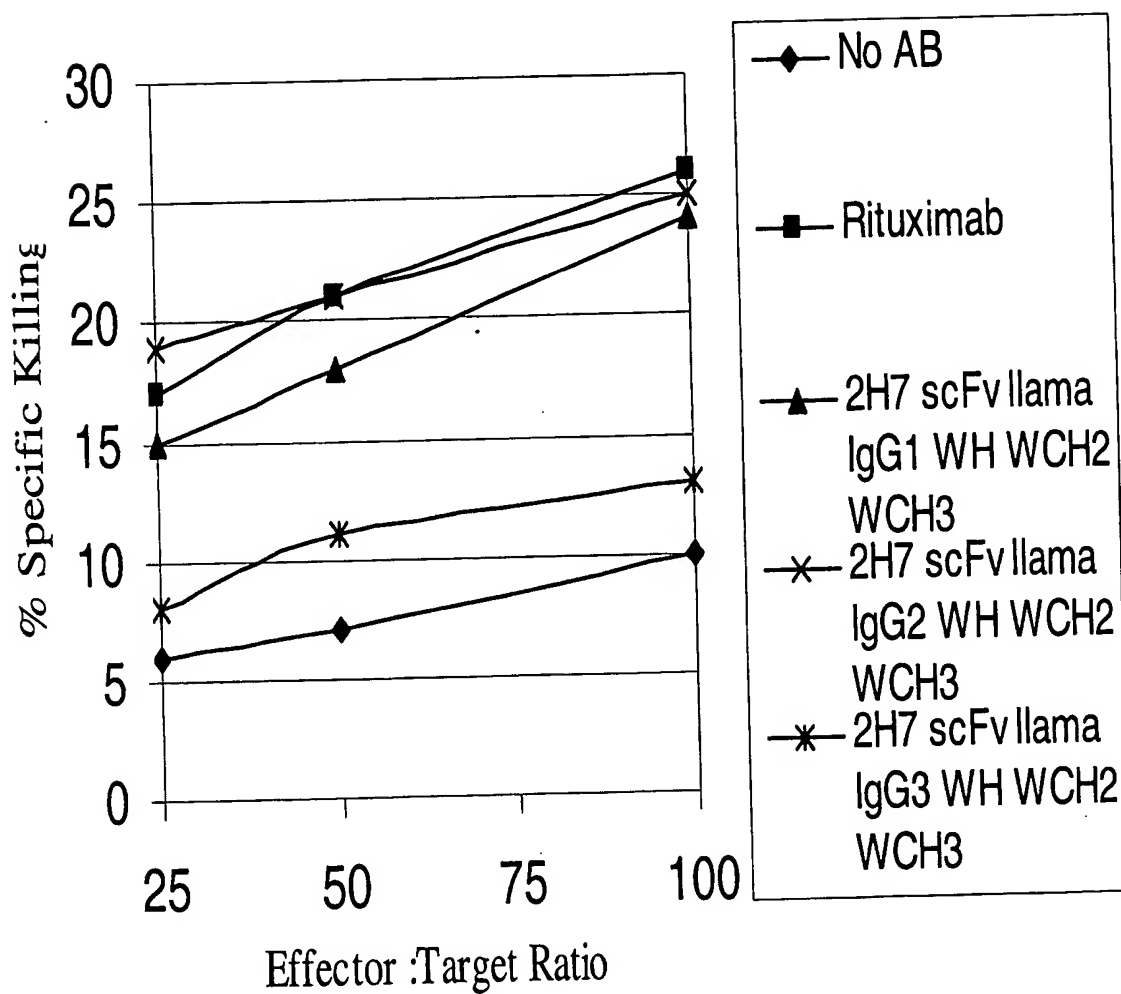


Fig. 29

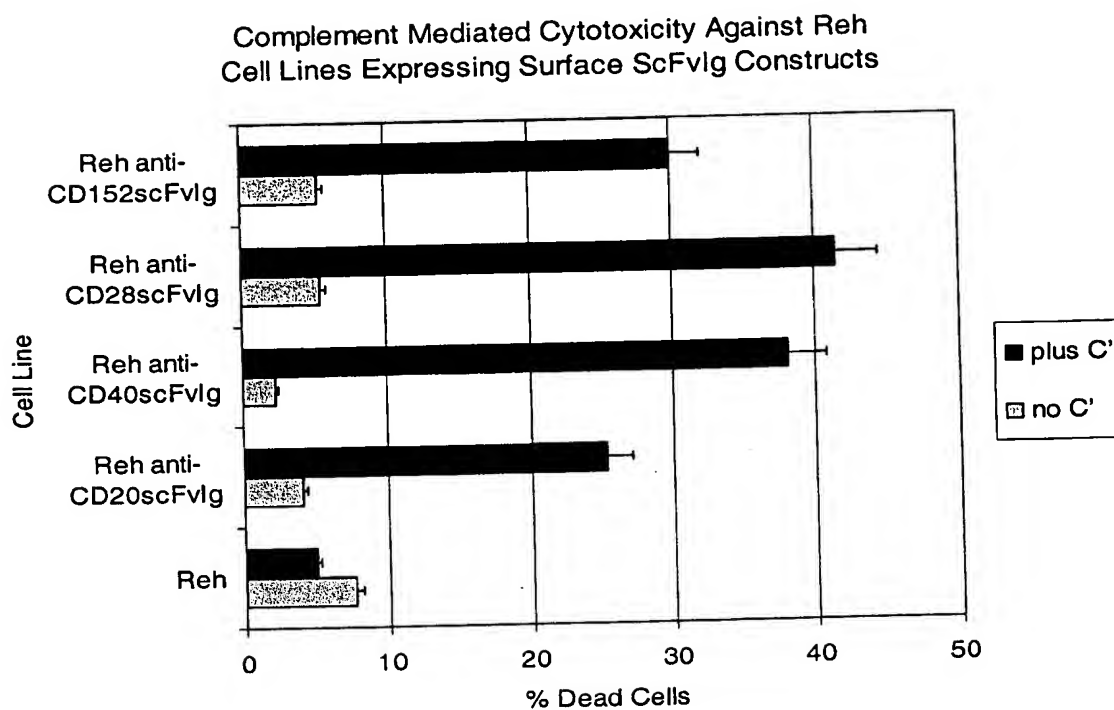
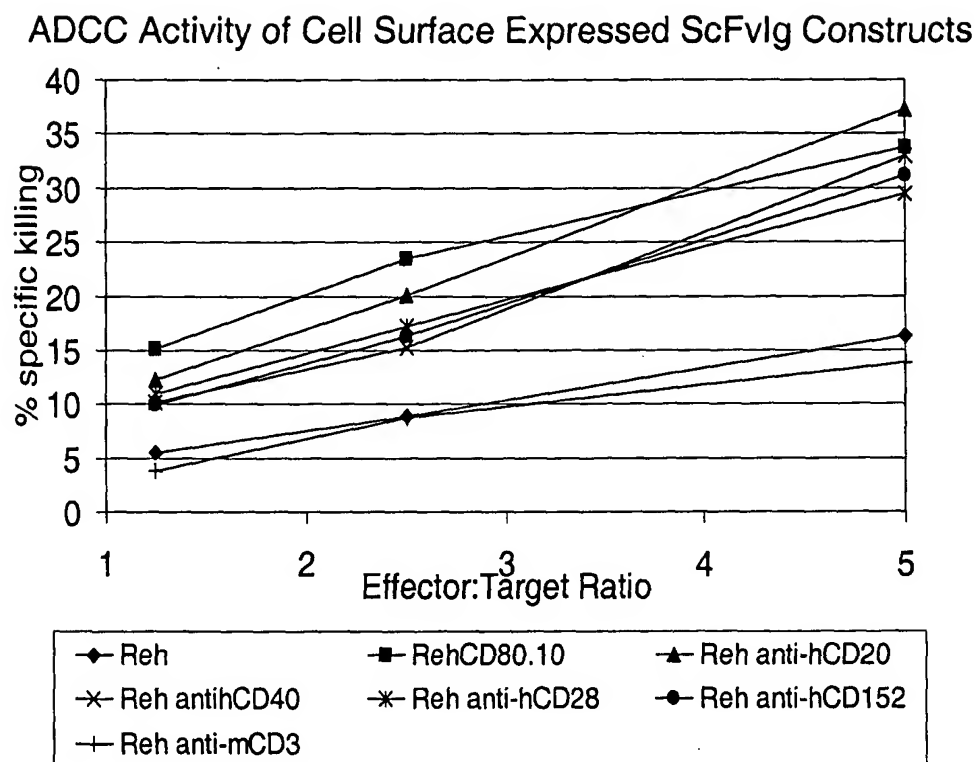


Fig. 30



Surface scFvlg and Effector Functions

**Fig. 31**  
**Ig Constructs and Nomenclature:**

<b>Name Identifier</b>	<b>Hinge Sequence</b>	<b>CH2 Sequence</b>	<b>CH3 Sequence</b>
hIgG1 (CCC-P)H WCH2 WCH3	IgG1 WT Hinge (CCC-P)	Wild Type CH2	Wild Type CH3
hIgG1 (SSS-S)H WCH2 WCH3	IgG1 Mutant Hinge (SSS-S)	Wild type CH2 (IgG1)	Wild type CH3 (IgG1)
VH L11S hIgG1 (SSS-S)H WCH2 WCH3	IgG1 Mutant Hinge (SSS-S)	Wild type CH2 (IgG1)	Wild type CH3 (IgG1)
IgG1 (SSC-S)H WCH2 WCH3	IgG1 Mutant Hinge (SSC-S)	Wild type CH2 (IgG1)	Wild type CH3 (IgG1)
IgG1 (SCS-S)H WCH2 WCH3	IgG1 Mutant Hinge (SCS-S)	Wild type CH2 (IgG1)	Wild type CH3 (IgG1)
IgG1 (CSS-S)H WCH2 WCH3	IgG1 Mutant Hinge (CSS-S)	Wild type CH2 (IgG1)	Wild type CH3 (IgG1)
IgG1 (SSS-S)H P238S CH2 WCH3	IgG1 Mutant Hinge (SSS-S)	Mutant CH2 (IgG1) Pro→Ser 238	Wild type CH3 (IgG1)
IgA WH hIgG1 WCH2 WCH3	IgA Hinge	Wild type CH2 (IgG1)	Wild type CH3 (IgG1)
IgA WH IgA WCH2 WCH3	IgA Hinge	Wild type CH2 (IgA)	Wild type CH3 (IgA)
IgA WH IgA WCH2 T4CH3	IgA Hinge	Wild type CH2 (IgA)	Truncated CH3 (IgA) Missing 4 aa at COOH

Fig. 32

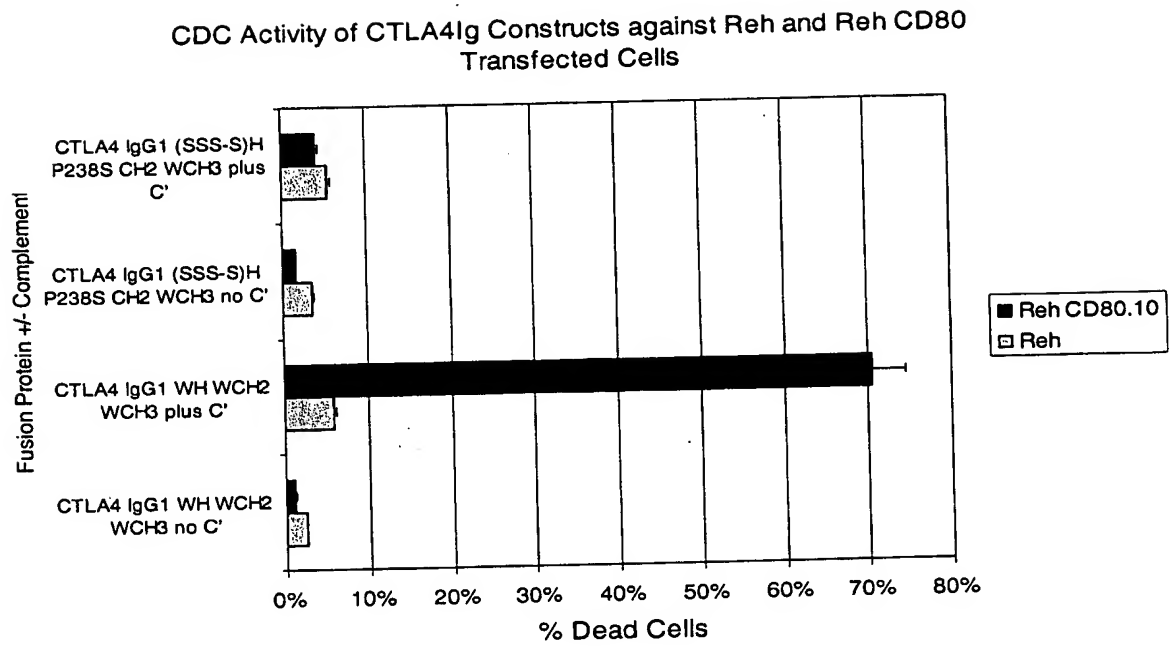


Fig. 33

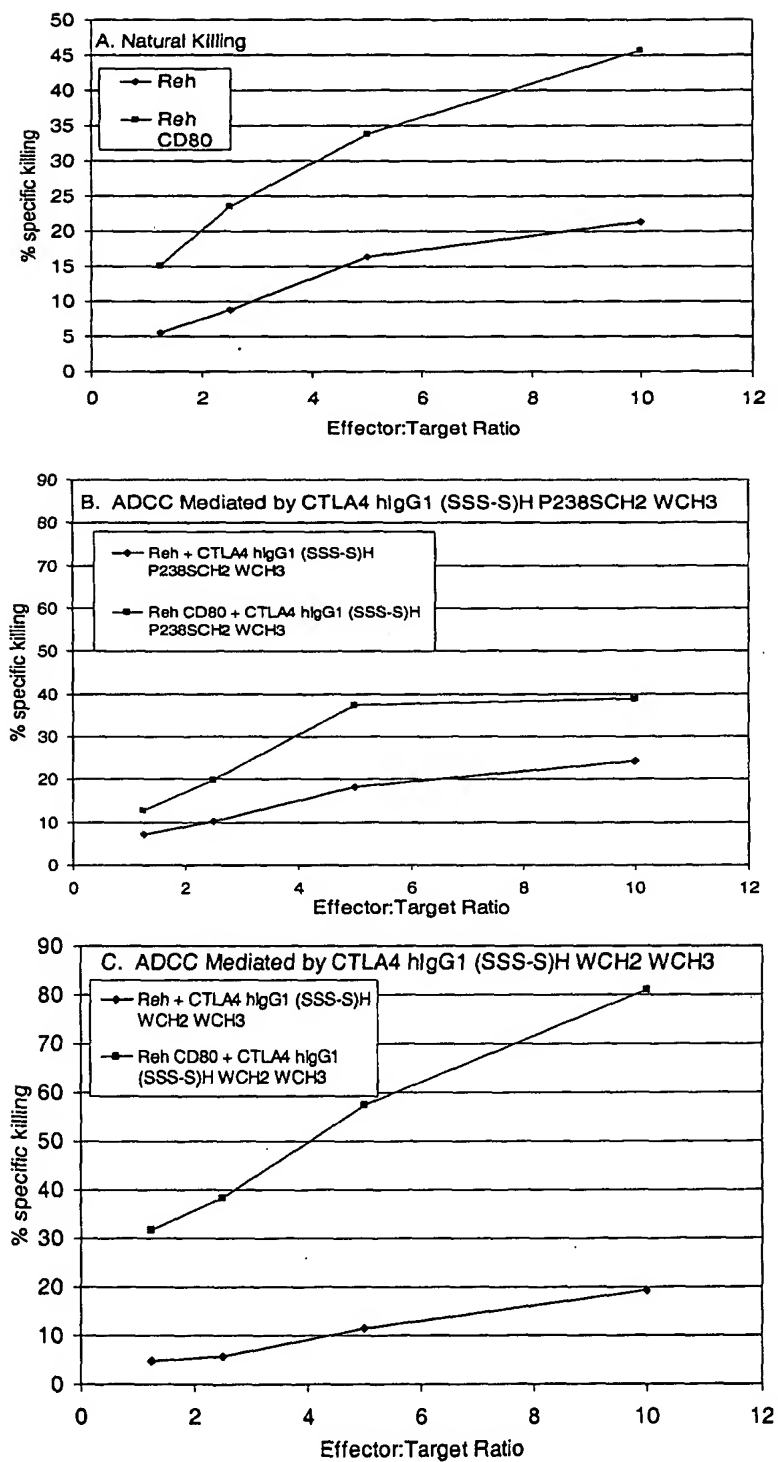
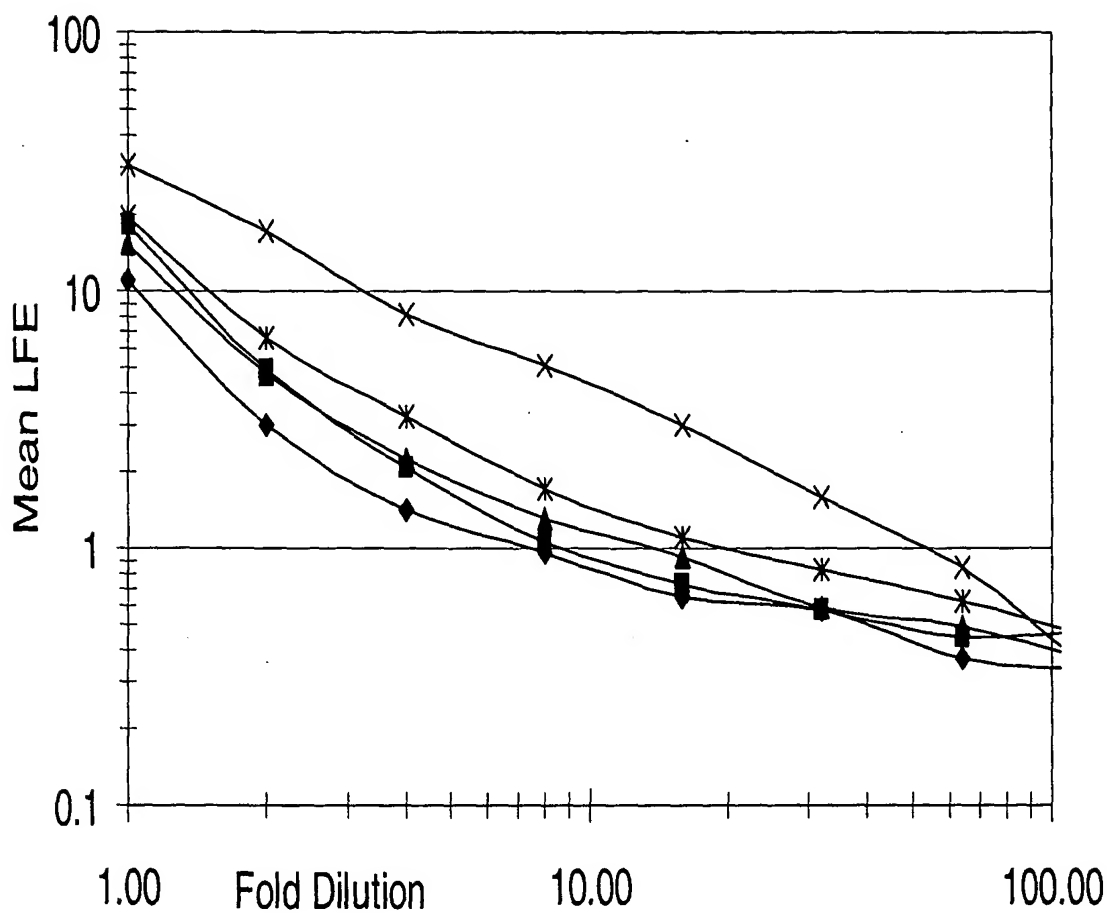


Fig. 34

Binding of 2H7 scFvIg Constructs  
with Alternative Tails to CD20 CHO Cells



- |  |                                     |
|--|-------------------------------------|
| ◆ 2H7 scFv hIgG1 (CCC-P)H WCH2 WCH3        | ■ 2H7 scFv hIgG1 (CSS-S)H WCH2 WCH3 |
| ▲ 2H7 scFv hIgG1 (SCS-S)H WCH2 WCH3        | ✕ 2H7 scFv hIgG1 (SSC-S)H WCH2 WCH3 |
| ✱ 2H7 scFv VH L11S hIgG1(CCC-P)H WCH2 WCH3 |                                     |

Fig. 35  
Immunoblot Analysis of protein immunoprecipitates  
from COS transfections of 2H7 scFvIg Constructs

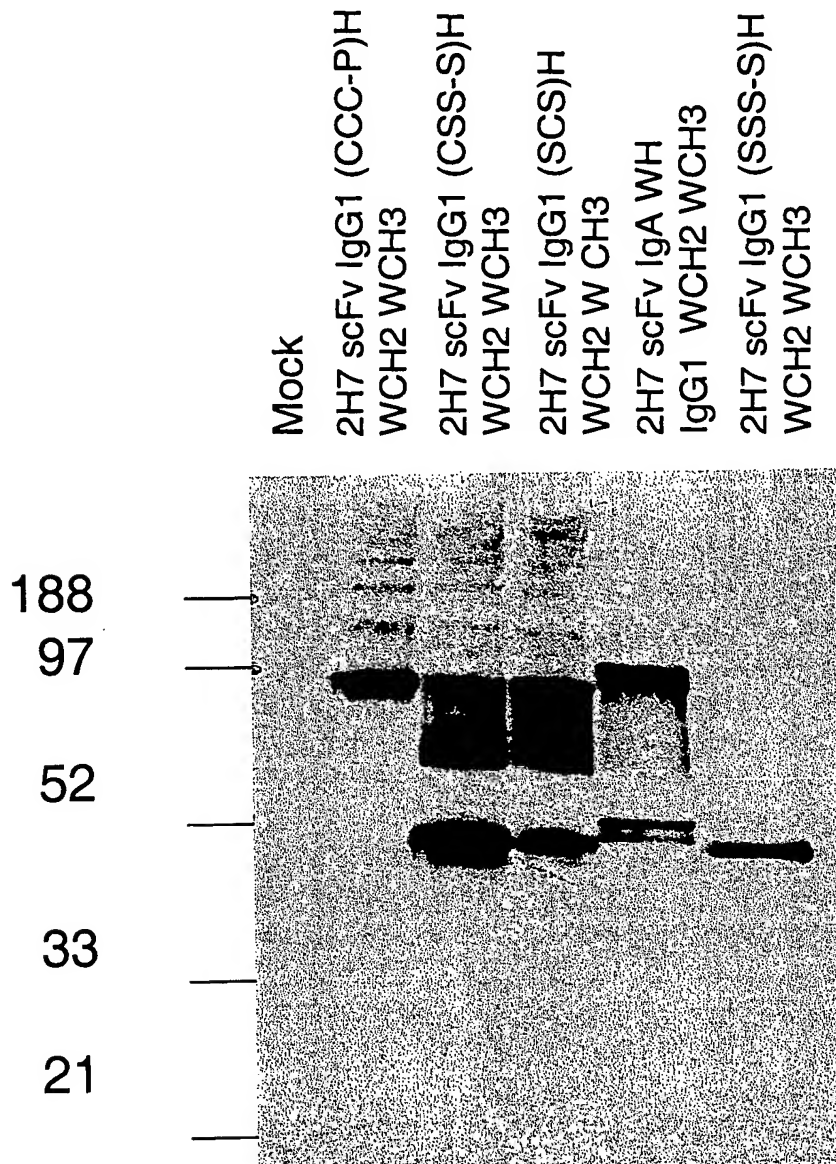


Fig. 36

Binding to CD20 CHO cells by constructs  
that link anti-CD20 scFv to IgA Fc Domains

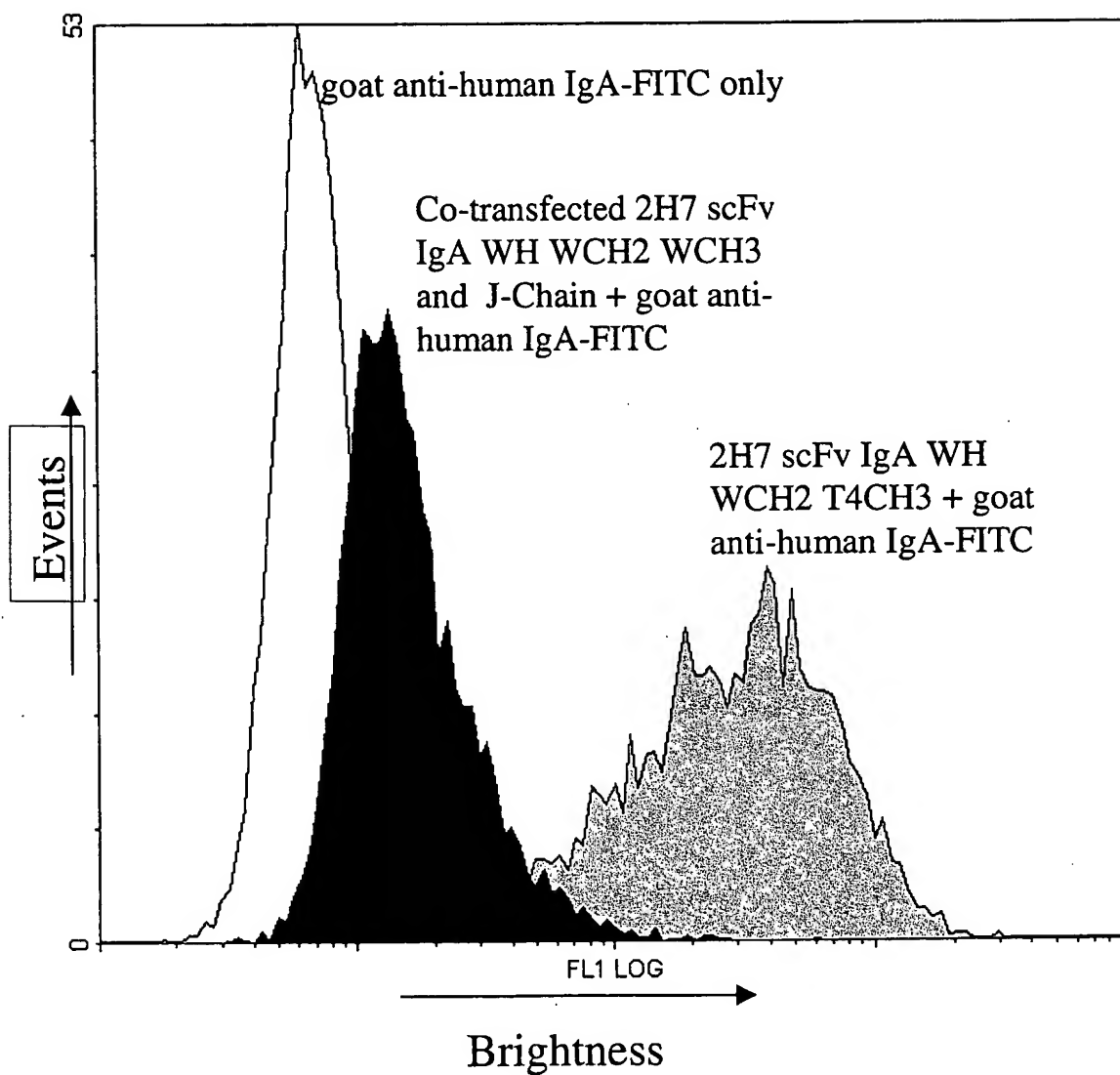


Fig. 37

Titration of CD20 specific scFvIg Constructs  
for ADCC Activity Using Whole Blood Effectors

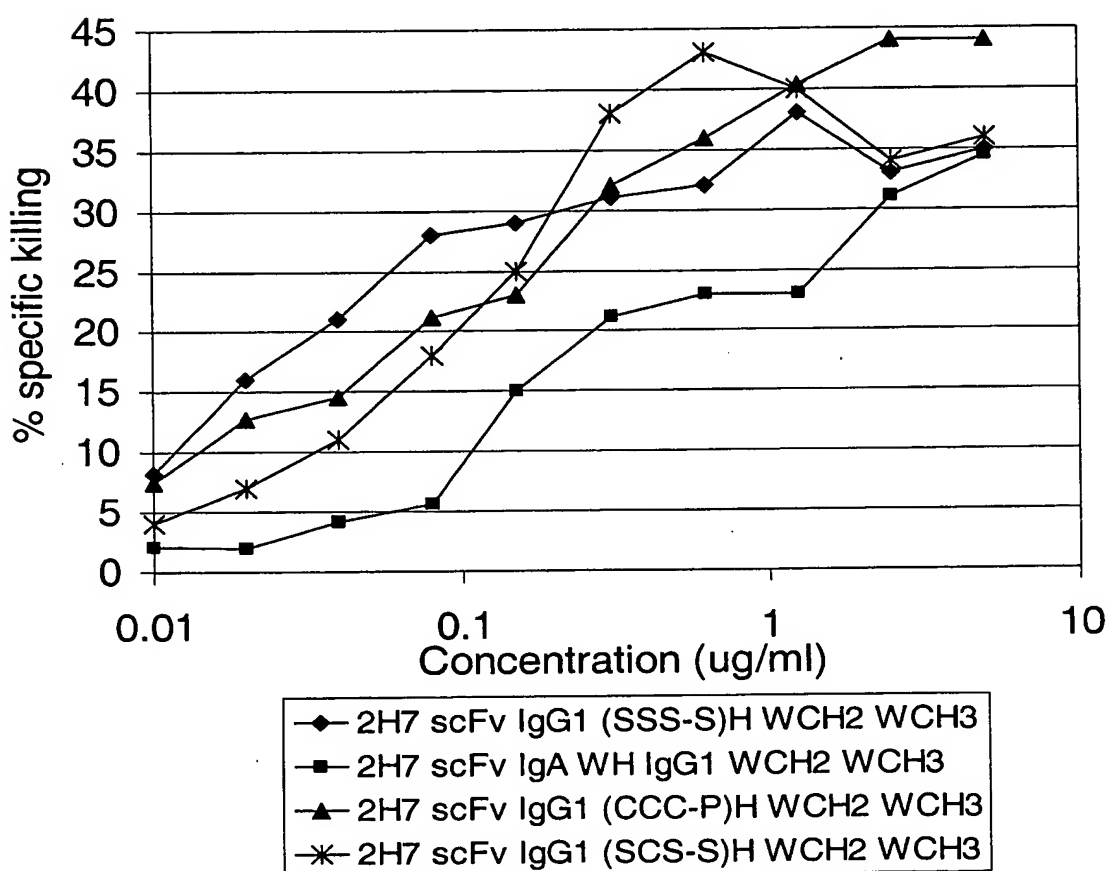


Fig. 38

ADCC Assay of anti-CD20 constructs with alternative tails  
(Whole Blood Effectors / BJAB Targets)

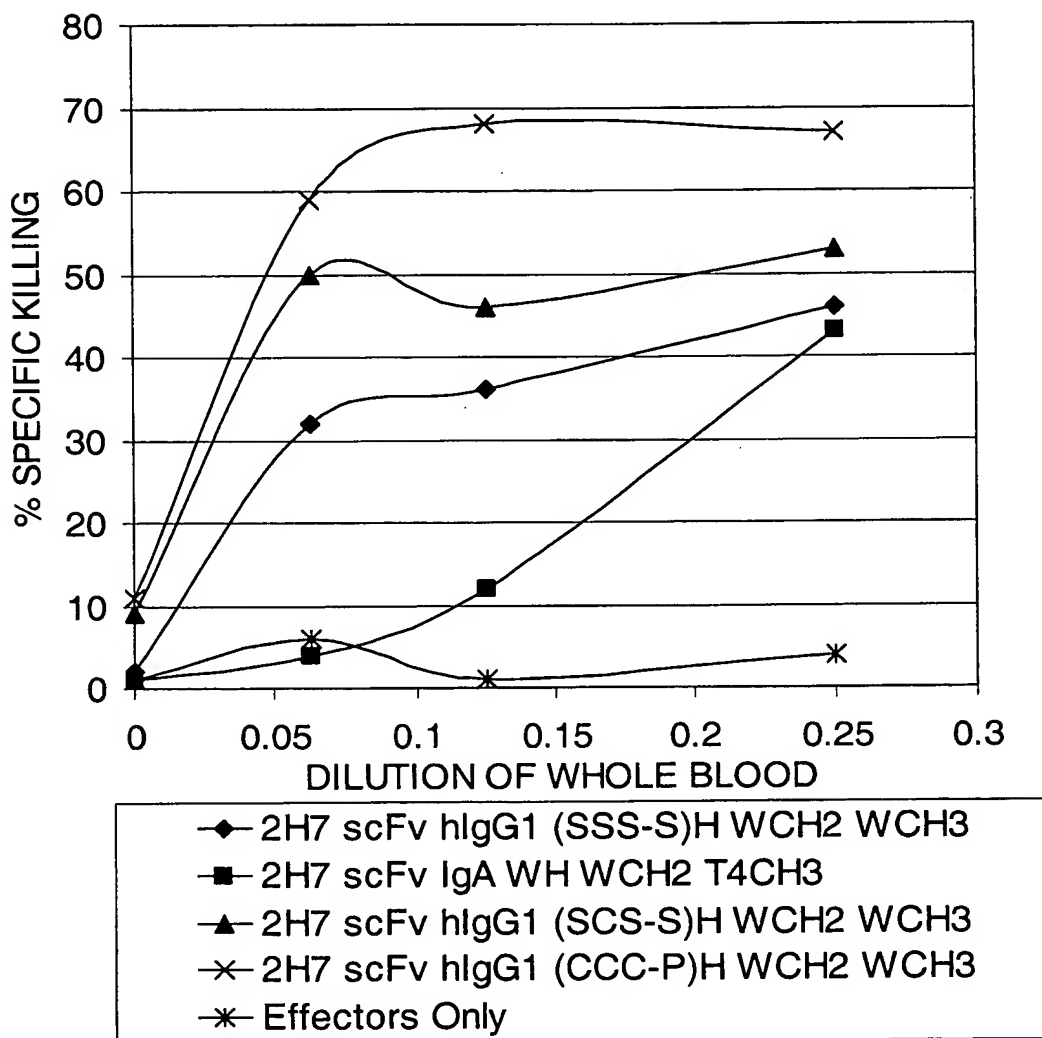


Fig. 39

ADCC Assay of Anti-CD20 scFvIg Constructs  
Using Different Effector Populations Against BJAB Targets

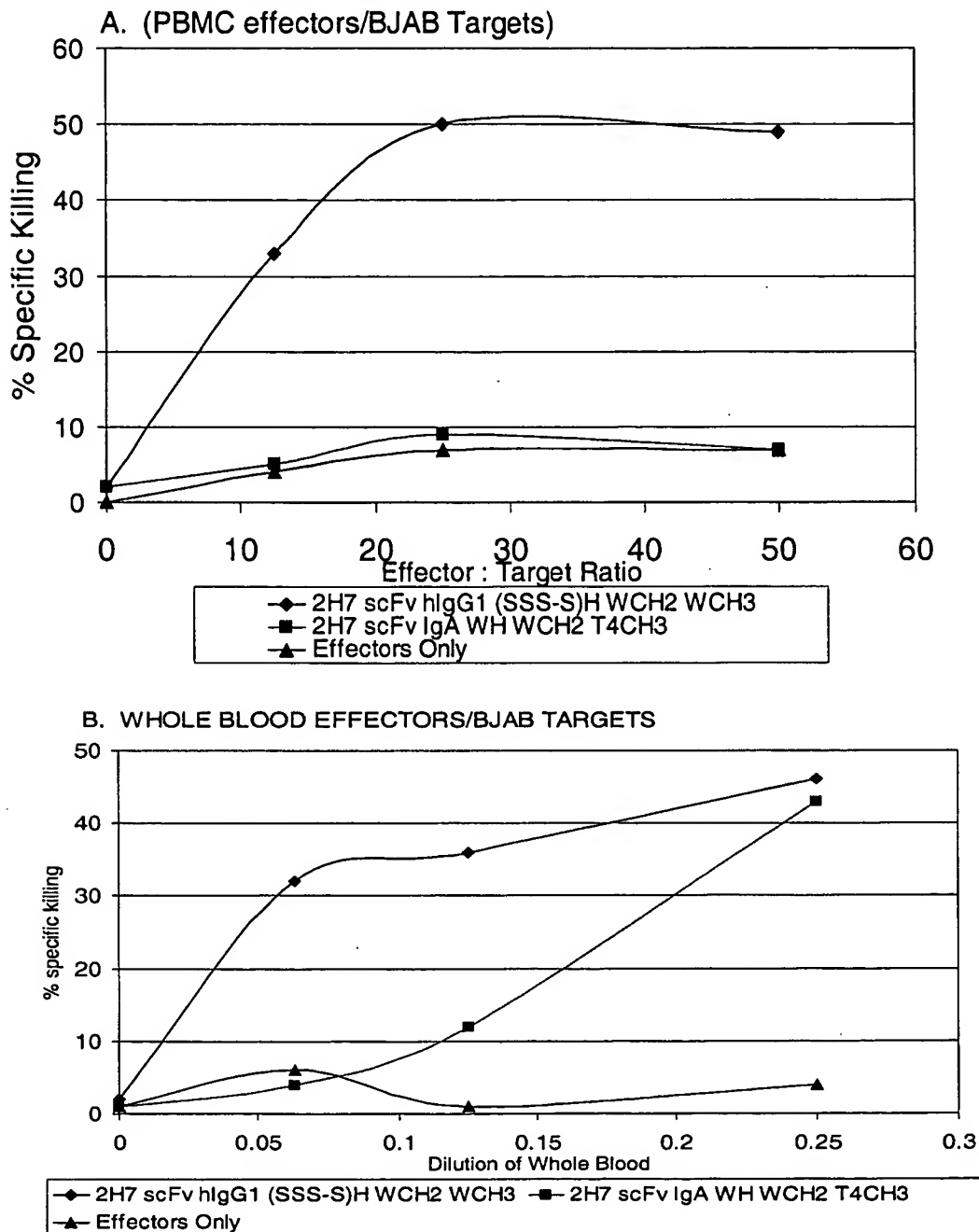
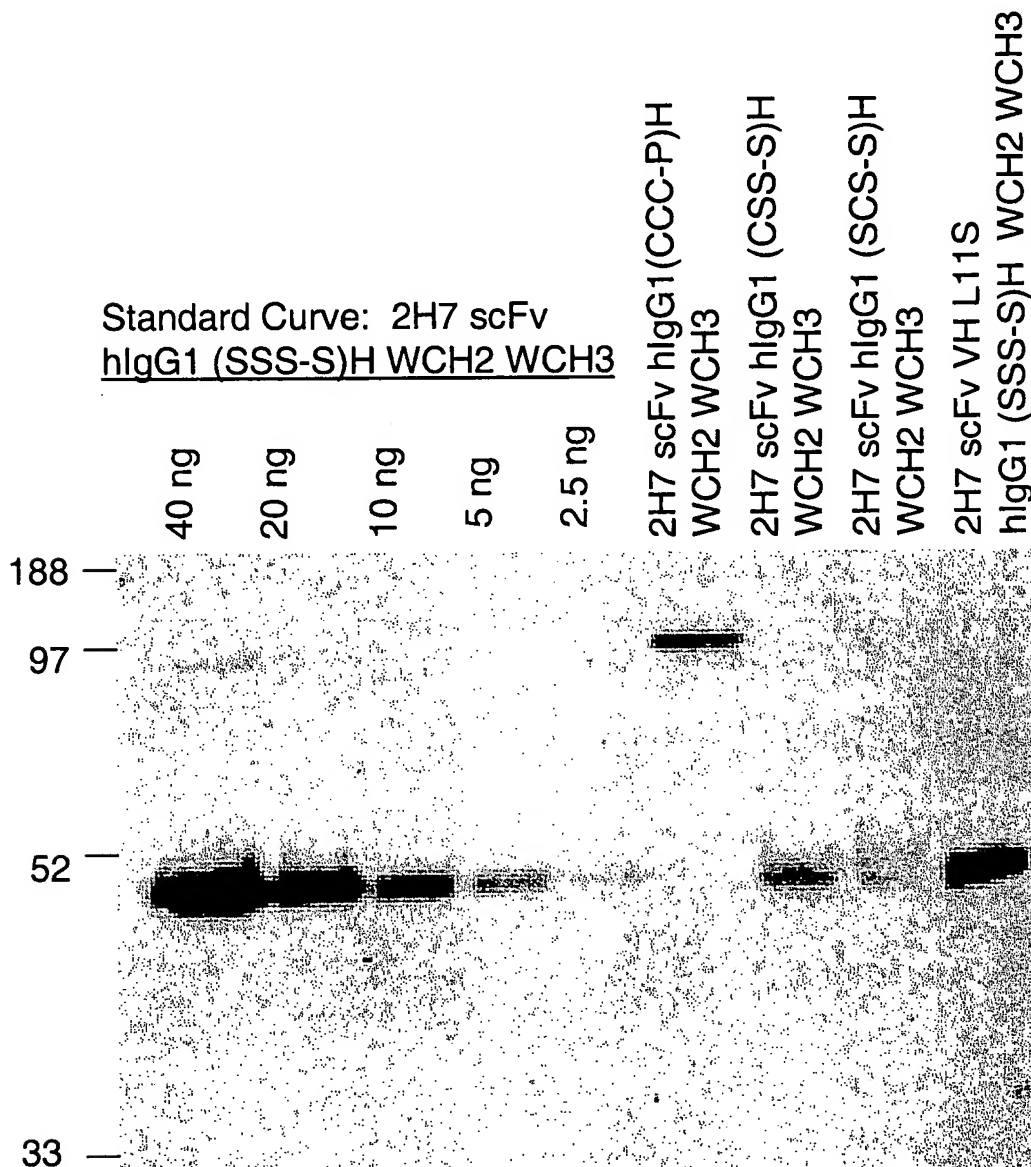


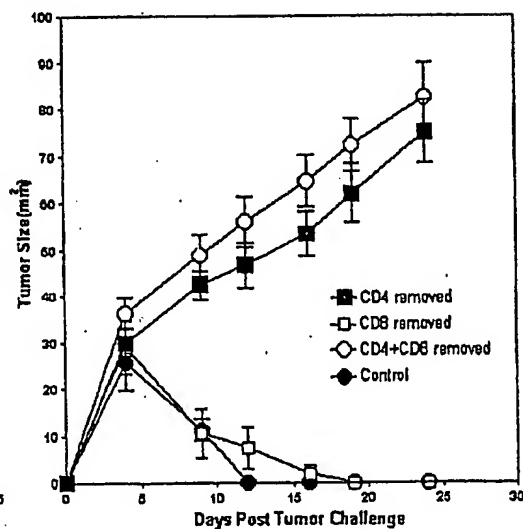
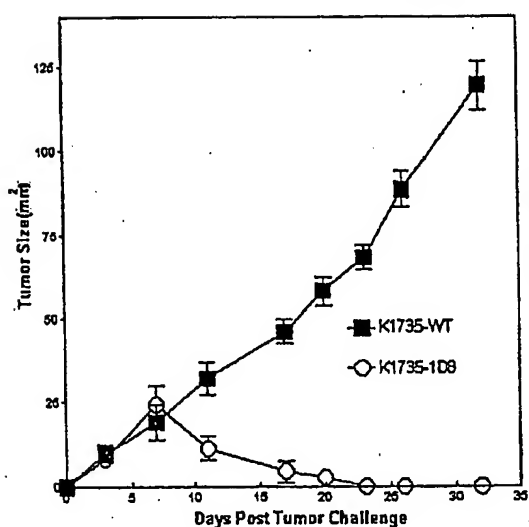
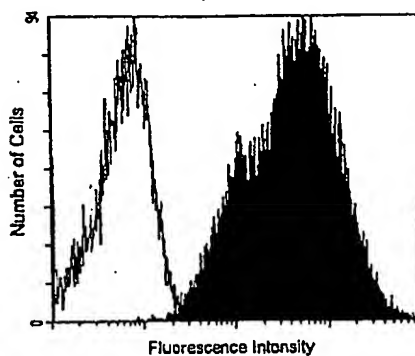
Fig. 40

Immunoblot of 2H7 scFv Ig constructs from COS  
Transfections (1 µl/well) compared to a Concentration Standard



Figures 41A, 41B and 41C

A.



Sheet 45 of 53

B.

C.

Fig. 42

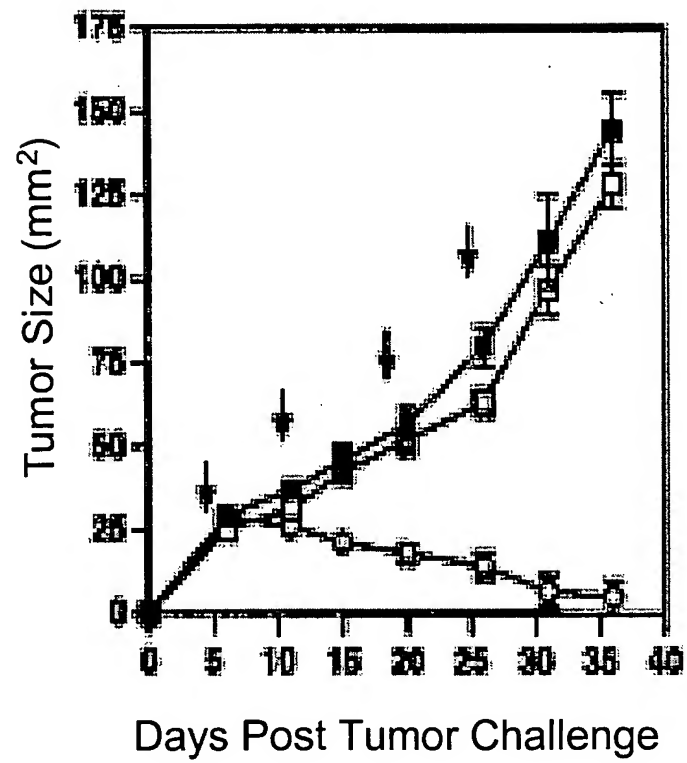


Fig. 43

Mixtures of K1735-WT and K1735-1D8 transfected tumor lines  
inhibit tumor outgrowth in C3H mice

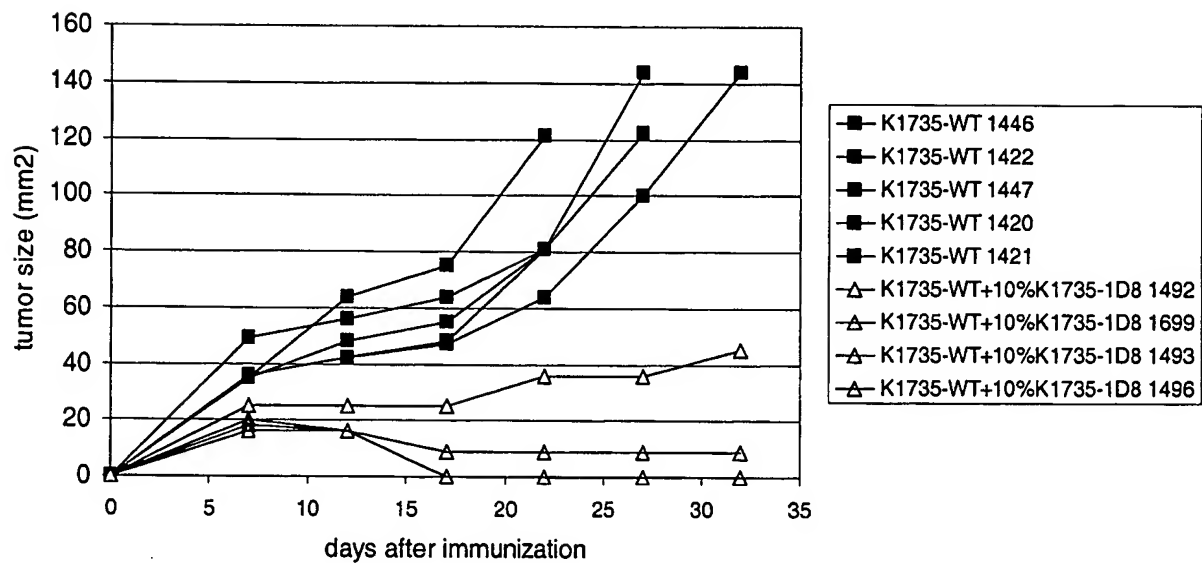


Fig. 44

Expression of anti-mouse CD137 (1D8) scFv-hIgG1 (SSS-S)H P238SCH2 WCH3  
On the surface of panned Ag104-1D8 Transfected Tumor Cells

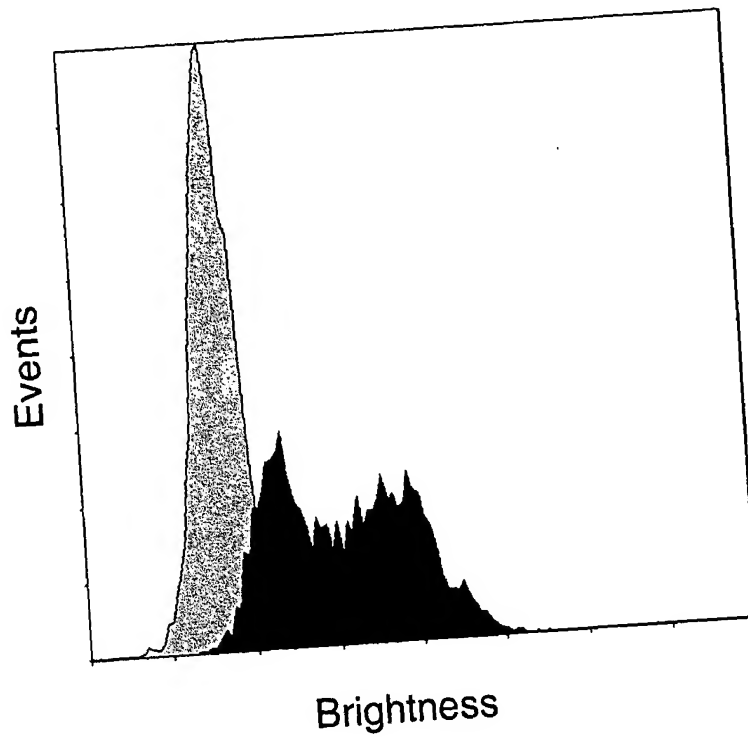


Fig. 45  
Coomassie Stained SDS-PAGE Gel of 2H7 scFv Ig  
Constructs

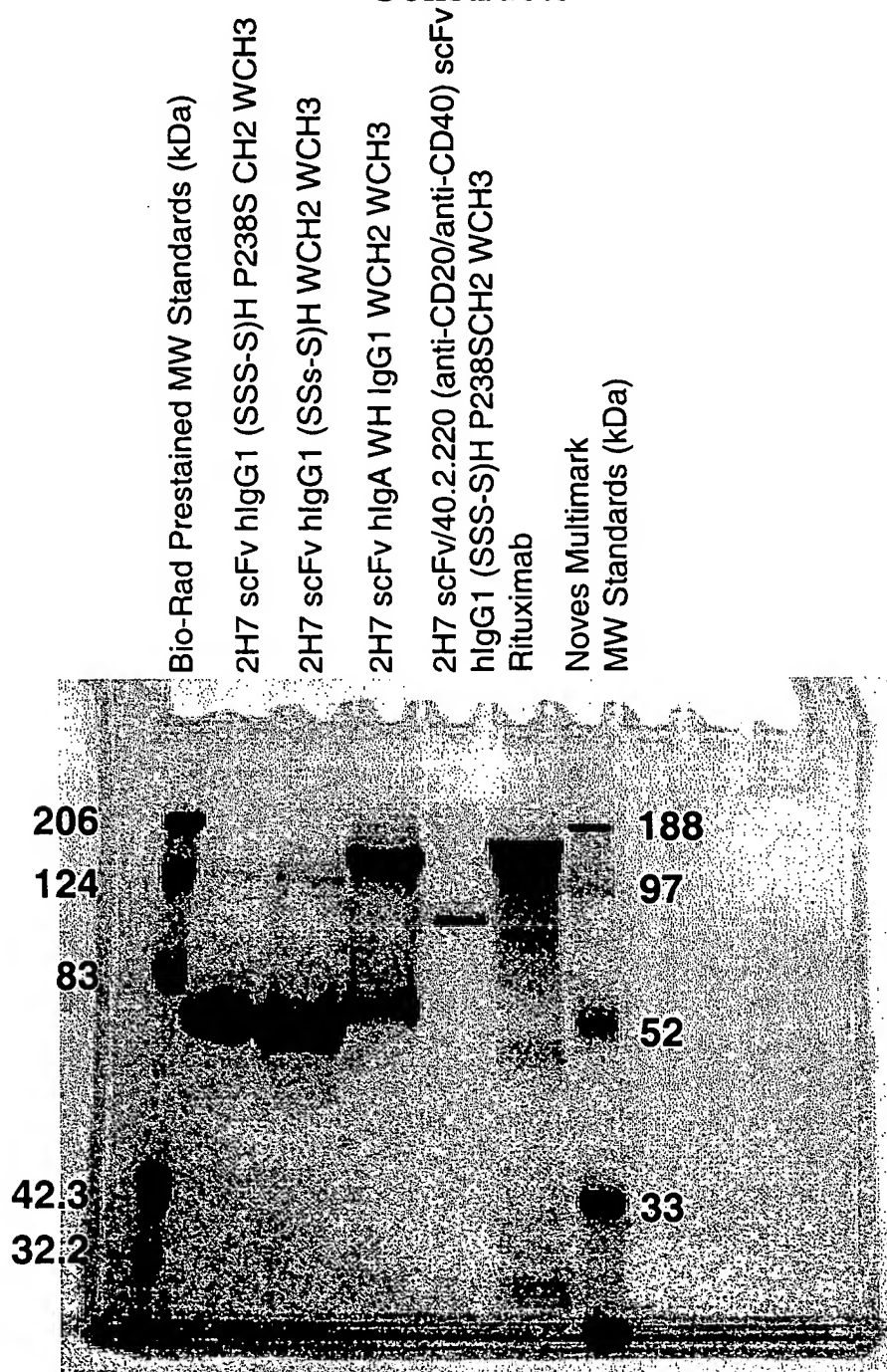
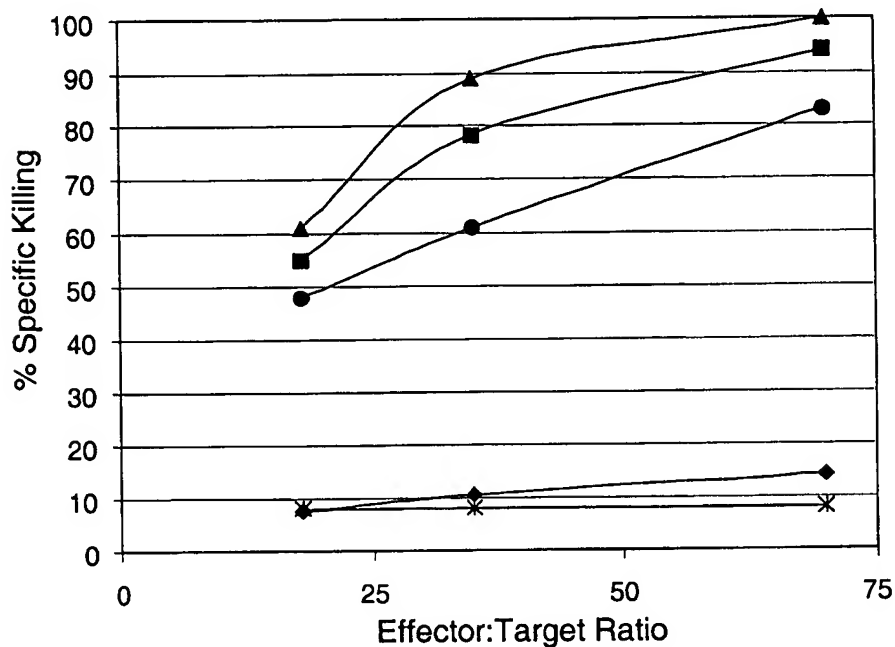


Fig. 46  
ADCC mediated by 2H7 scFvIg Constructs by human  
PBMC effector cells against Bjab targets

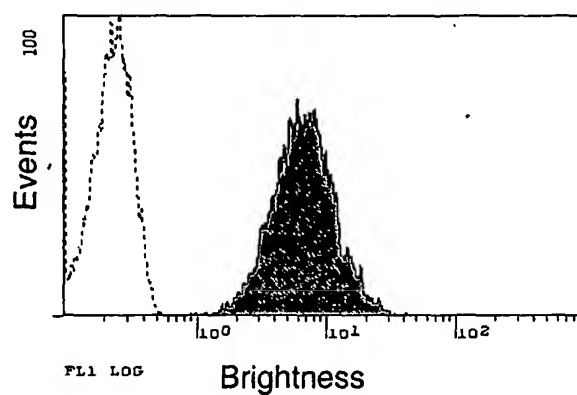


- |  |                        |
|--|------------------------|
| ◆ 2H7 scFv hlgG1(SSS-S)H P238SCH2 WCH3 | ● RITUXIMAB            |
| ▲ 2H7 scFv hlgA WH IgG1 WCH2 WCH3      | * CELLS ALONE (W/O AB) |
| ■ 2H7 scFv hlgG1 (SSS-S)H WCH2 WCH3    |                        |

Fig. 47

Cell surface expression of anti-human CD3 G19-4  
scFv hIgG1 (SSS-S)H P238SCH2 WCH3-  
hCD80TM/CT on Reh and T51 Cells.

Reh anti-CD3 (G19-4) scFv hlgG1 (SSS-S)H  
P238SCH2 WCH3-hCD80TM/CT



T51 G19-4 scFv hlgG1 (SSS-S)H  
P238SCH2 WCH3-hCD80TM/CT:

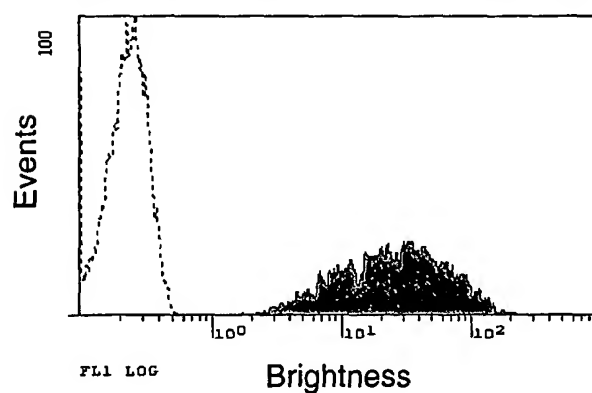
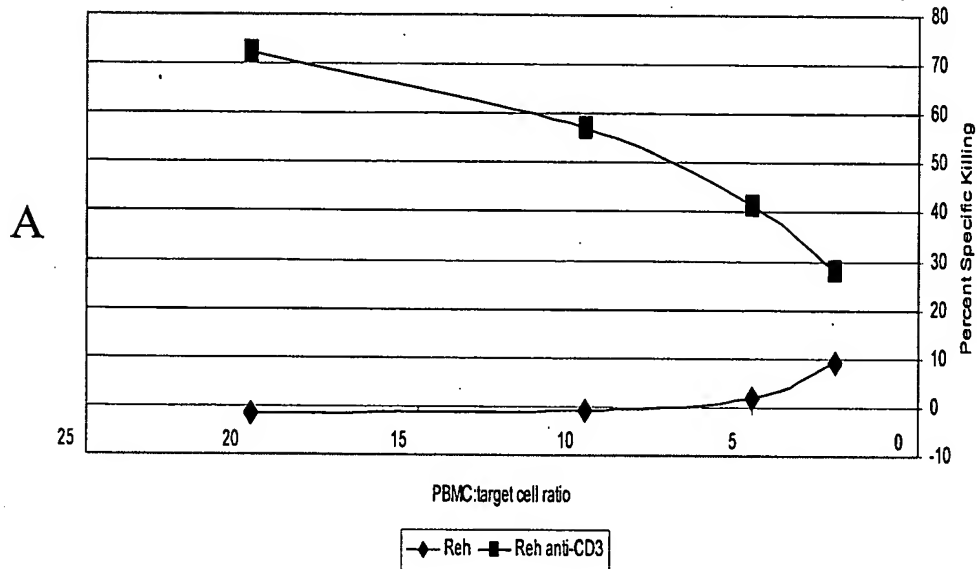


Figure 48.  
Targeting of Cytotoxicity to Transfected Cell Lines  
by Surface expression of CD3 scFvIg  
Cytotoxic activity of resting PBMC towards transfected Reh cells



Cytotoxic activity of resting PBMC towards transfected T51 lymphoblastoid cells

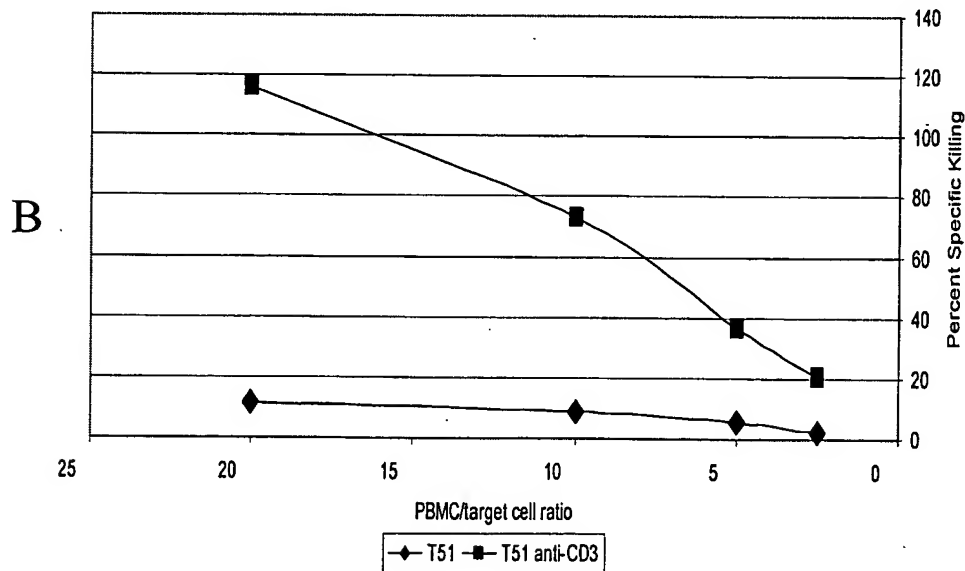


Fig. 49  
Binding of 5B9, a mouse anti-human CD137 scFv hIgG1  
(SSS-S)H WCH2WCH3 to stimulated human PBMC

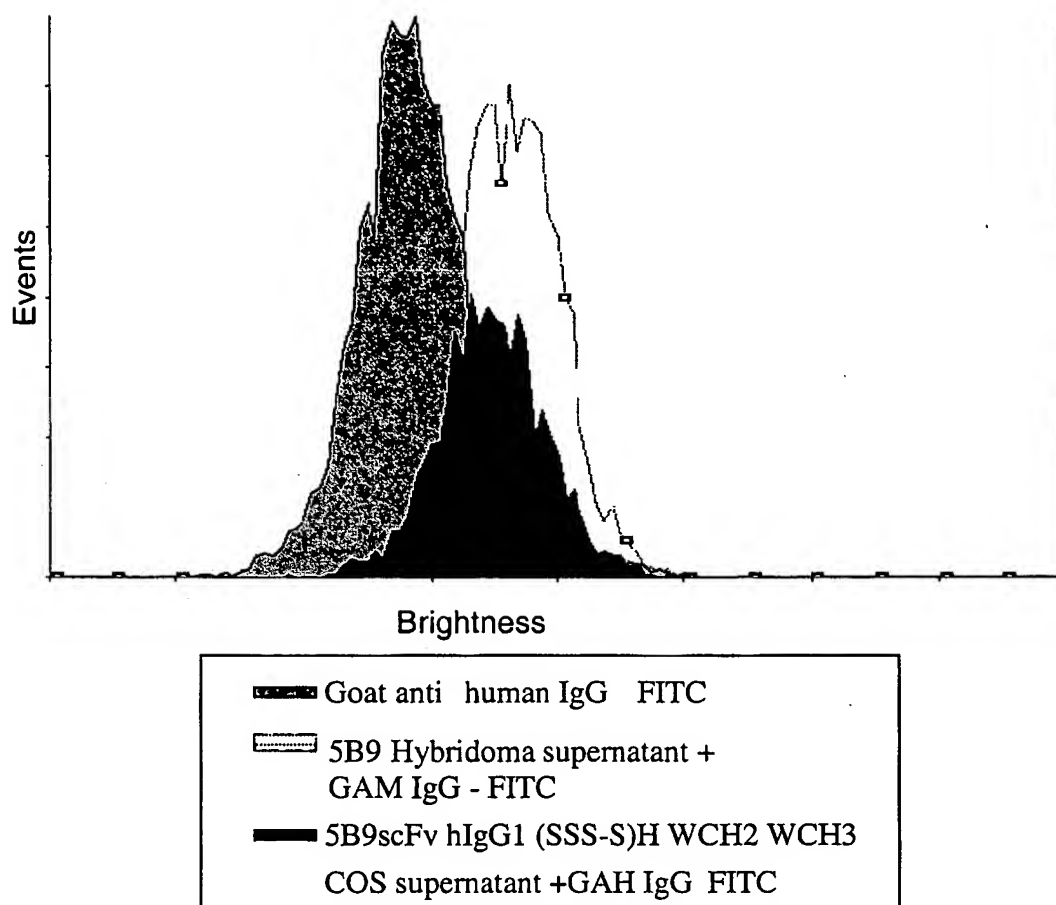
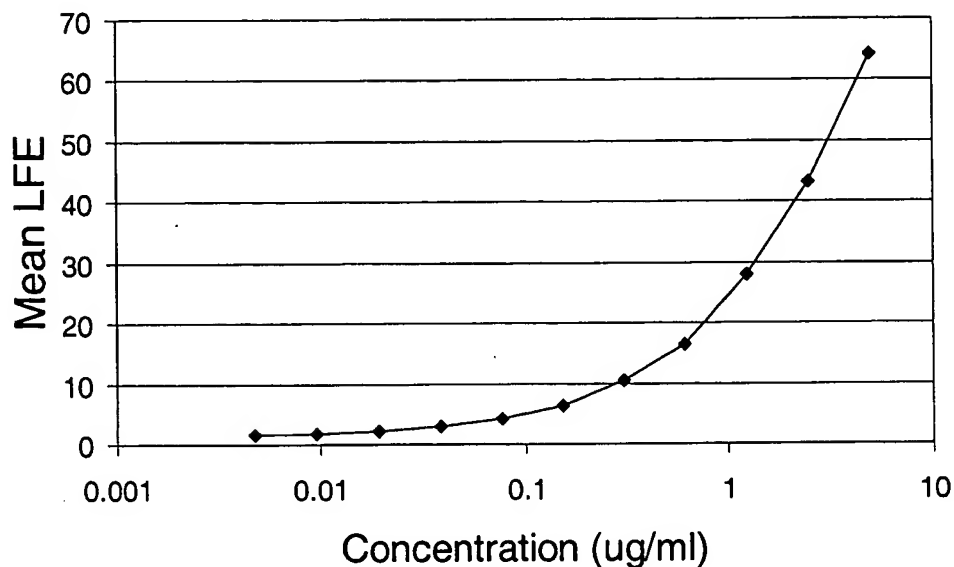


Fig. 50  
Effect of V<sub>H</sub>L11S Mutation on Cytox B20  
2H7 scFv hIgG1 (SSS-S)H WCH2 WCH3 Protein Expression

50A. Standard Curve: 2H7VH-L11S-IgG1 (SSS-S)H WCH2 WCH3



50B. CHO supernatant Brightness and Estimation of Protein concentrations from Standard Curve:

	CHO clone name				
	4F2	4F5	3E5	6B11A	2B8A
Mean LFE					
1/100	71.7	40.6	31.5	99.7	101.5
1/500	27.1	12.4	11.2	40.8	43
approx conc. μg/ml	600	225	125	1000	1250

Fig. 51  
Production Levels of 2H7scFv VH L11S hIgG1  
(SSS-S)H WCH2 WCH3  
From CHO Clone Culture Supernatants

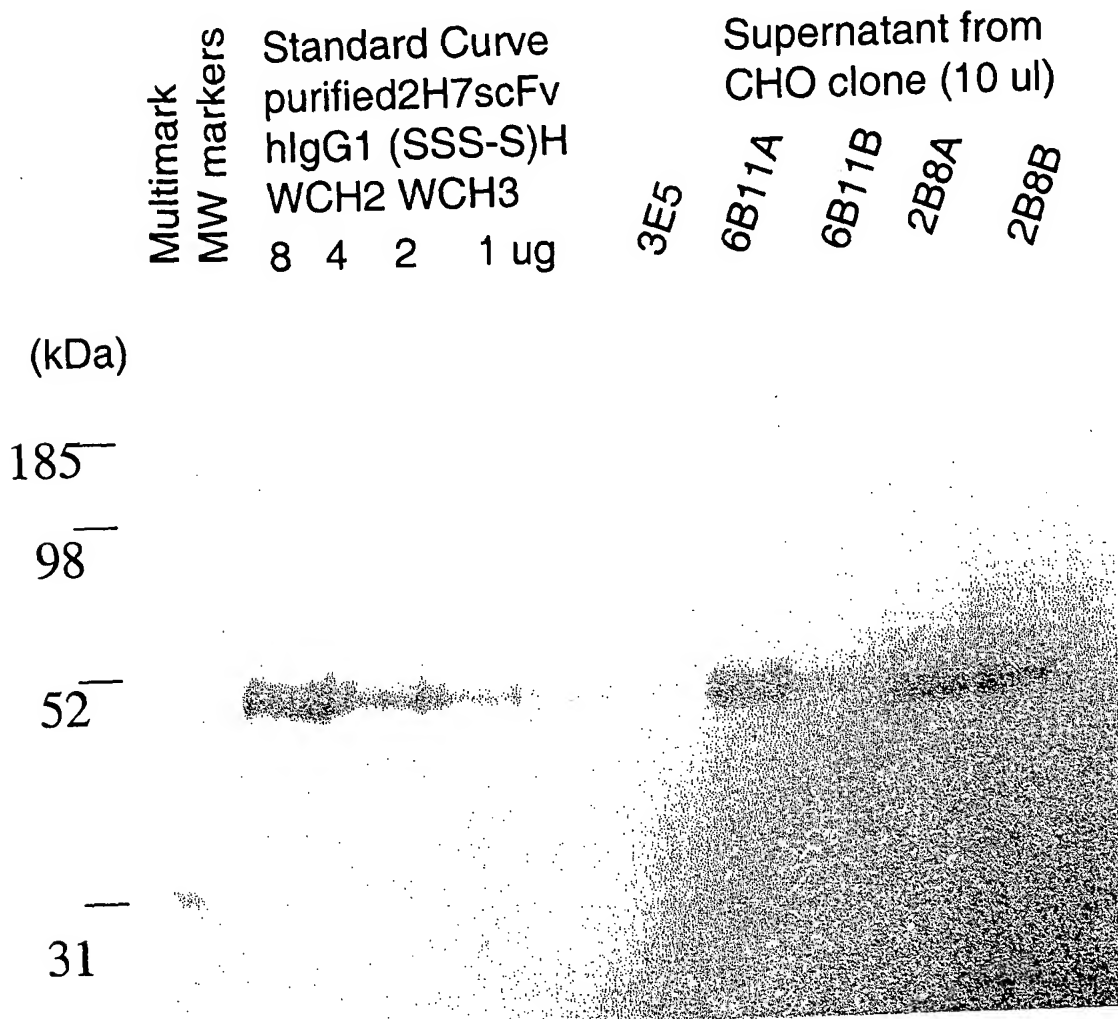
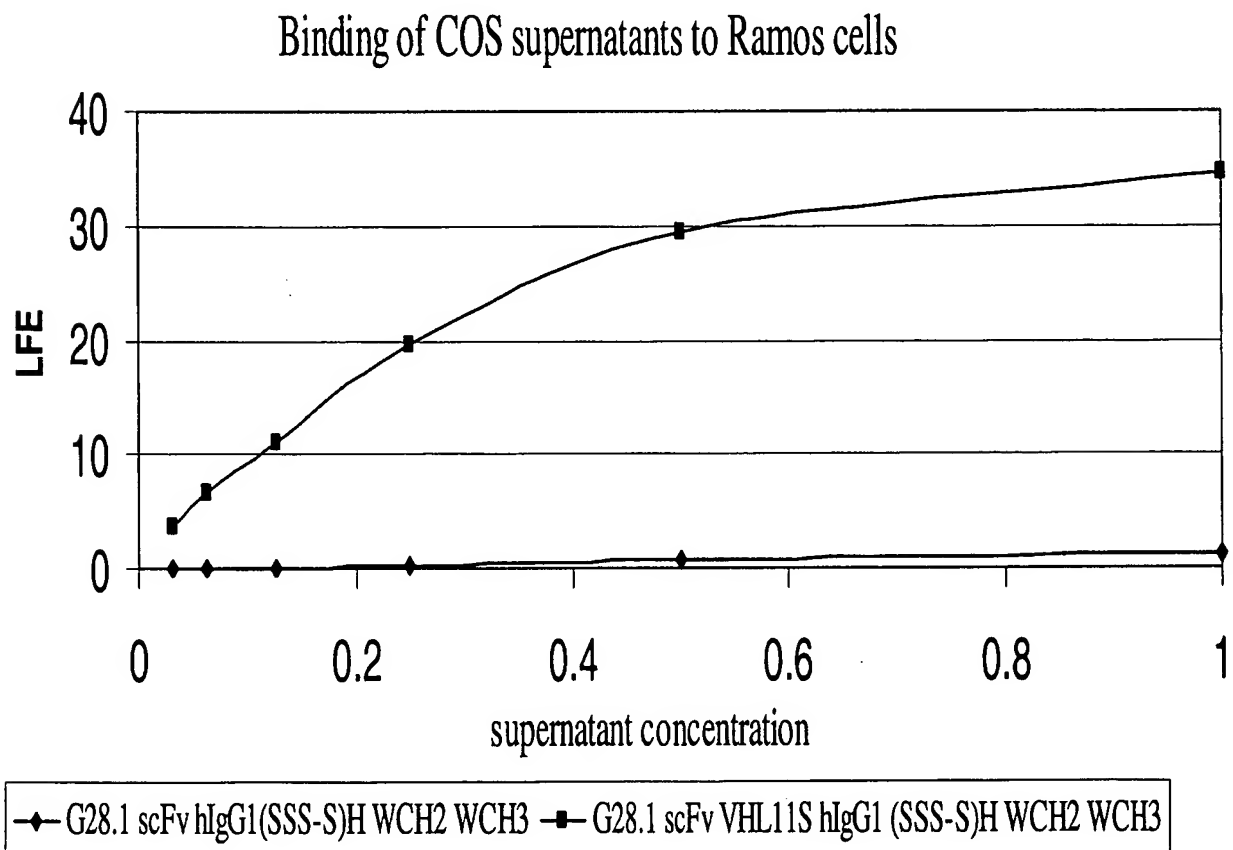


Fig. 52  
Effect of VHL11S Mutation on G28-1 scFvIg Construct  
Protein Production from COS cells



## Fig. 53

### Immunoblot of G28-1 scFvIg Constructs

Increased Protein Levels in COS supernatants  
transfected with G28-1scFv hlgG1 (SSS-S)H WCH2 WCH3  
After Substitution of Leucine with Serine at position 11 of VH (VHL11S)

Fig. 53A.

Purified G28-1 (11/6/01)				G28-1 scFv hlgG1 (SSS-S)H				
scFv IgG1 (SSS-S)H				WCH2 WCH3				
WCH2 WCH3				1 ul/well				
80ng	40ng	20ng	10ng	A	B	C	D	E

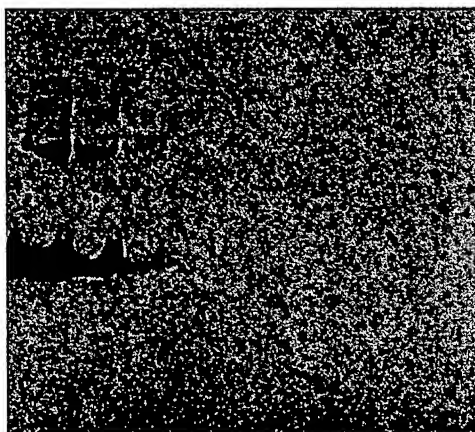


Fig. 53B.

Purified G28-1 (11/6/01)				G28-1VHL11S scFv hlgG1 (SSS-S)H				
scFv hlgG1(SSS-S)H				WCH2 WCH3				
WCH2 WCH3				1 ul/well				
80ng	40ng	20ng	10ng	A	B	C	D	E

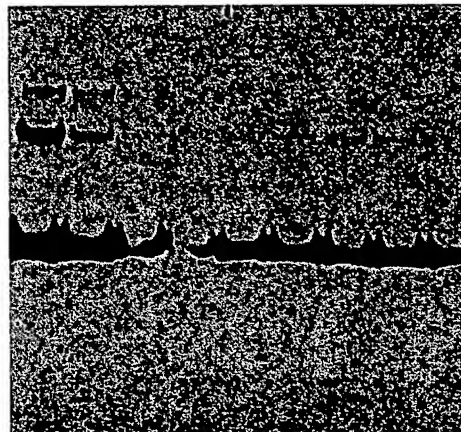


Fig. 54

Binding of 2H7 scFvIg Constructs with Altered  
Hinges and CH3 domains to CD20 CHO Cells

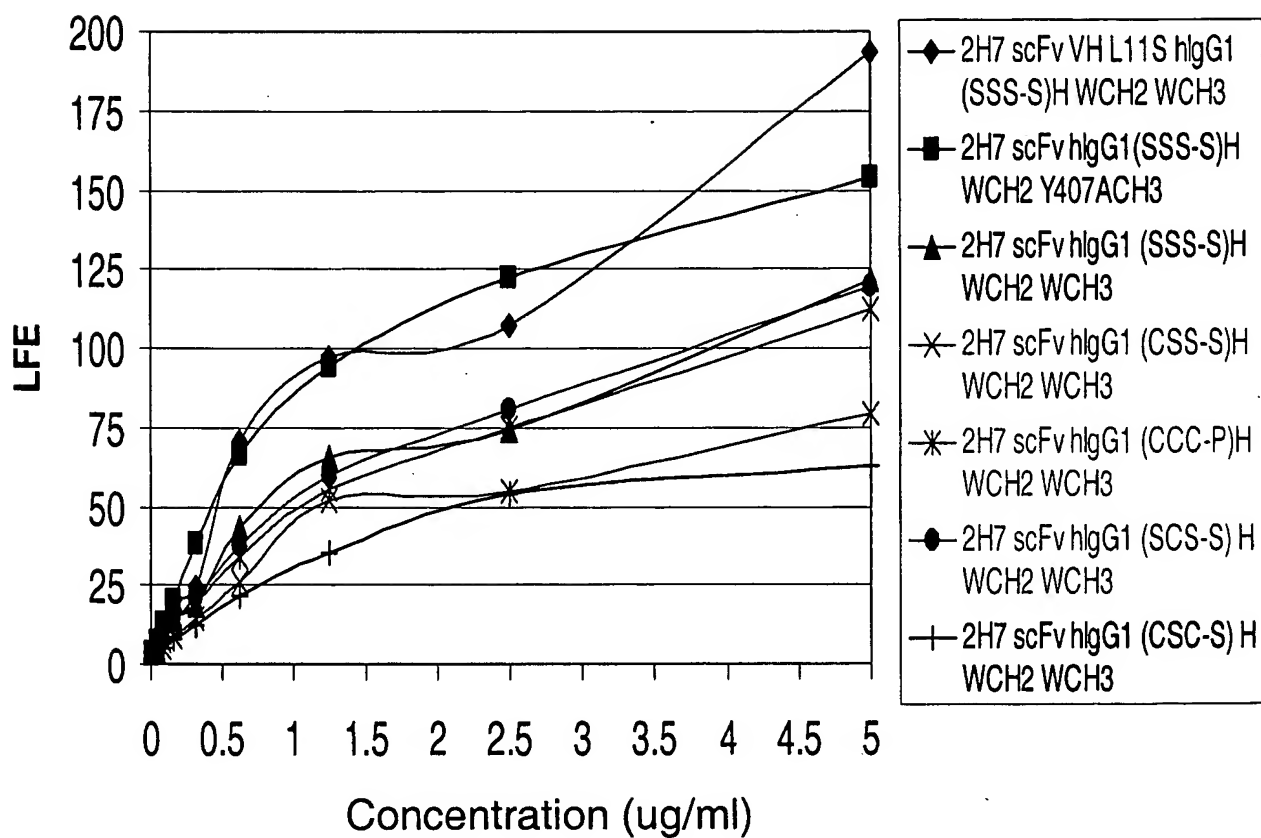


Fig. 55

ADCC Activity of 2H7 scFvlg constructs Against  
BJAB Targets and PBMC Effectors

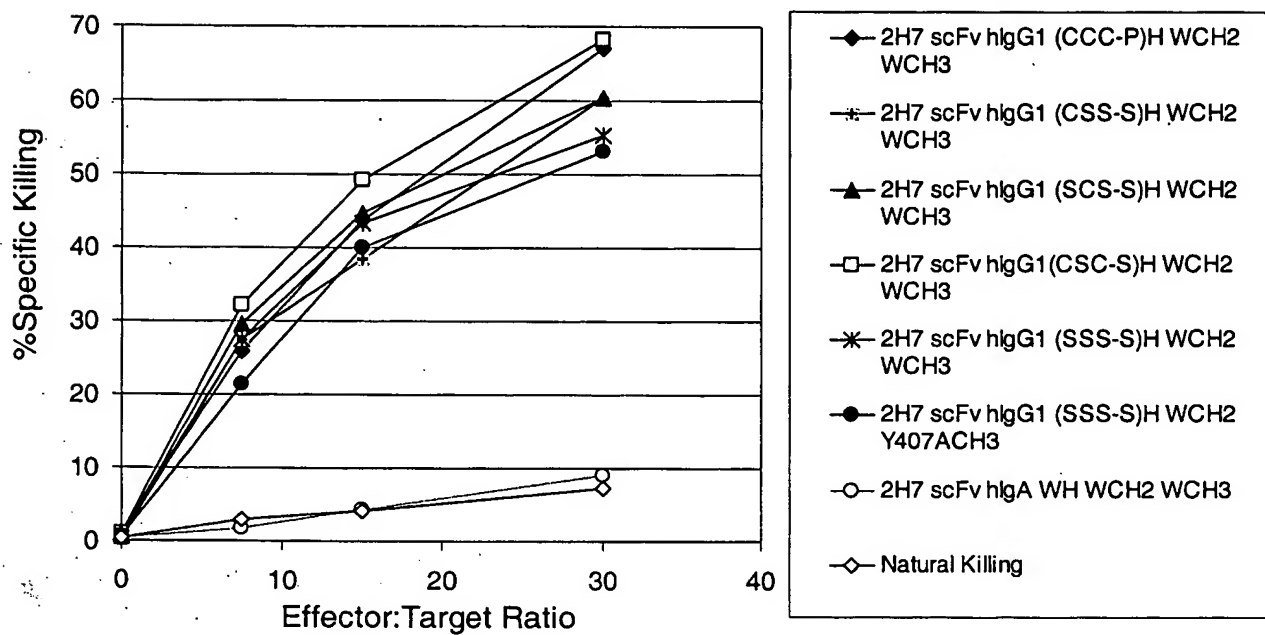


Fig. 56

Complement Activity of 2H7 scFvIg Constructs  
With Ramos Target Cells

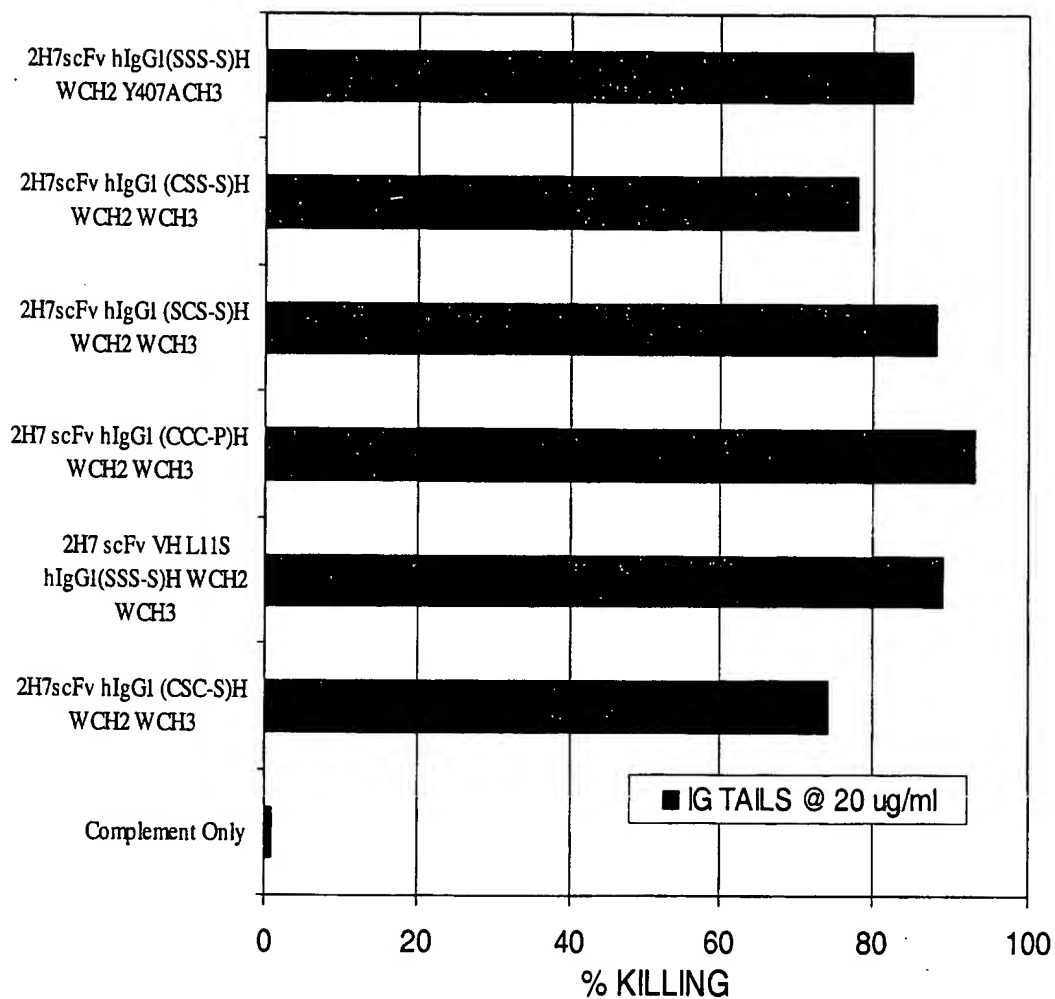
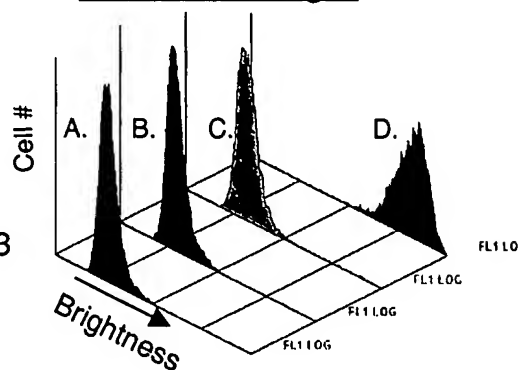


Fig. 57

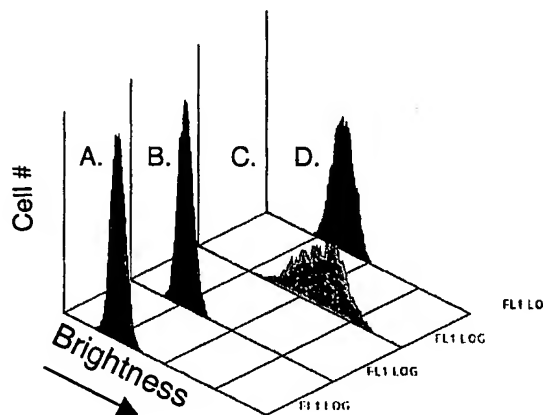
Binding of 2H7 scFvIg Derivatives to CD20CHO Cells

- A. ■ No fusion protein
- B. ■ 2H7 scFv hlgE CH2CH3CH4
- C. ■ 2H7 scFv hlgA WH WCH2 WCH3
- D. ■ 2H7 scFv hlgG1 (SSS-S)H WCH2 WCH3

FITC anti-hlgG



FITC anti-hlgA



FITC anti-hlgE

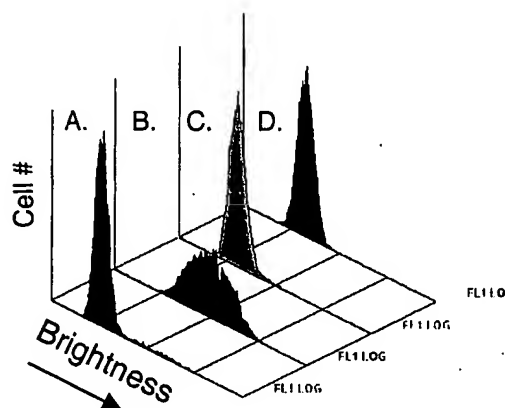


## Fig. 58

Fig. 58A. 2H7 scFv VH L11S human IgE (WCH2 WCH3 WCH4)  
Binding to CD20 CHO at 30 ug/ml

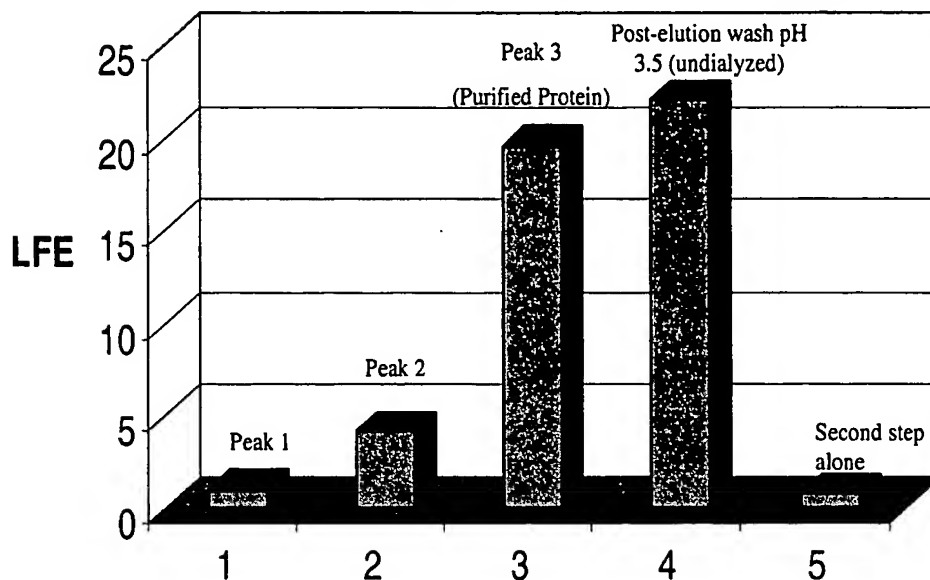


Fig. 58B. ADCC Activity of 2H7 VHL11S IgE (WCH2 WCH3 WCH4)  
Protein Fractions with **PBMC** Effectors and Bjab Targets

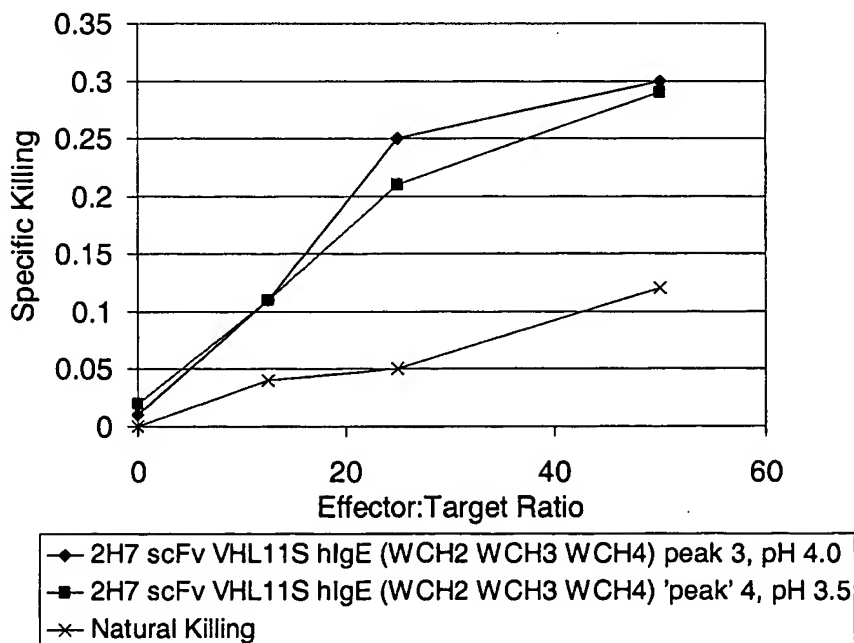
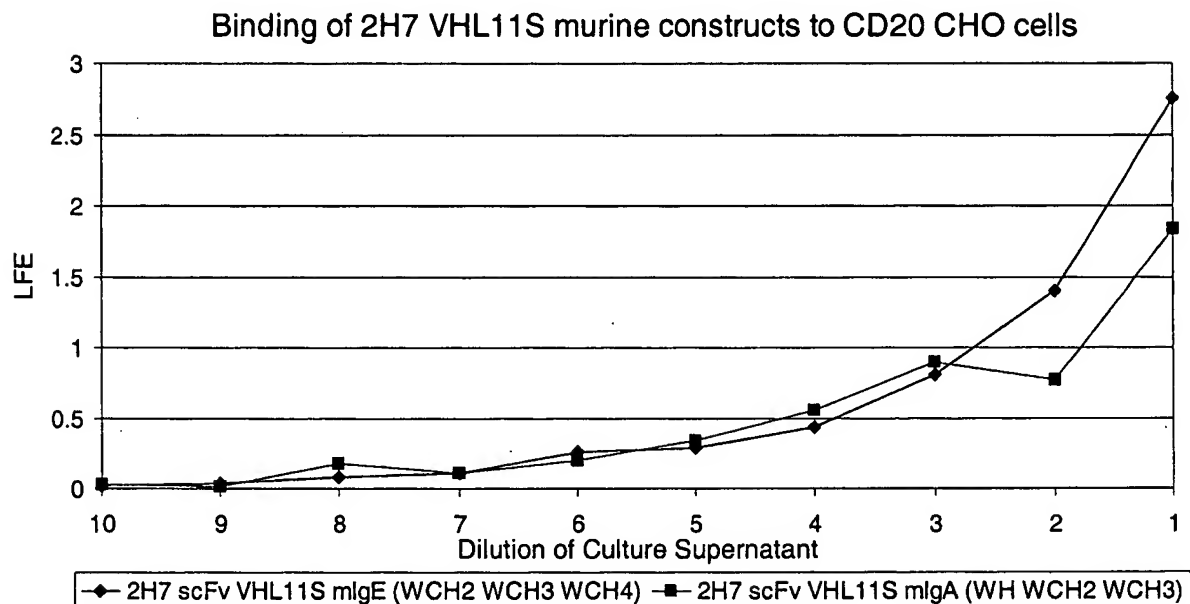
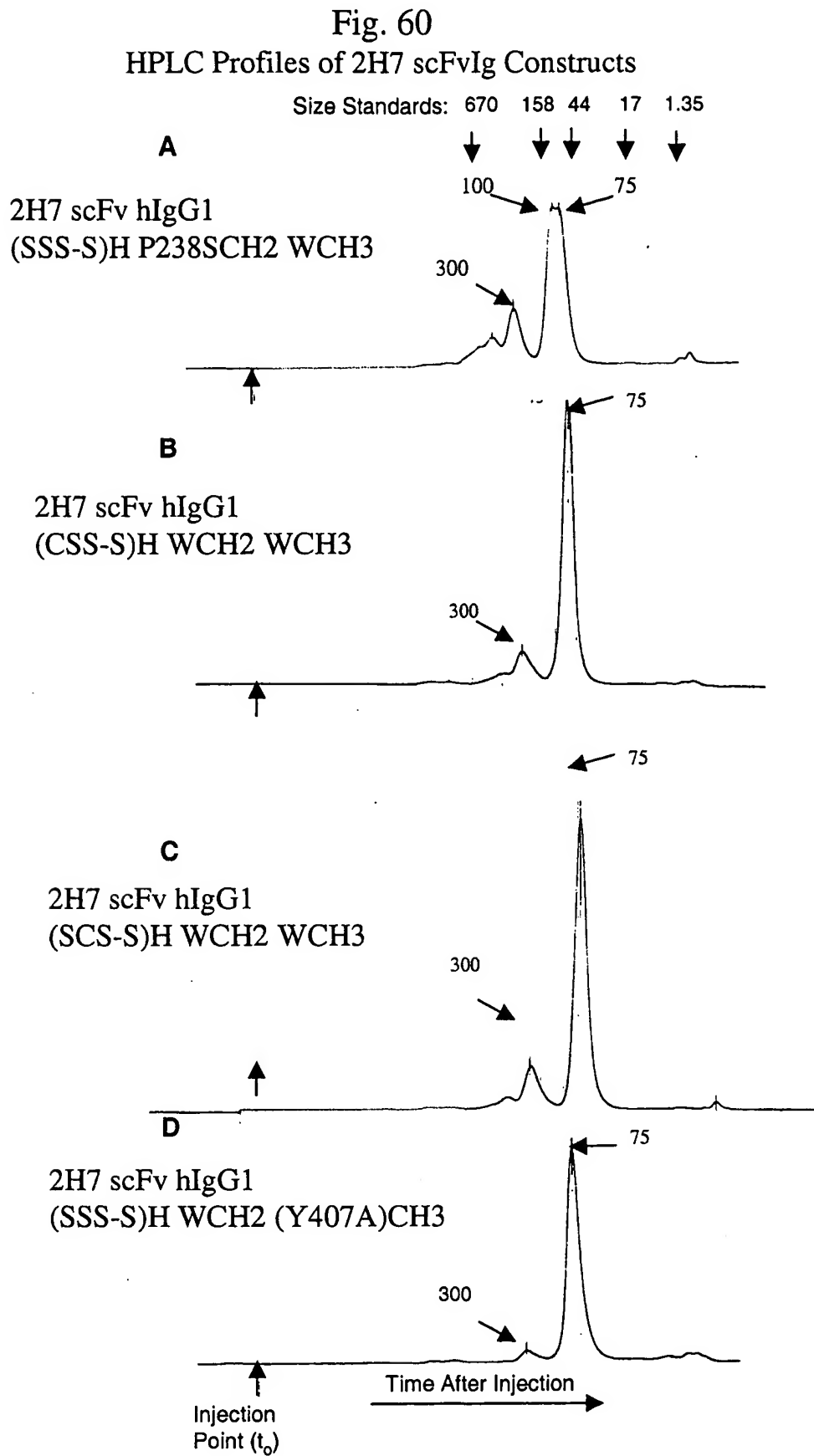


Fig. 59

Binding Data for COS derived  $\alpha$ -CD20 (2H7) scFv VHL11S  
mIg E (WCH2 WCH3 WCH4) and  
mIgA (WH WCH2 WCH3)Tailed Molecules





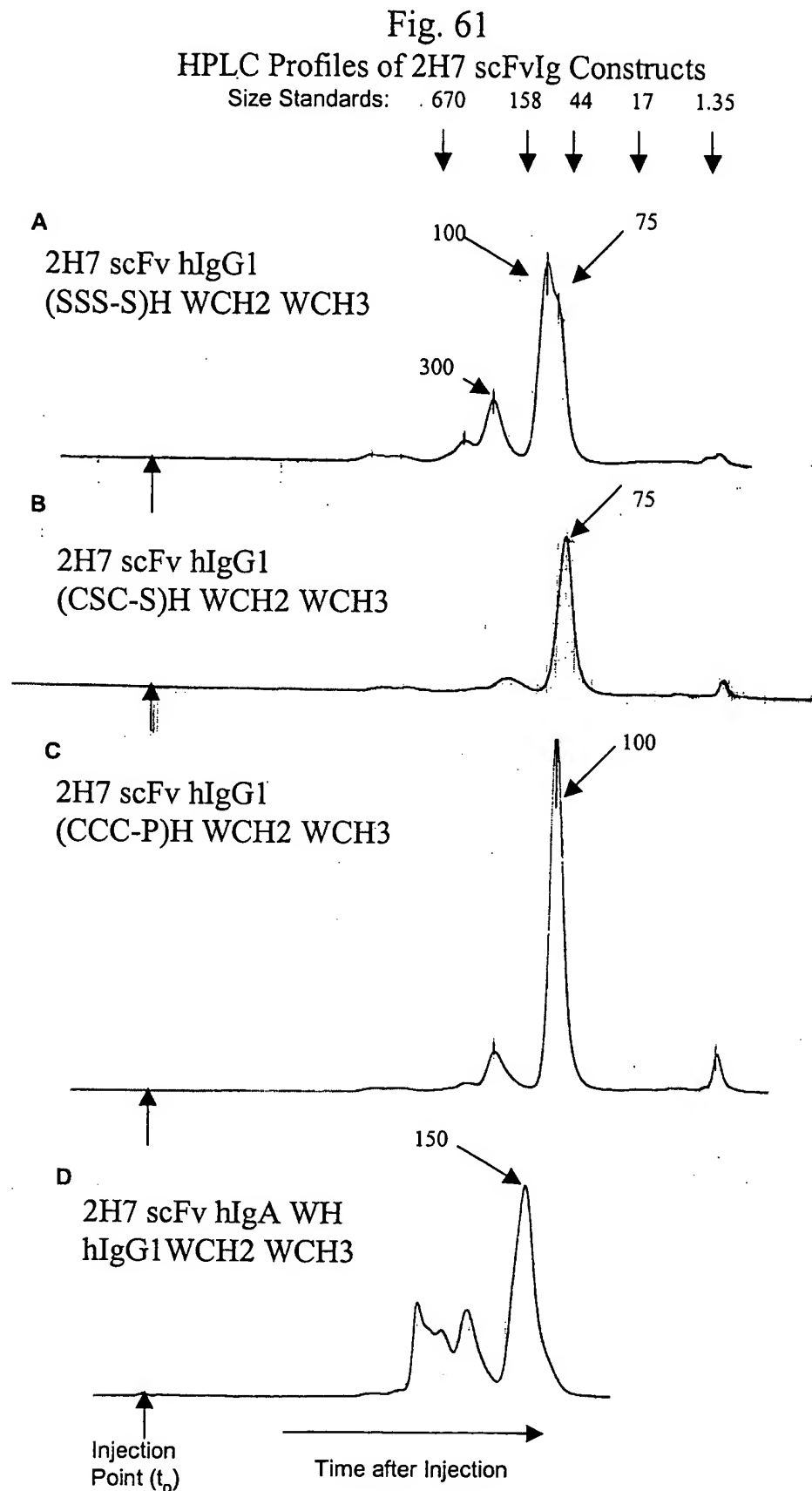


Fig. 62

HPLC Profiles of 2H7 scFvIg Constructs:

Size Standards: 670 158 44 17 1.35

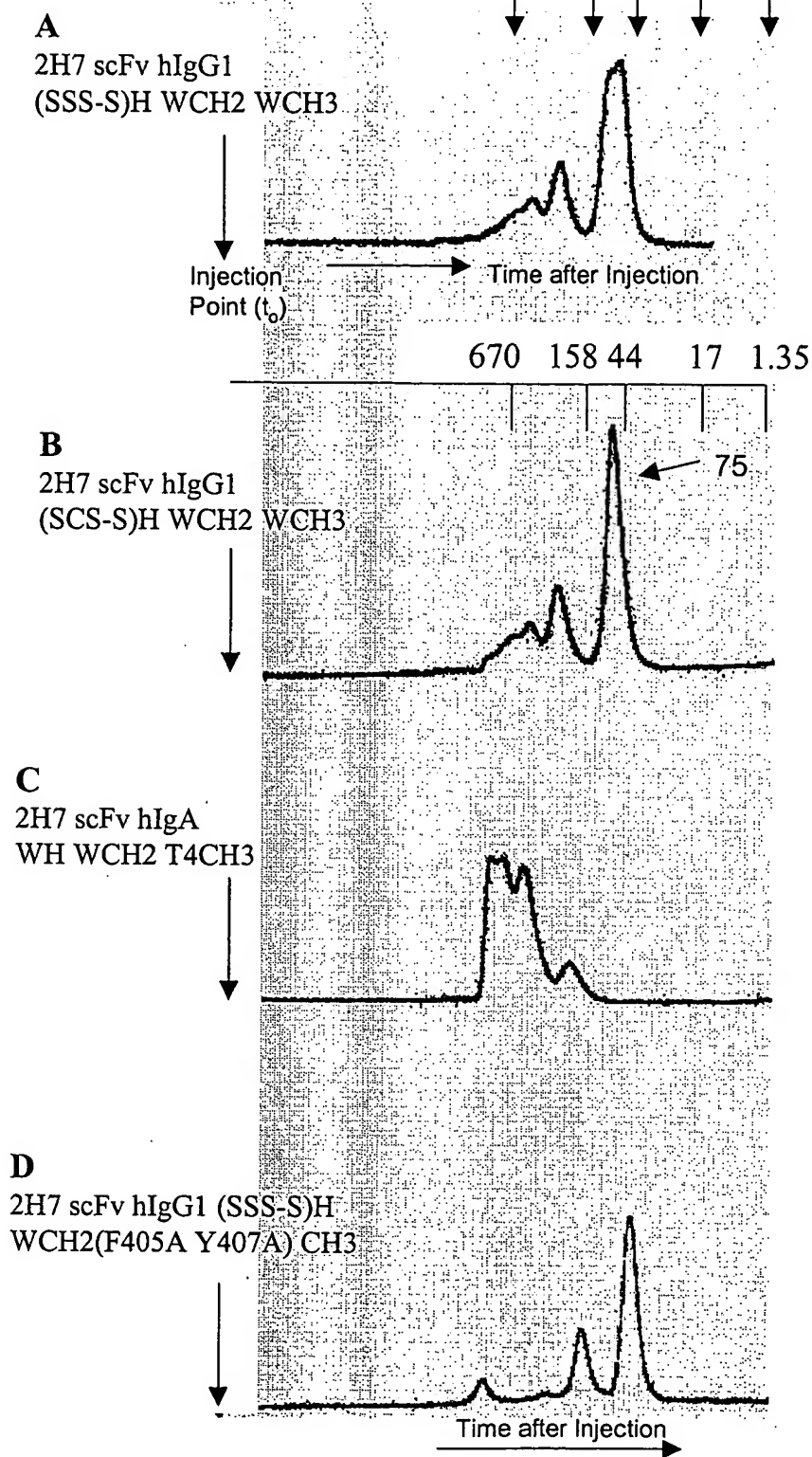


Fig. 63

Binding of Purified Proteins from COS Supernatants  
to CD20 CHO cells:  
Differential Effects of CH3 Mutations on Binding

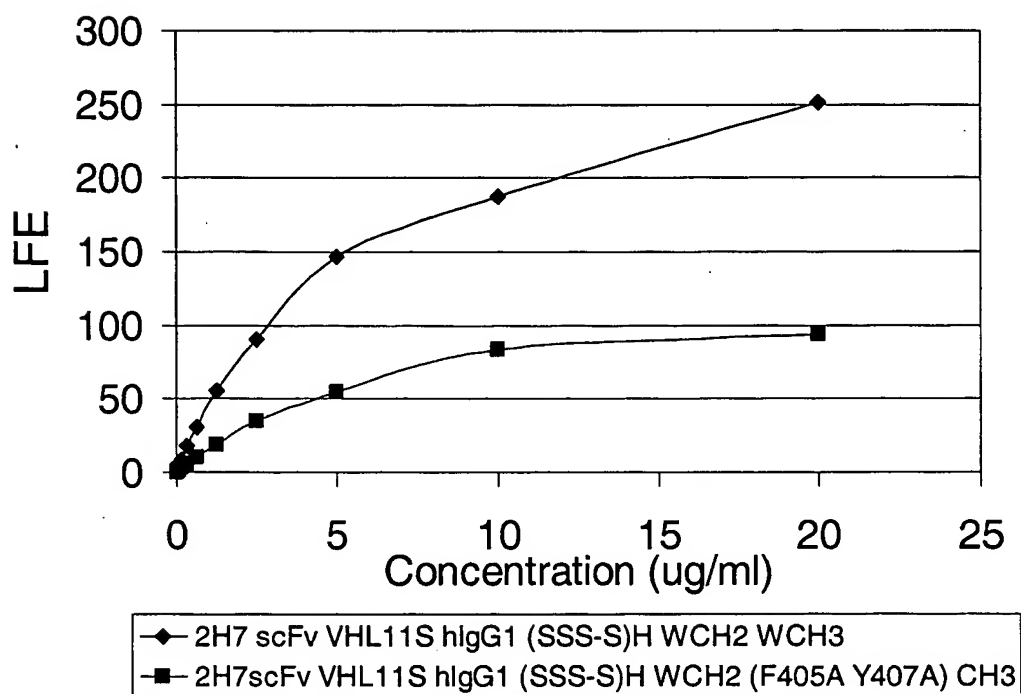


Fig. 64

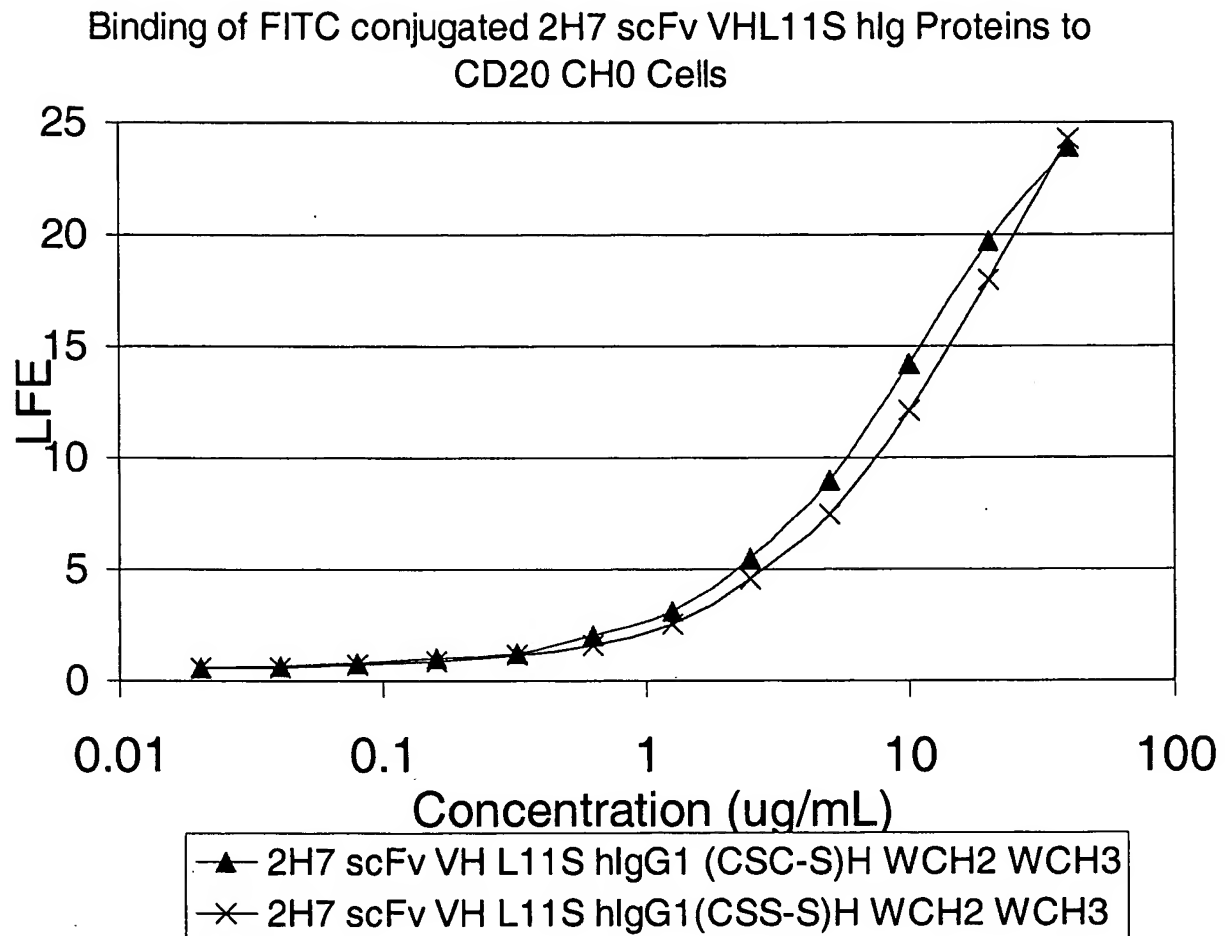


Fig. 65

Nonreducing SDS-PAGE on Protein A-Purified Lots  
of 2H7 scFv VHL11S hlg Constructs (10 ug/lane)

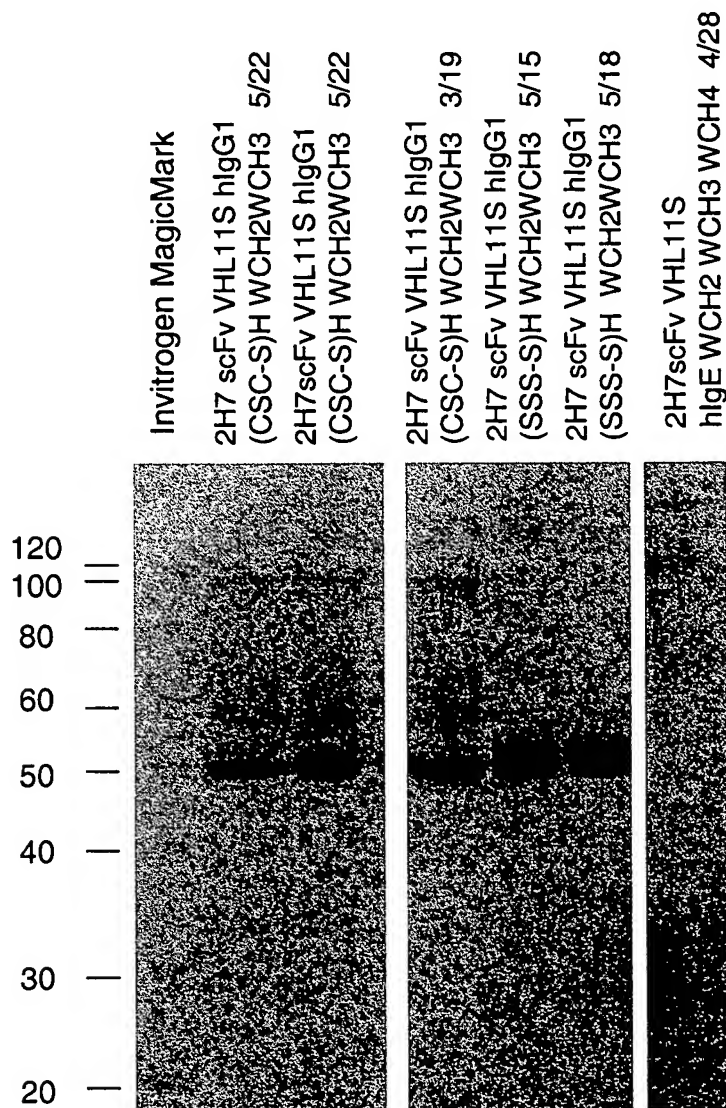


Fig. 66  
Alterations in Human IgG Fc sequence  
that differentially change effector function efficiency

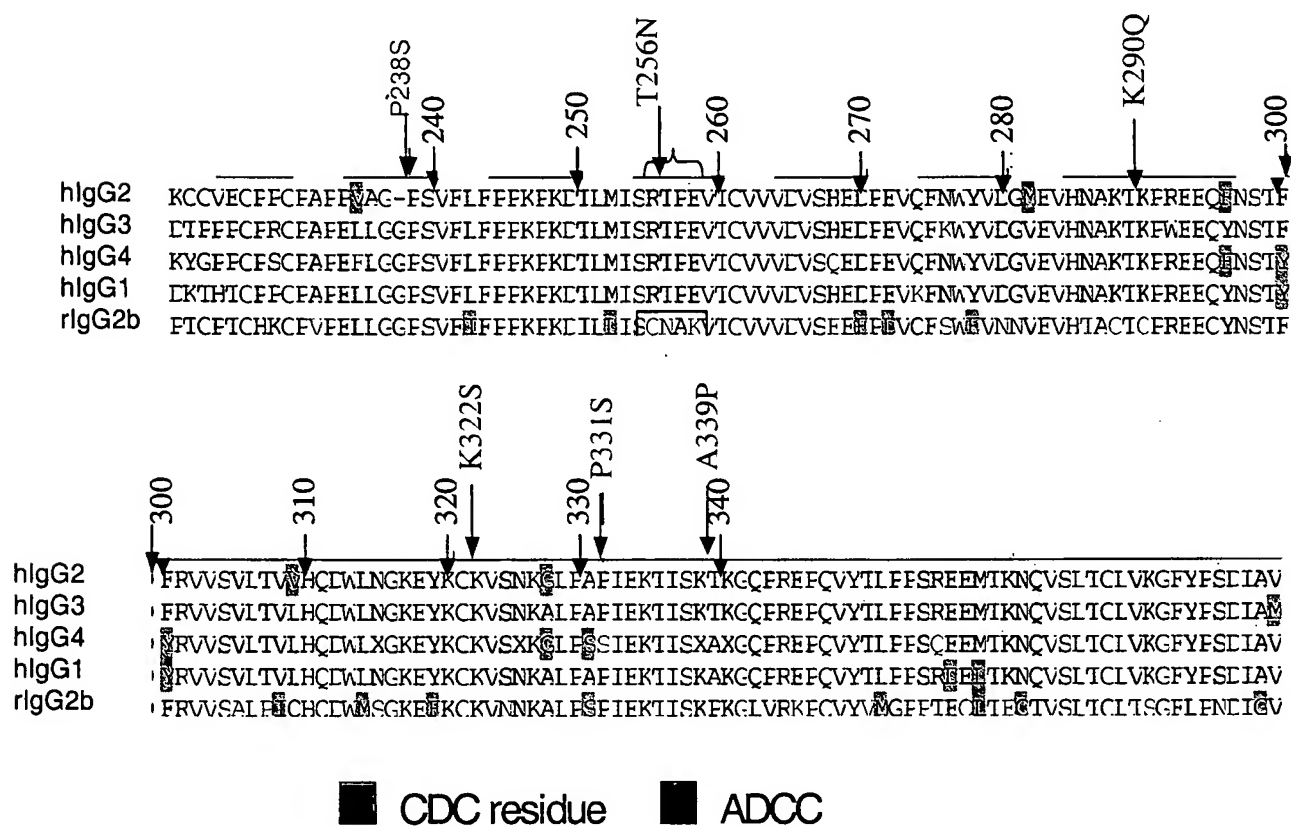


Figure 67.

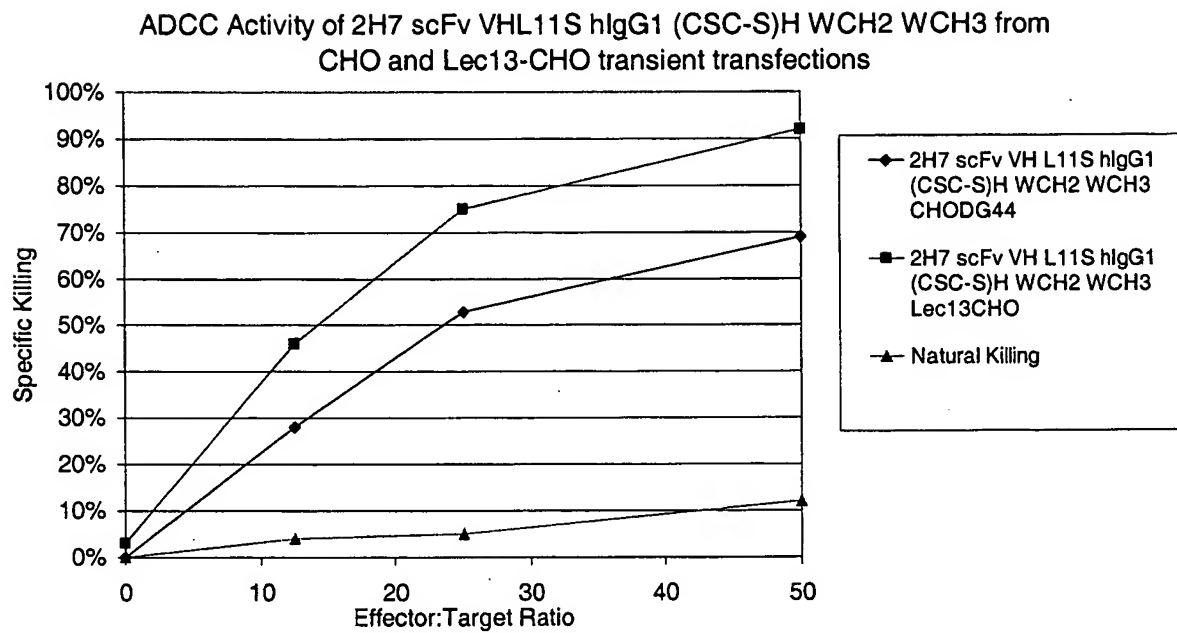


Fig. 68

CD16(ED) hIgG1(SSS-S)H P238S CH2 WCH3 high and low affinity alleles expressed as soluble molecules

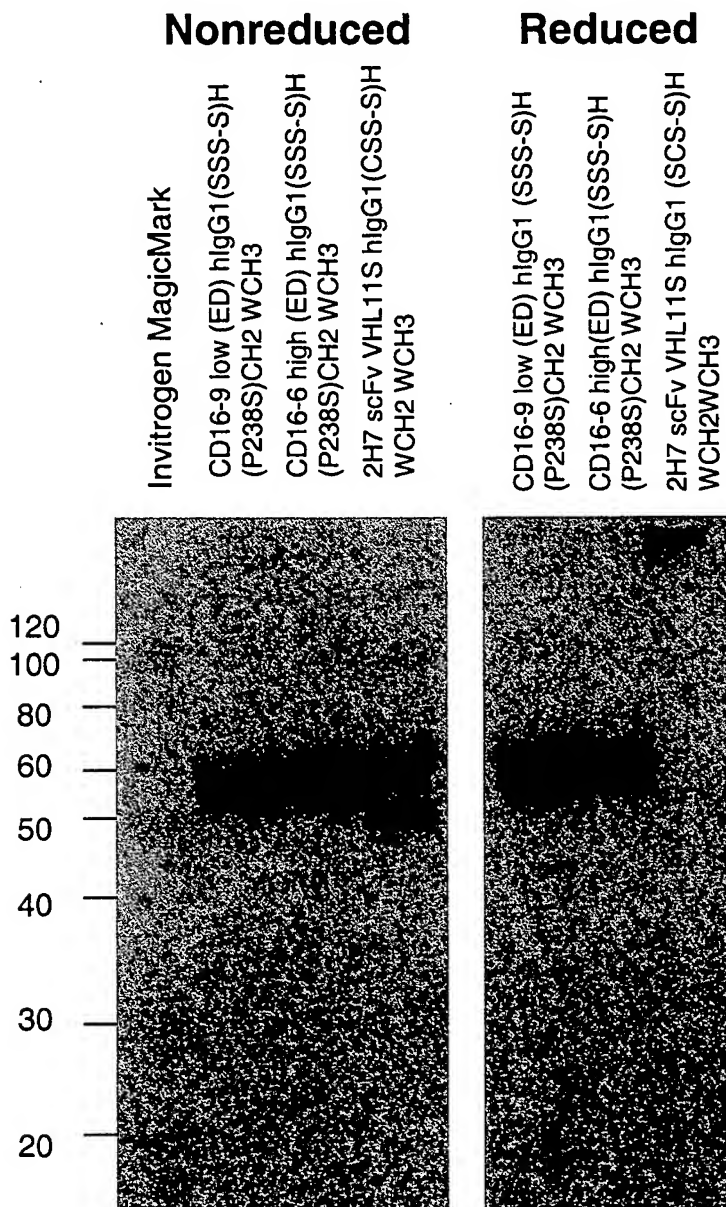


Fig. 69

Binding of soluble CD16-FITC high and low affinity fusion proteins to 2H7 scFv VHL11S hlgG1 (CSC-S)H WCH2WCH3 or (SSS-S)H (P238S)CH2WCH3 on CD20CHO Targets

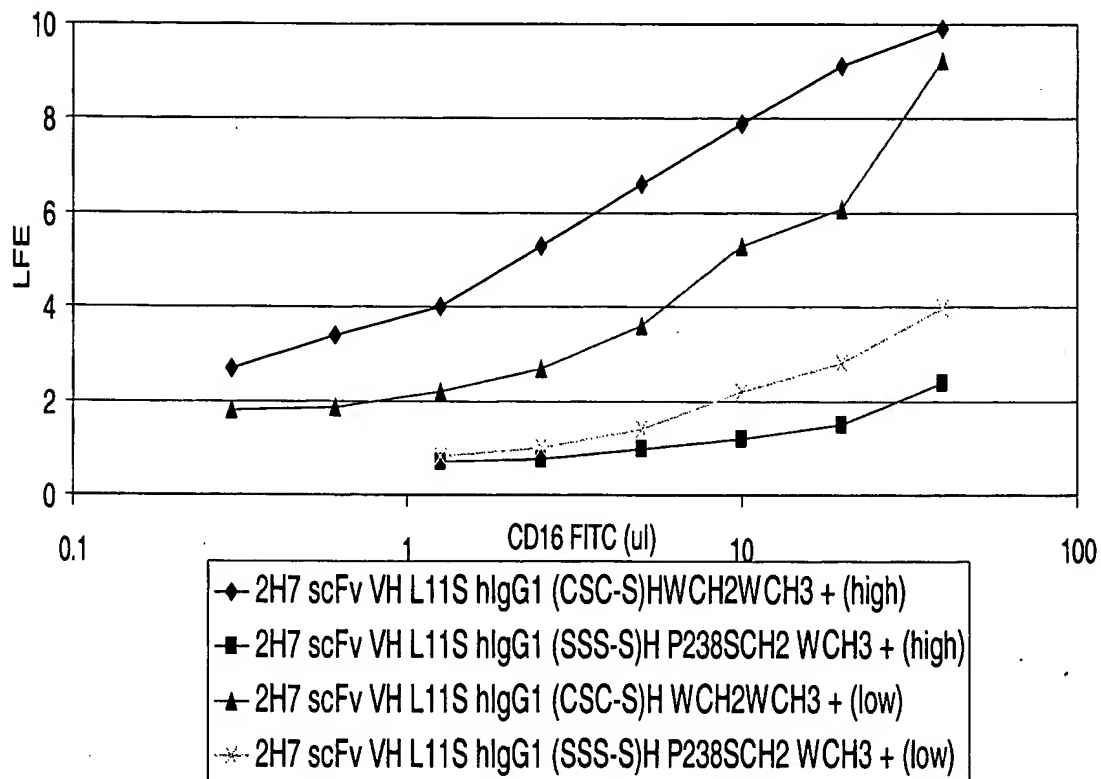
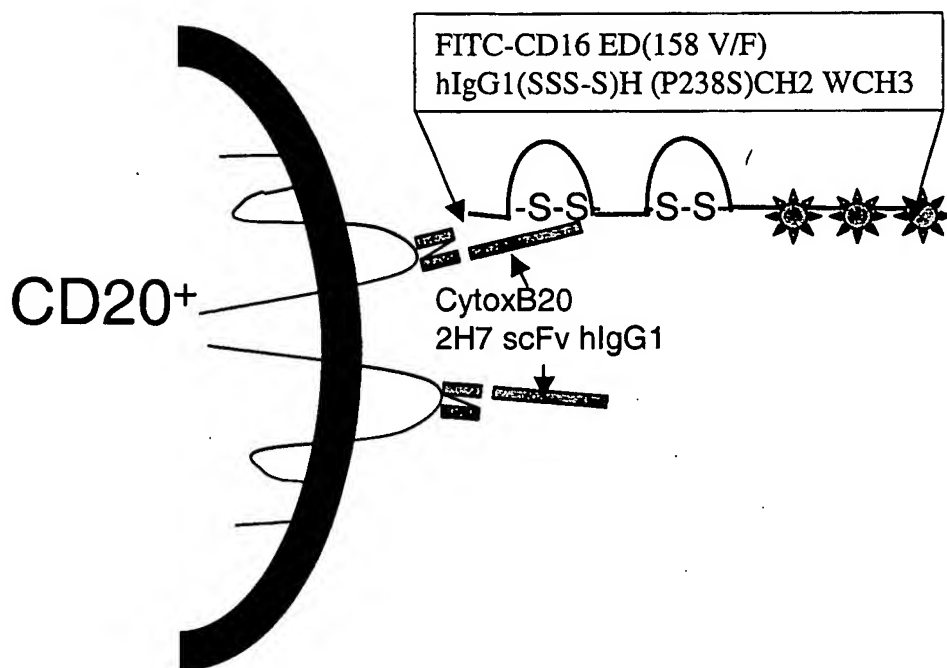


Fig. 70

Binding of FITC Labeled, Recombinant Human  
CD16(ED) extracellular domain -Ig Fusion Protein to  
Cytox B Derivatives on CD20 CHO Cells



Expression of surface displayed SMIPs links  
modified cDNAs with the altered fusion proteins

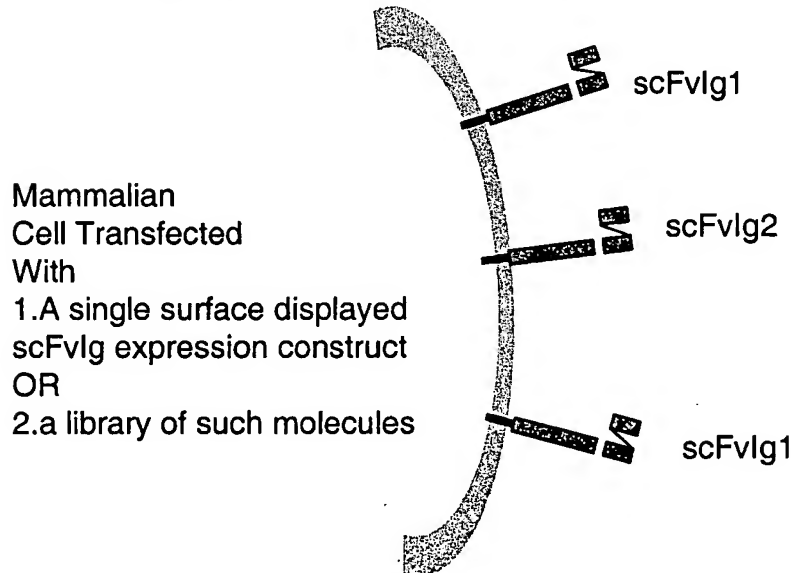


Fig. 71  
CD37 mAbs and scFvIg Induce Apoptosis

scFvIg	Bjab Staining	Annexin V Positive	
	No scFvIg	17.5	
	2H7 MH	27	
	G28-1 MH	30.6	
	G28-1 IgAH	28.9	
	HD37 MH	29.1	
	(2H7+G28-1)MH	41	
	(2H7+HD37) MH	37.1	
	(G28-1+HD37) MH	35.3	
mAbs			plus GAM
	Ramos	AnnexinV Positive	AnnexinV positive
	cells alone	3	3.3
	2H7 Mab	1.4	3.1
	G28-1 Mab	18.3	8.7
	HD37 Mab	3.7	3.1
	G28-5	3.9	8.3
	2H7+G28-1	32.3	35.7
	2H7+HD37	5	10.5
	2H7+G28-5	5.7	19.4
	HD37+G28-1	26.9	50
	HD37+G28-5	8.2	18.4
	G28-1+G28-5	39.5	68.3